SEA
GRANT
PROJECT
OFFICE

CHARACTERISTICS OF CONDENSER WATER DISCHARGE ON THE SEA SURFACE (CORRELATION OF FIELD OBSERVATIONS WITH THEORY)

by

Stephen C. Doret

Donald R.F. Harleman

Arthur T. Ippen

and

Bryan R. Pearce

Massachusetts Institute of Technology

Cambridge, Massachusetts 02139

Report No. MITSG 73-12

Index No. 73-312-Cd

CHARACTERISTICS OF CONDENSER WATER DISCHARGE ON THE SEA SURFACE

[CORRELATION OF FIELD OBSERVATIONS WITH THEORY]

BY

STEPHEN C. DORET

DONALD R. F. HARLEMAN

ARTHUR T. IPPEN

and

BRYAN R. PEARCE

MASSACHUSETTS INSTITUTE OF TECHNOLOGY
CAMBRIDGE, MASSACHUSETTS 02139

Report No. MITSG 73-12
June 26, 1973

MASSACHUSETTS INSTITUTE OF TECHNOLOGY
CAMBRIDGE, MASS. 02139

SEA GRANT PROJECT OFFICE

Administrative Statement

Considerable public and governmental awareness has arisen with regard to possible environmental effects from thermal changes in natural water bodies which are produced by condenser water discharges from electric power stations. This report applies a previously developed steady state analytical model to the heated discharge of a particular power station at the seashore and predicts the heat affected zone. The condenser water is discharged into the coastal water as a free surface stream under tidal conditions. The results of the mathematical model were compared with the surface temperature contours obtained by field measurements offshore from the Pilgrim Nuclear Power Station located at Plymouth, Massachusetts.

Funding for the publication of CHARACTERISTICS OF CONDENSER WATER DISCHARGE ON THE SEA SURFACE (CORRELATION OF FIELD OBSERVATIONS WITH THEORY) was provided by:

The National Sea Grant Program, Grant No. NG-43-72
The Henry L. and Grace Doherty Charitable Foundation, Inc.
The Boston Edison Company
The Division of Mineral Resources, Commonwealth of Massachusetts

Alfred H. Keil
Director

June, 1973

ROOM 3-282 (617) 253-7041

ABSTRACT

CHARACTERISTICS OF CONDENSER WATER DISCHARGE ON THE SEA SURFACE
[CORRELATION OF FIELD OBSERVATIONS WITH THEORY]

BY

STEPHEN C. DORET

DONALD R. F. HARLEMAN

ARTHUR T. IPPEN

and

BRYAN R. PEARCE

Field measurements of the condenser water discharge plume at the Pilgrim Nuclear Power Station were conducted during three survey periods between January and April 1973. Horizontal temperature profiles of the plume were obtained for two water depths. Vertical temperature profiles were obtained in the far field to establish the ambient water conditions for the various survey periods. Plume centerline temperature reduction versus distance and surface isotherm areas were determined from the field data. The field data collected was compared to an analytical model developed for prediction of the heat affected zone.

ACKNOWLEDGEMENTS

This study represents a part of a major research program on the "Sea Environment in Massachusetts Bay and Adjacent Waters", and adds a further step in the continuing investigations of heated water discharges from power stations at the Ralph M. Parsons Laboratory for Water Resources and Hydrodynamics. Funding for this project was provided under Sea Grant Project, DSR 80344 and by matching funds from the Boston Edison Company, DSR 80507. Under this funding the equipment described herein was developed and tested for use in the field.

This study developed from the need for comprehensive field data on temperature distributions caused by heated surface discharges. The scope and difficulties involved in collecting field data in a sea environment are not to be underestimated. For this reason many people were involved. Major participants in the data collection were Dr. John D. Ditmars, Dr. Ole S. Madsen, Dr. Bryan R. Pearce, Mr. Douglas A. Briggs, Mr. William Leimkuhler, Mr. Robert F. Paquette, and Mr. John Wang. Instrumentation development and maintenance was provided by Mr. Edward F. McCaffrey. Mr. E. Eric Adams and Dr. Gerhard Jirka provided valuable assistance in data evaluation and in obtaining the analytical results. Technical advice and guidance throughout the project was provided by Dr. Arthur T. Ippen and Dr. Donald R. F. Harleman of the Department of Civil Engineering.

The authors gratefully acknowledge the excellent typing of this report by Miss Susan M. Johnson and Mrs. Stephanie M. Demeris.

TABLE OF CONTENTS

LIST OF FIGURES

LIST OF PLATES

LIST OF TABLES

LIST OF SYMBOLS

A	the discharge channel aspect ratio = h_o/b_o
a	the coefficient of thermal expansion = $-\partial\rho/\partial T$
b	horizontal distance from the centerline to the jet boundary
b_o	one half the width of a rectangular discharge channel
c	specific heat of water
$\mathbb{F}$	densimetric Froude number = $\dfrac{u}{\sqrt{\frac{\Delta\rho}{\rho} gh}}$
$\mathbb{F}_o$	the densimetric Froude number of the discharge channel = $\dfrac{u_o}{\sqrt{\frac{\Delta\rho_o}{\rho_a} gh_o}}$
h	vertical distance from the jet centerline to the jet boundary
h_o	depth of the discharge channel
K	the surface heat loss coefficient
k	the thermal conductivity of water = $K/\rho c$
L_r	the scale ratio for horizontal lengths between model and prototype
p	the pressure
Q_o	the discharge flow
r	the vertical distance from the jet centerline to the boundary of the core region
S_x	the bottom slope
s	the horizontal distance from the jet centerline to the boundary of the core region

T	the temperature
$T_a, T_{ambient}$	the ambient temperature
T_c	the jet centerline temperature
ΔT	temperature rise above ambient in the jet = $T - T_a$
ΔT_c	the surface temperature rise above ambient at the jet centerline = $T_c - T_a$
u,v,w	the velocity components in the field coordinate system
$\tilde{u},\tilde{v},\tilde{w}$	the velocity components in the coordinate system relative to the centerline of a deflected jet
u_o	the velocity of the discharge channel
u_i	the velocity in the intake opening
V	the ambient cross flow velocity
v_e	the lateral velocity of the entrained flow at the jet boundary
v_h	the lateral velocity in the jet at $y = s$ and $-h < z < \eta$
v_s	the lateral velocity in the jet at $y = s$ and $-r < z < \eta$
w_b	the vertical velocity in the jet at $z = -r$ and $s < y < b$
w_e	the vertical velocity of the entrained flow at the jet boundary
w_r	the vertical velocity in the jet at $z = -r$ and $0 < y < x$
x,y,a	the fixed coordinate directions
$\tilde{x},\tilde{y},\tilde{z}$	the coordinate directions relative to the centerline of a deflected jet

η	the water surface elevation
Θ	the angle between jet centerline ($\tilde{x}$ axis) and the y axis
Θ_o	the angle between the discharge channel centerline and y axis
ρ	the density of water
ρ_a	the density of the ambient water
ρ_o	density of the heated discharge
$\Delta\rho$	the difference between the density of the heated flow in the discharge channel and the ambient density = $\rho_o - \rho_a$

CHAPTER 1

INTRODUCTION

1.1 The Site

Pilgrim Nuclear Power Station is located at Rocky Point in the town of Plymouth, Massachusetts. It is a 650 megawatt, General Electric Boiling Water Reactor, which has a cooling water flow rate of 720 cubic feet per second. The plant raises the intake water temperature 28.7°F above ambient. The intake structure is located at the end of a dredged channel and is protected by a stone armored break water running northeast to southeast, as shown in Figure 1.1. The discharge channel is of trapezoidal configuration with a bottom width of 30 feet and side slopes of 1 on 2 as shown in Figure 1.2. The discharge channel is constructed in the same manner as the breakwater. The invert elevation of the discharge channel at the seaward end is 0 feet mean low water.[1] The sea bottom slopes from the discharge, as shown in Figure 1.3. The sea bottom slope has been schematized with a slope of 1 foot vertical for every 60 feet horizontal.

1.2 Statement of the Problem

The growing demand for electric power in New England and in the United States has created a reduced level of reserve electric power production capacity.[4] The electric companies of New England have met this challenge by construction of new production capacity. One of the new power plants constructed to meet the power demand of this region is

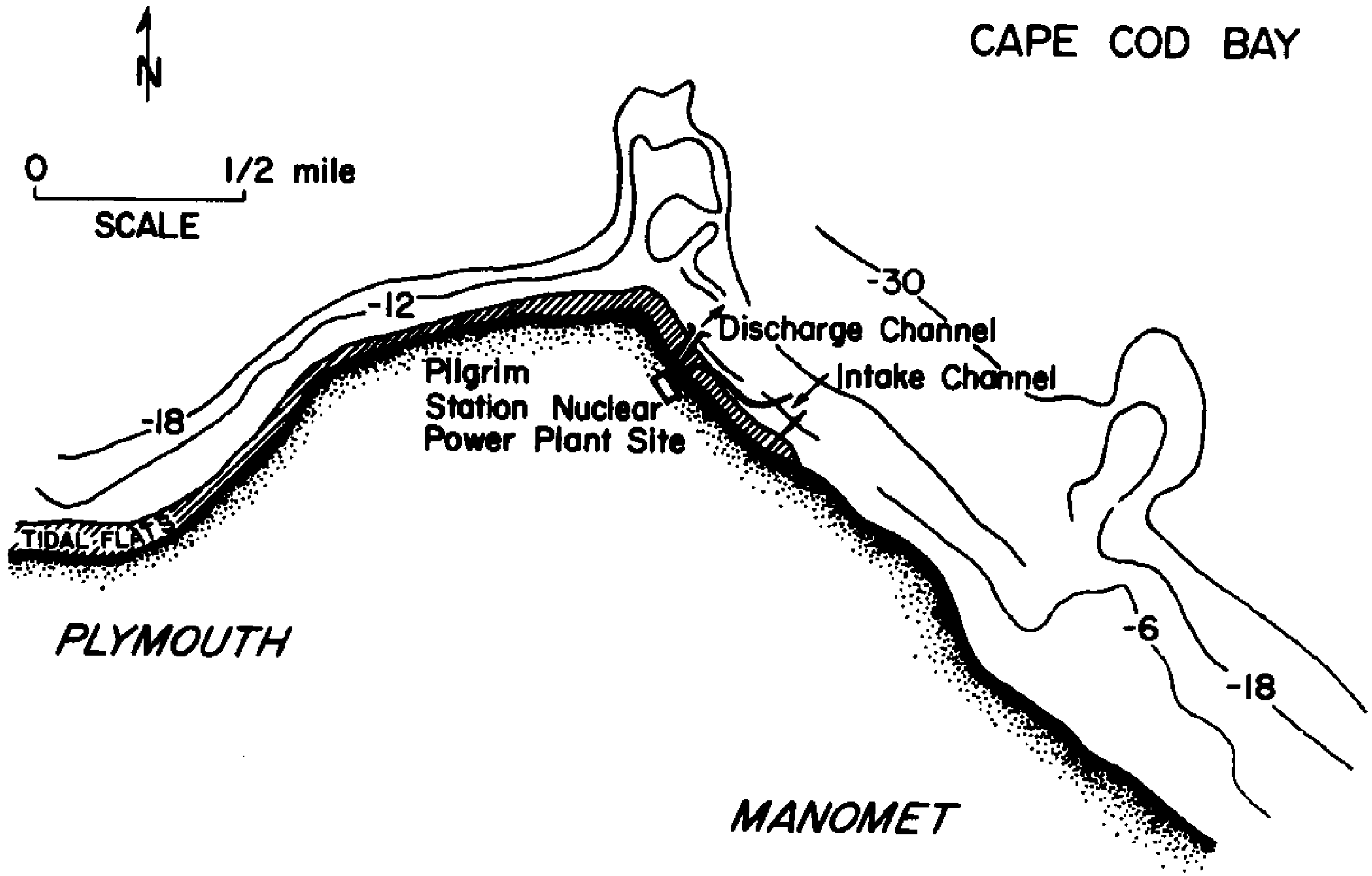

FIGURE 1.1 LOCATION OF POWER PLANT (REF. 1)

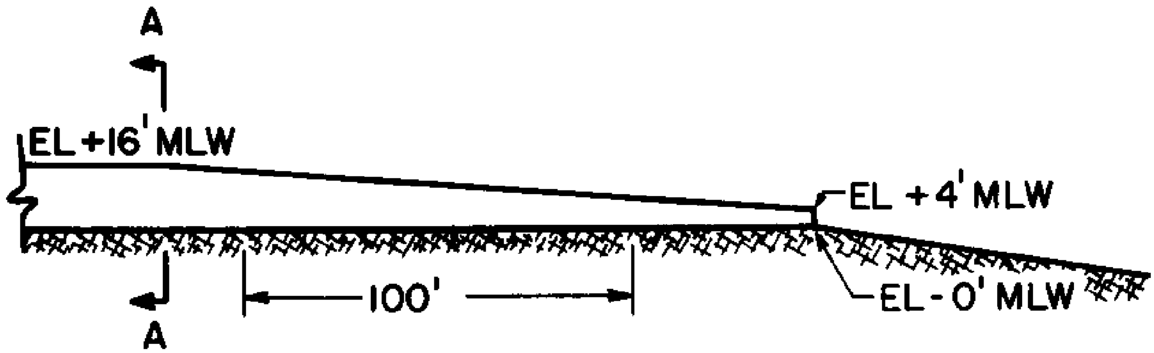

ELEVATION OF DISCHARGE STRUCTURE

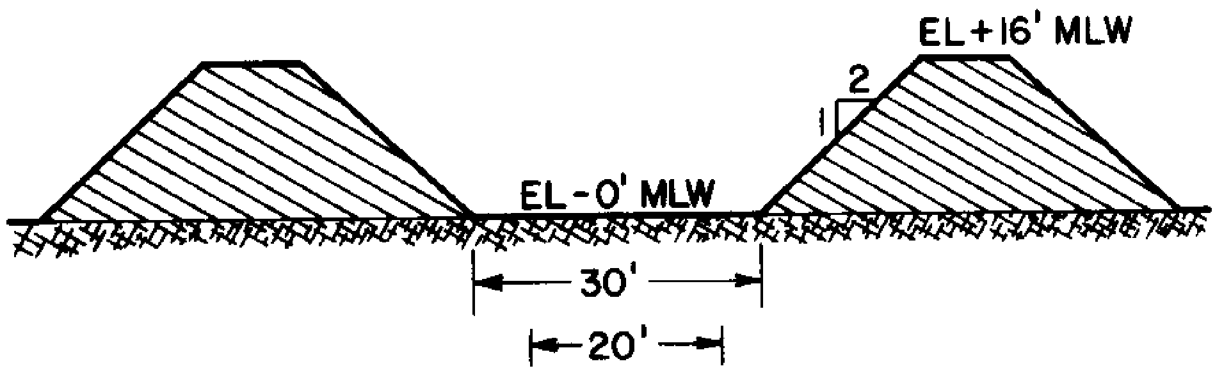

DISCHARGE CHANNEL CROSS SECTION
SECTION A-A

FIGURE 1.2 AS BUILT DISCHARGE CHANNEL

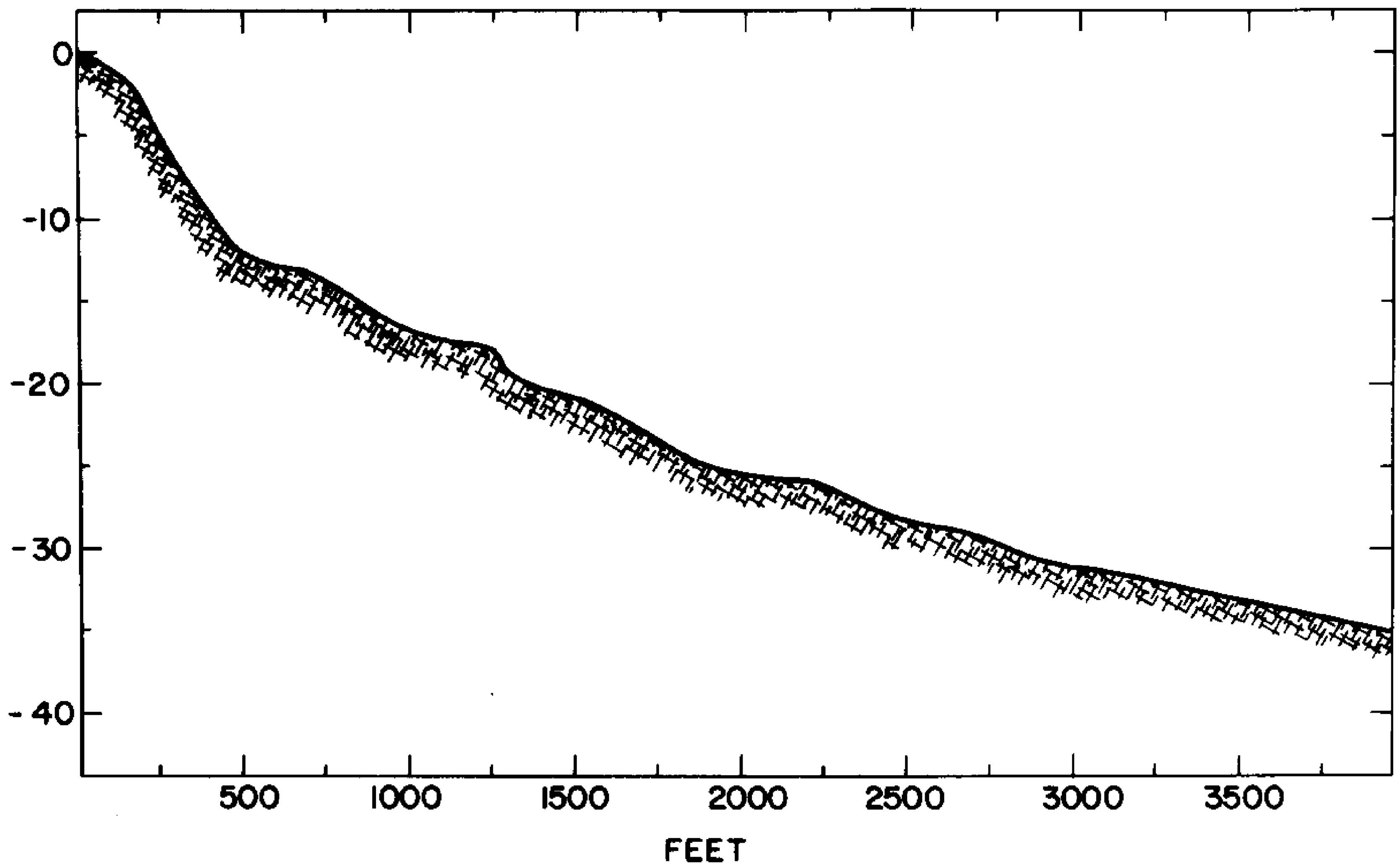

FIGURE 1.3 SHORE BOTTOM ALONG DISCHARGE CHANNEL ℄

the Pilgrim Nuclear Power Station located about 50 miles south of Boston, at Plymouth, Massachusetts. The construction of this facility has coincided with an increased awareness of the public and governmental sectors of potential pollution of our environment. With the advent of this new awareness, federal and state governments have enacted legislation affecting the operation of such power plants.

Electric generating facilities, particularly nuclear generating plants, must have a heat sink into which waste heat can be discharged. The most efficient heat sink for condenser cooling purposes is a natural water body, either a river, lake or ocean. Since the thermal efficiencies of fossil fuel plants are about 40% and nuclear plants are about 30%,[2] it is evident that a significant amount of the input heat energy is discharged to the environment. The area of the heat affected zone must be known before the environmental effects can be ascertained.

1.3 Time Varying Froude Number

The condenser water from the power plant is discharged to the sea through the structure mentioned above. This structure is subject to the rise and fall of the tide during the operation of the power plant. Since the cross section of the discharge is trapezoidal, the width and depth of the water flowing in the channel is directly related to the tidal elevation of the sea. The cross-sectional area of the discharge channel increases as the tidal elevation increases, this in turn decreases the flow velocity since the same amount of water is discharged through an increased area. The discharge velocity and the depth of flow in the discharge channel determine the densimetric Froude number. The initial densimetric Froude number at the invert is one of the important parameters used as input to the analytical model considered in this study.

Another important parameter affected by the tidal elevation is the aspect ratio which is related to the dimensions of the discharge channel. The aspect ratio will be discussed in a later chapter. Determination of the densimetric Froude number proceeds from the depth due to the tidal elevation, sea water density and the velocity of flow. The densimetric Froude number is defined as

$$\mathbb{F}_o = \frac{u_o}{\sqrt{\frac{\Delta\rho}{\rho} g h_o}}$$

where u_o is the initial velocity of the discharge, $\Delta\rho$ is the water density difference caused by the temperature rise across the condenser, g is the gravitational acceleration and h_o is the water depth in the channel.

The value of the Froude number is directly proportional to the dilution of the discharge jet. Thus the variation of the Froude number over the tidal range is an important consideration.

The construction of the discharge channel as described above affects the variation of the densimetric Froude number at low tide. Since the invert of the channel is at elevation 0 feet, MLW, the depth of water flowing in the channel reaches a minimum at the critical flow depth, after which a decrease in tidal elevation below the critical depth of flow will not reduce the depth of water flowing but causes a free overfall to occur. The critical depth of flow in the Pilgrim Nuclear Power Station discharge channel is +2.48 feet MLW. The maximum tidal difference at Plymouth (Boston) as determined from tide tables is ~ 10 feet. Thus the free overfall case represents a significant part of the tidal period where the discharge velocity and densimetric Froude number do not vary. It is important to note that the jet has a vertically downward component in trajectory of varying magnitude at the tidal elevation of 2.48 feet and below. This fact has some significance in evaluation of the field data.

CHAPTER 2

BACKGROUND

2.1 Pilgrim Physical Model

In an earlier study a hydraulic model of the discharge and intake structures of the Pilgrim Nuclear Power Station was constructed in the Ralph M. Parsons Laboratory for the Boston Edison Company. A laboratory study of various discharge schemes was conducted using a distorted physical model.[1] The model had a horizontal length scale of 1 to 240, and a vertical scale ratio of 1 to 40. The horizontal scale was chosen to allow reproduction of a sufficient length of coastline in the experimental basin. The vertical scale was chosen to maintain similarity for the far field surface heat loss. The purpose of the study was to evaluate a number of discharge configurations and the effects of variable discharge rates. The physical model study was conducted prior to the development of the Stolzenbach-Harleman analytical model.[2]

2.2 The Stolzenbach-Harleman Analytical Model

Under a research grant supported by the Environmental Protection Agency an analytical model[2] was developed for the prediction of the temperature distribution in a heated surface discharge. The analytical model does not require the specification of any empirical parameters. One of the objectives of this study is the comparison of the field measurements at the Pilgrim site with the analytical predictions. A user's manual[3] has been prepared to facilitate use of the model.

The analytical model developed by Stolzenbach and Harleman deals with buoyant surface discharges through rectangular orifices. The trapezoidal discharge geometry is resolved by substituting a width to preserve an equivalent rectangular channel area while keeping both the original trapezoidal channel and final channel depths constant. This results in values of h_o and b_o, the initial depth and half width, respectively, where

$$b_o = \frac{\text{channel area}}{2h_o} \quad \text{and} \quad A, \text{ the aspect ratio } = \frac{h_o}{b_o}$$

A schematic drawing of an idealized discharge is presented in Figure 2.1.

The factors which affect the temperature distribution considered in the model are:

1. entrainment of ambient water
2. buoyancy
3. discharge channel geometry
4. bottom slope
5. surface heat loss
6. ambient cross flow

The model is limited to the region of flow where jet induced turbulence dominates over ambient turbulence (i.e. the near-field region). The cross flow in the receiving water is assumed to be parallel to the shore line; however, its magnitude may vary, as shown in Figures 2.2 and 2.3. Far from the jet the ambient water surface is uniform at $z = 0$ and has a temperature, $T_{ambient}$. The model uses only <u>steady</u> <u>mean</u> <u>flows</u> to

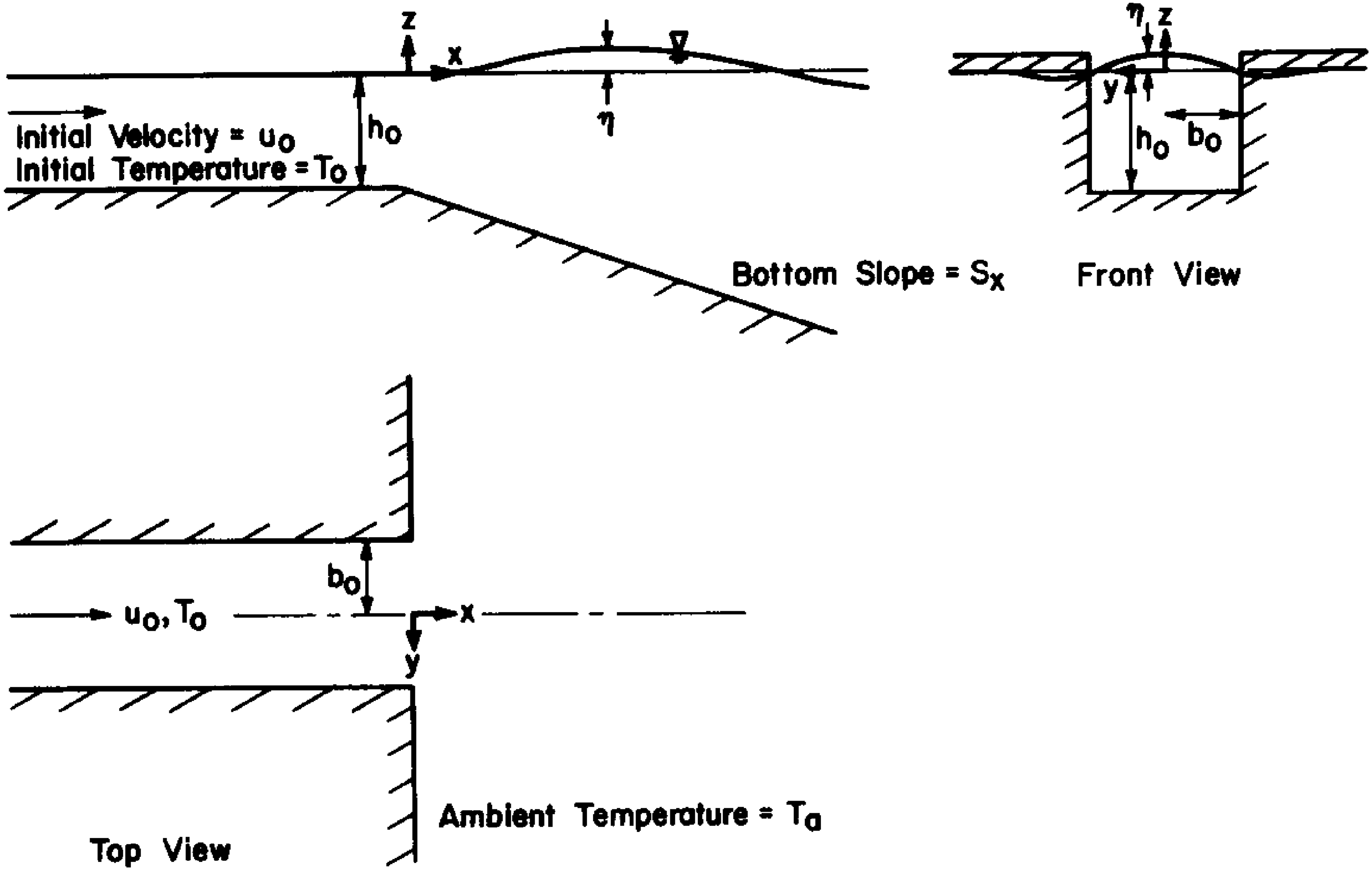

FIGURE 2.1 CHARACTERISTICS OF THE DISCHARGE CHANNEL
(REF. 2)

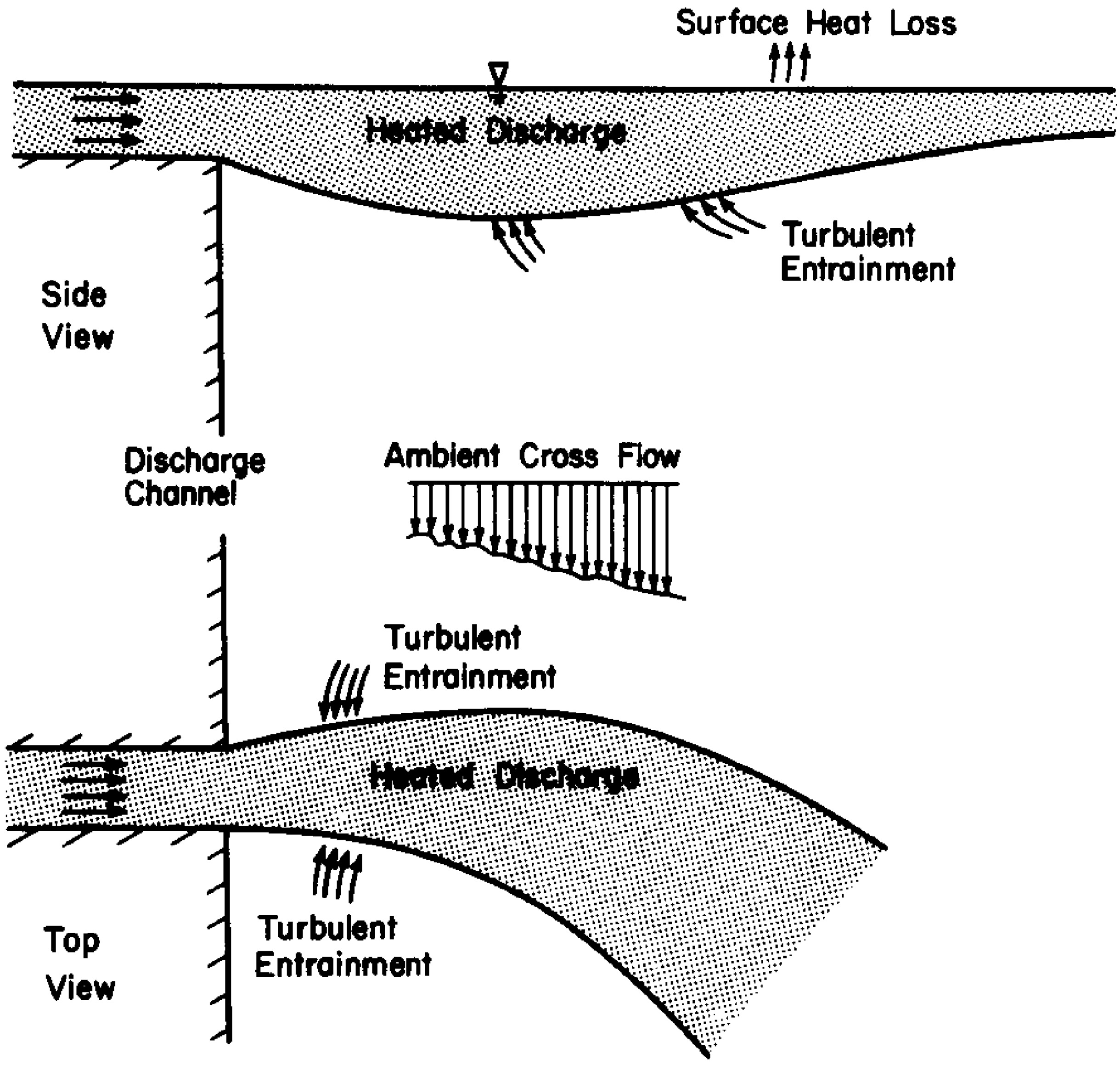

FIGURE 2.2 SCHEMATIC OF HEATED DISCHARGE (REF. 3)

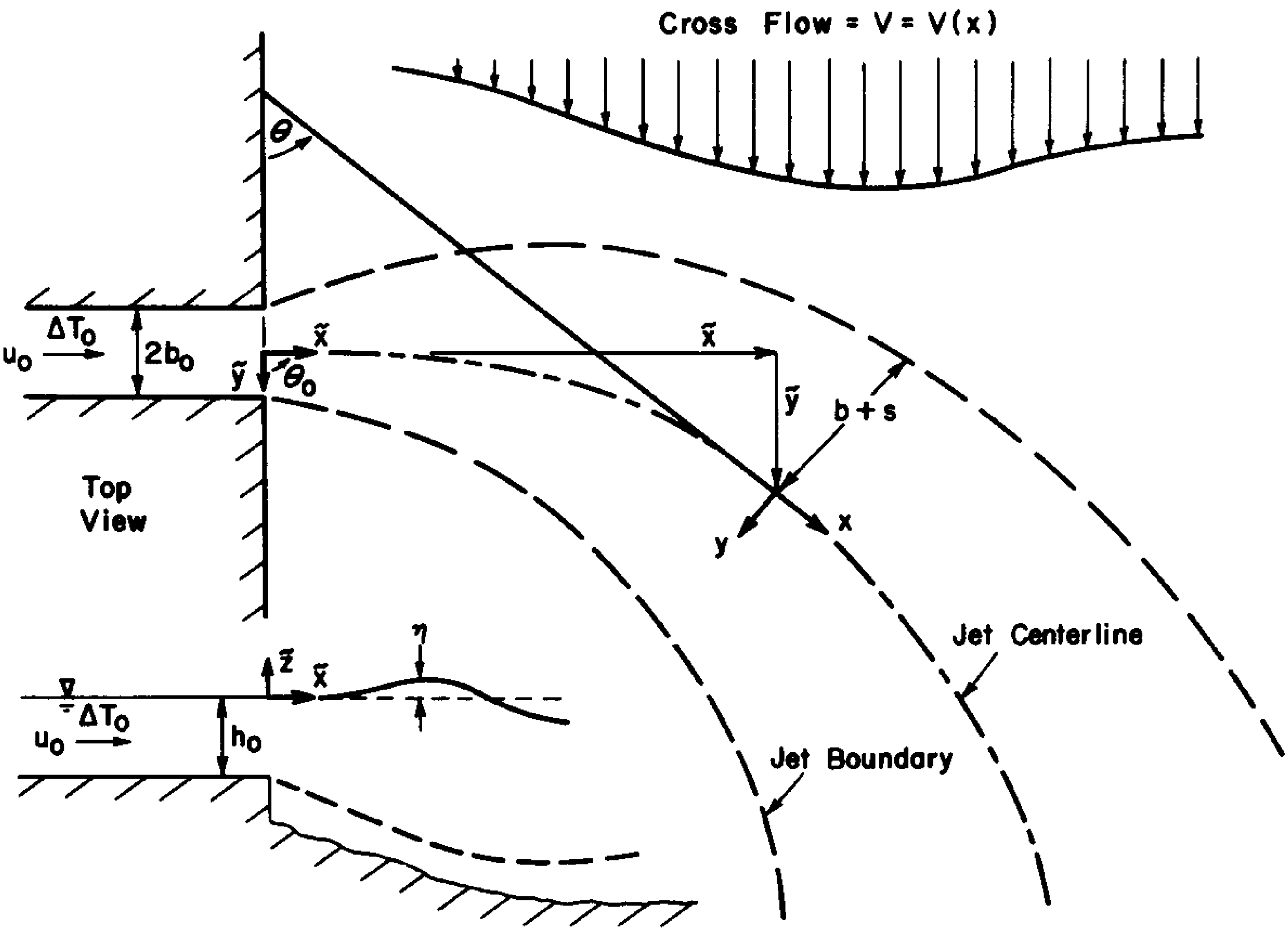

FIGURE 2.3 COORDINATE DEFINITIONS (REF. 3)

generate the turbulent mass, momentum, and heat equations. Thus the model is a steady state model. The conservation of mass equation assumes the change in the coefficient of thermal expansion as very small and therefore, changes in density can be neglected in the mass conservation equation which becomes the familiar continuity equation.

$$\frac{\partial u}{\partial x} + \frac{\partial v}{\partial y} + \frac{\partial w}{\partial z} = 0$$

The density difference can not be neglected in the conservation of momentum equations since the pressure difference term is of the same order of magnitude as the momentum terms. The solutions for the buoyant jet equation are built from the non-buoyant jet solutions with addition of the heat equation and the equation of state. The density difference $\Delta\rho$, is replaced by $a(T-T_{ambient}) = a(\Delta T)$. The structure of the jet is divided into four regions. The core region, with a half width of S and depth of R; the turbulent shear region expanding horizontally with a width b; a vertical sheared region with a depth h; and a region sheared in both directions, as shown in Figures 2.4 and 2.5. The boundary conditions at $x = 0$, the end of the discharge channel are $r = h_o$, $s = b_o$, $b = h = 0$ and $u_c = u_o$. Vertical entrainment is considered since horizontal entrainment was already included in the non-buoyant jet solution. Deflections of the jet are considered by input of a variable ambient cross flow, $u = v(x)$. Bottom slope and, therefore the solid boundary associated with it invalidates a number of assumptions made in the general solution and thus, this solution can not be used.

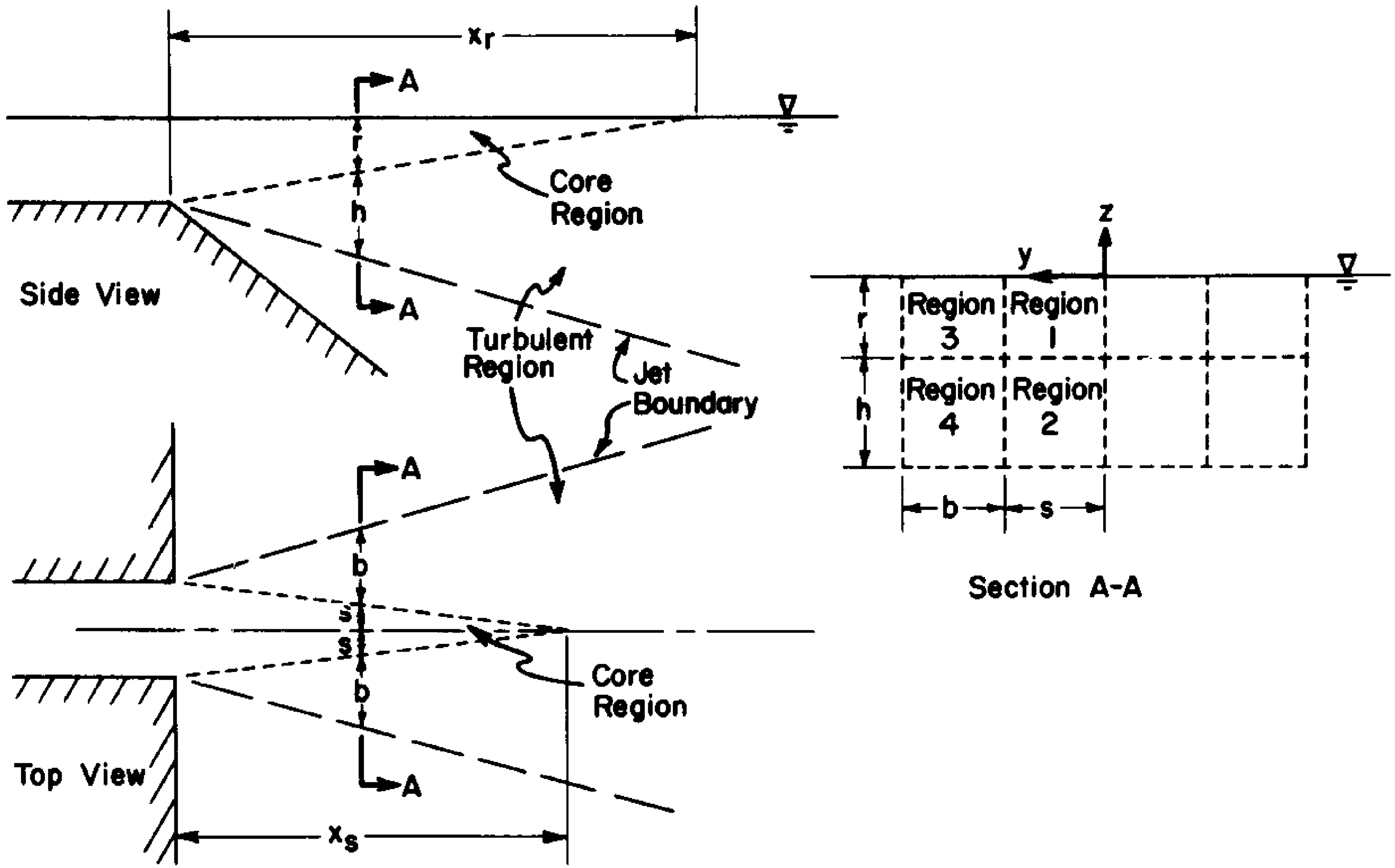

FIGURE 2.4 GEOMETRICAL CHARACTERISTICS OF THE JET (REF. 2)

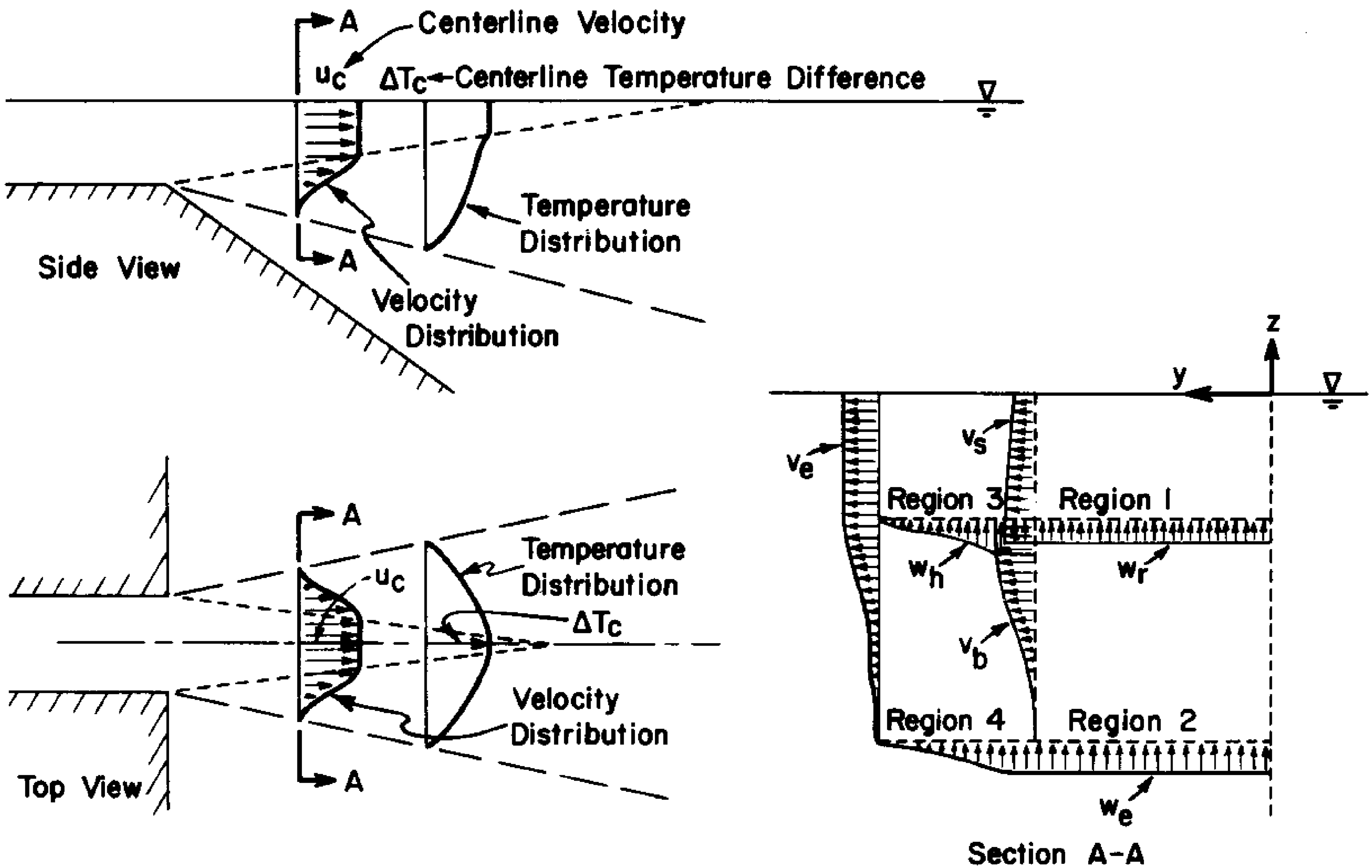

FIGURE 2.5 VELOCITY AND TEMPERATURE CHARACTERISTICS OF THE JET (REF. 2)

It can be used, however, by dropping the non-buoyant y equations. A test is made to determine whether the jet is spreading faster than the bottom allows. If this is the case, the bottom slope defines the lower limit of the jet and the solution continues until the vertical spreading is less than the bottom slope allows and control returns to the original set of y equations.

Model input parameters necessary for temperature predictions are the densimetric Froude number, the aspect ratio A, which defines the channel geometry, the specification of the maximum allowable truncation error at each time step, in each dependent variable, the heat loss coefficient, and the cross flow.

Since the publication of the original analytical model, a second report dealing with the analytical model was published: "A User's Manual for Three Dimensional Heated Surface Discharge Computations".[3] In this report the analytical model was modified by eliminating the capability of modeling the shore-bottom interference with the discharge jet. It was shown by later laboratory experiments that the original analytical model underpredicted the lateral spreading of the discharge jet and the point of jet separation from the bottom. Nevertheless, both the original and the modified model can be used since there are no other existing models with the capability of predicting bottom interference.

At the Pilgrim Station bottom interference with the discharge jet takes place except for the low Froude discharges near the time of high tide. The variation of the vertical jet penetration is caused by the variation of the densimetric Froude number related to the change in tidal elevation as discussed in Chapter 1. Thus this study considers both the original analytical model including bottom slope interference as well as the modified model listed in the "User's Manual".[3]

Comparisons of center line temperature reduction, jet spreading, and isotherm areas will be made between the analytical models and data collected in the field. An evaluation of the steady state assumption used in the analytical models as well as jet spreading and site geometry will be presented in this report. The relative usefulness of the analytical models will be assessed.

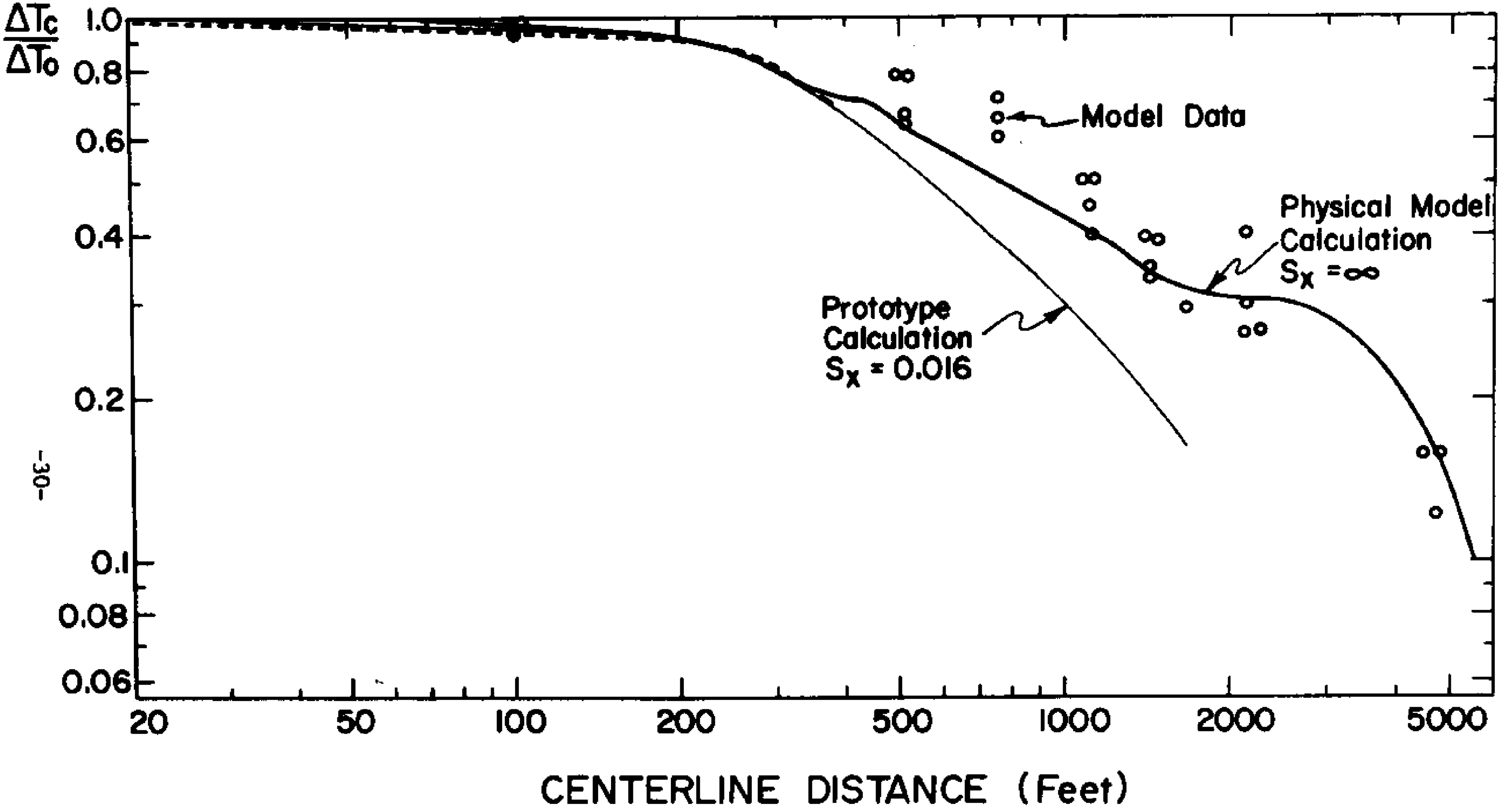

FIGURE 2.6 COMPARISON OF MODEL WITH THEORY

2.3 Comparison: Physical Model and Analytical Results

A comparison of the distorted physical model and the analytical model was made in Reference 2.

Figure 2.6 shows the hydraulic model data for centerline temperature variation at the water surface as a function of distance offshore of the discharge channel for a steady state run at MSL elevation and discharge Froude number of about 6. Since the physical model was vertically distorted by a factor of six to one, the prototype slope of 1/60 is represented in the model by a slope of 1/10 ($S_x = 0.1$). This slope is steep enough so that there is essentially no bottom interference at this Froude number.

An analytical calculation using the Stolzenbach-Harleman mathematical model, without bottom slope ($S_x = \infty$), was made. The Froude number $\mathbb{F} = 6$, and the aspect ratio of the discharge channel in the distorted model were used in this calculation and the results are in good agreement with the model data as shown in Figure 2.6. The analytical calculation for the prototype at the same Froude number was made using the prototype aspect ratio and the prototype bottom slope of 1/60 ($S_x = .016$). The difference between the two calculated curves shows the effect of distortion of the physical model.

It should be noted that the output of the mathematical model is in the form of $\Delta T_c/\Delta T_o$ as a function of the dimensionless distance $x/\sqrt{h_o b_o}$. In order to obtain the physical length x used in Figure 2.6, the dimensionless output must be multiplied by $\sqrt{h_o b_o}$. The physical model calculations ($S_x = \infty$) are scaled by the distorted model values of h_o and b_o and the horizontal length scale of 240. The prototype calculations are scaled by the true values of h_o and b_o.

CHAPTER III

PILGRIM NUCLEAR POWER STATION PRE-OPERATIONAL DATA STUDIES

3.1 Purpose of the Baseline Study

The thermal study of the Pilgrim Nuclear Power Station developed from both the proximity of the Pilgrim Nuclear Power Station to M.I.T. and the need for good on-line field data for heated surface discharges. The baseline study was the first part of the two part field collection program. Baseline information collected during the spring and summer of 1972 provided control information for the on line data collected after the power plant began operations.

3.2 Baseline Procedures and Measurement Equipment

3.2.1 Measurement Procedures

Measurements of salinity, temperature and ocean currents were made during the baseline study. Salinity and temperature were measured over as large an area as possible but an area small enough so as to allow frequent returns to the same stations. The area of study chosen was about one mile off the shore to the shore and two miles along the shore encompassing Rocky Point on the north and White Horse Rock on the south, as shown in Figure 3.1. The area was divided into five transects. The first transect began on leaving Plymouth Harbor and continued along the coast at a water depth of 60 feet to a point directly off White Horse Rock. The other transects began at a water

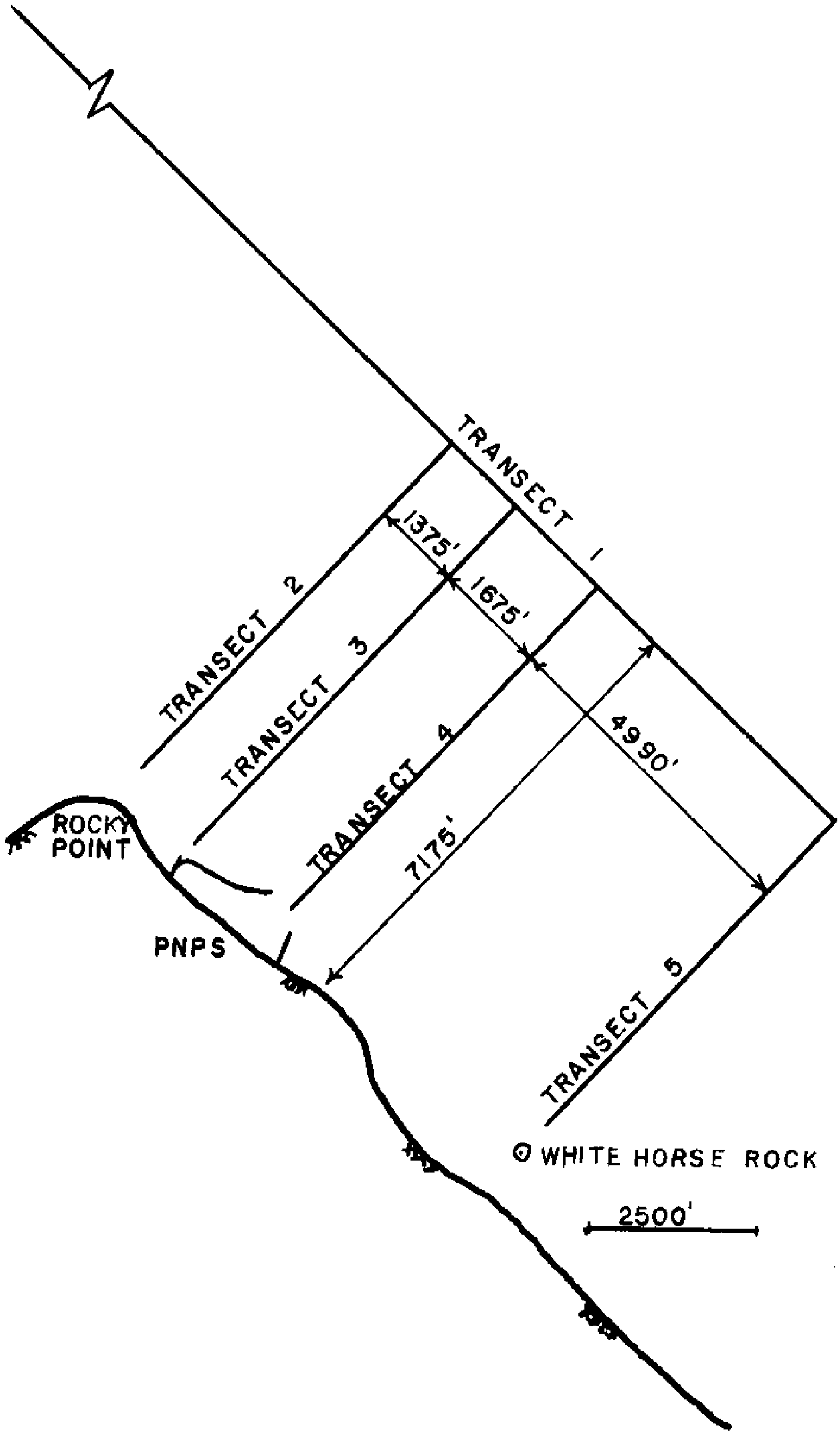

FIG. 3.1 BASELINE TRANSECTS

depth sufficient for safe operation and continued until they intersect transect #1. The transects ran on lines perpendicular to the shore originating at the mouth of the intake channel, discharge channel and on either side as control transects. During the period of the baseline study field trips were conducted in April, June and August, 1972. Salinity and temperature measurements were made on all three trips and current drogue studies only on the June and August field trips. The location and density of the salinity and temperature measurement over depth are shown in Figures 3.2, 3.3, and 3.4.

3.2.2 <u>The C.T.D.</u>

The C.T.D. is the Conductivity, Temperature, Depth instrument used during the baseline study to measure temperature and conductivity over the depth of the water column. This instrument was developed by the Ralph M. Parsons Laboratory for Water Resources and Hydrodynamics for oceanographic studies with funds provided by the Massachusetts Bay Sea Grant Program. The C.T.D. provides vertical profiles of temperature versus depth and conductivity versus depth and was designed for computer compatibility. The C.T.D. is shown in Figure 3.5. The sensors providing analog readout are a Standard Controls Company pressure transducer for depth Model #210-80-040-06; Rosemont Engineering Company, Model #171CG platinum element for temperature and a Plessey Instrument Company, Model #2600-3 conductivity head.

The analog output voltage signal from each sensor is converted to F.M. format by voltage control oscillators and recorded with a

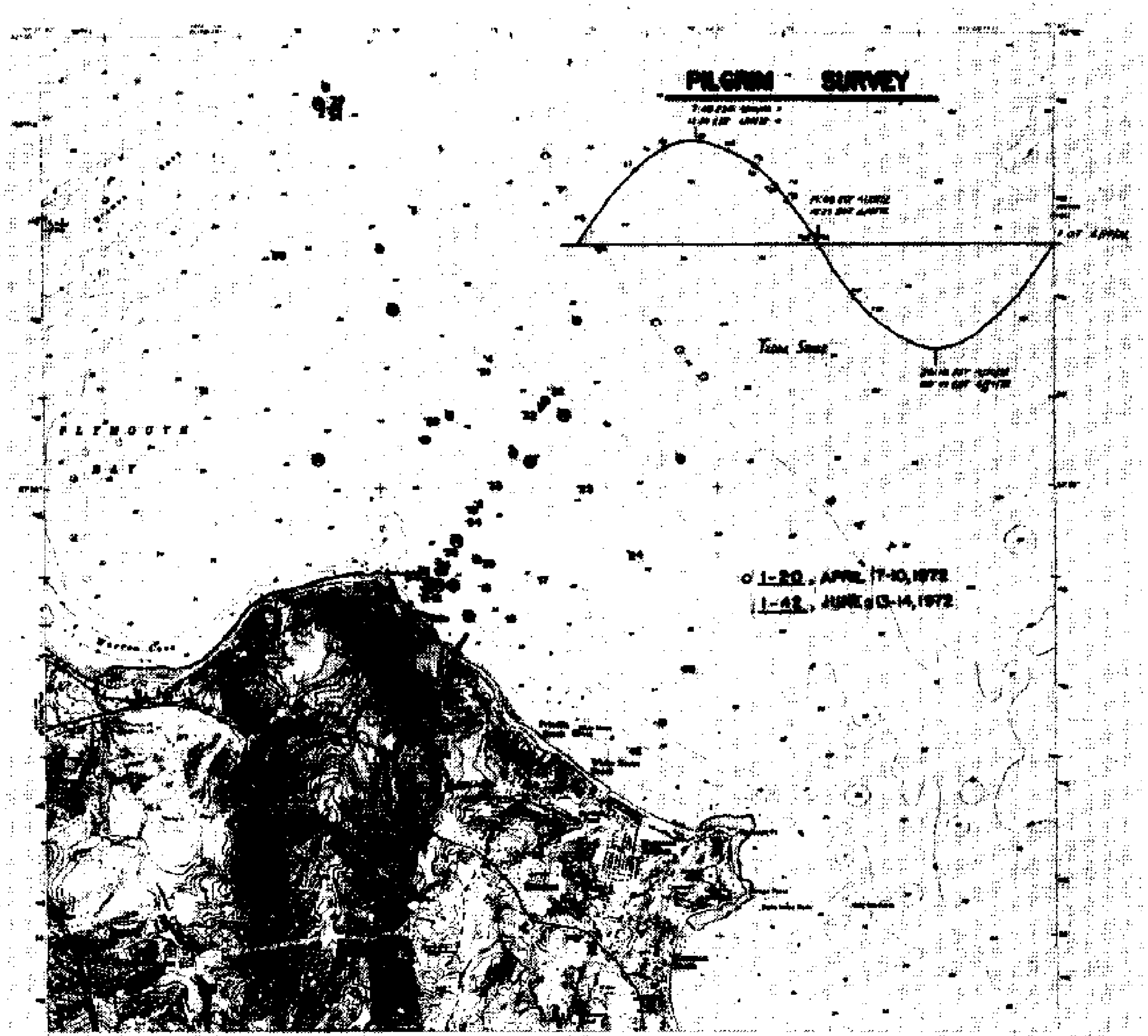

FIGURE 3.2 APRIL AND JUNE C.T.D. STATIONS

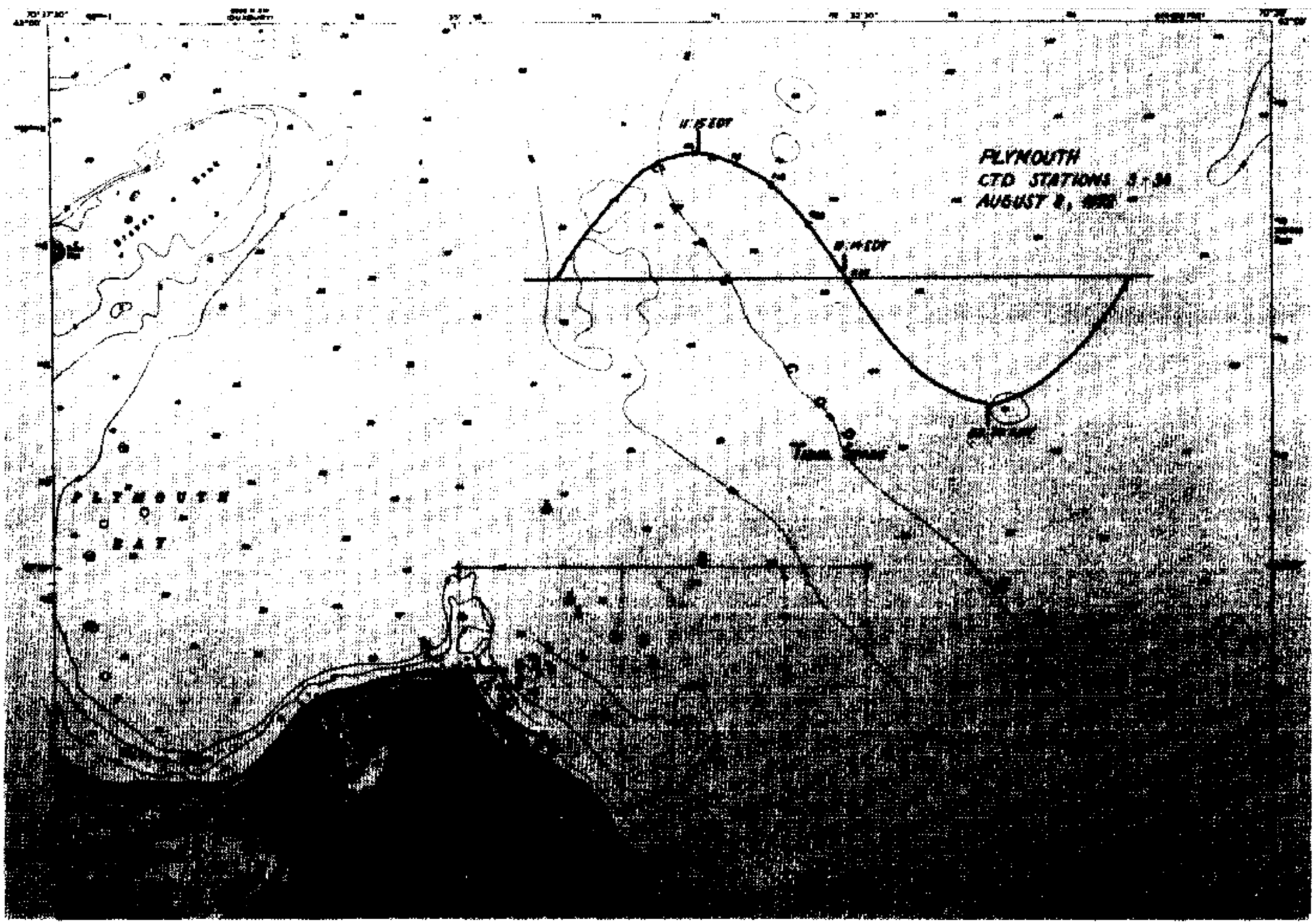

FIGURE 3.3 AUGUST 8 C.T.D. STATIONS

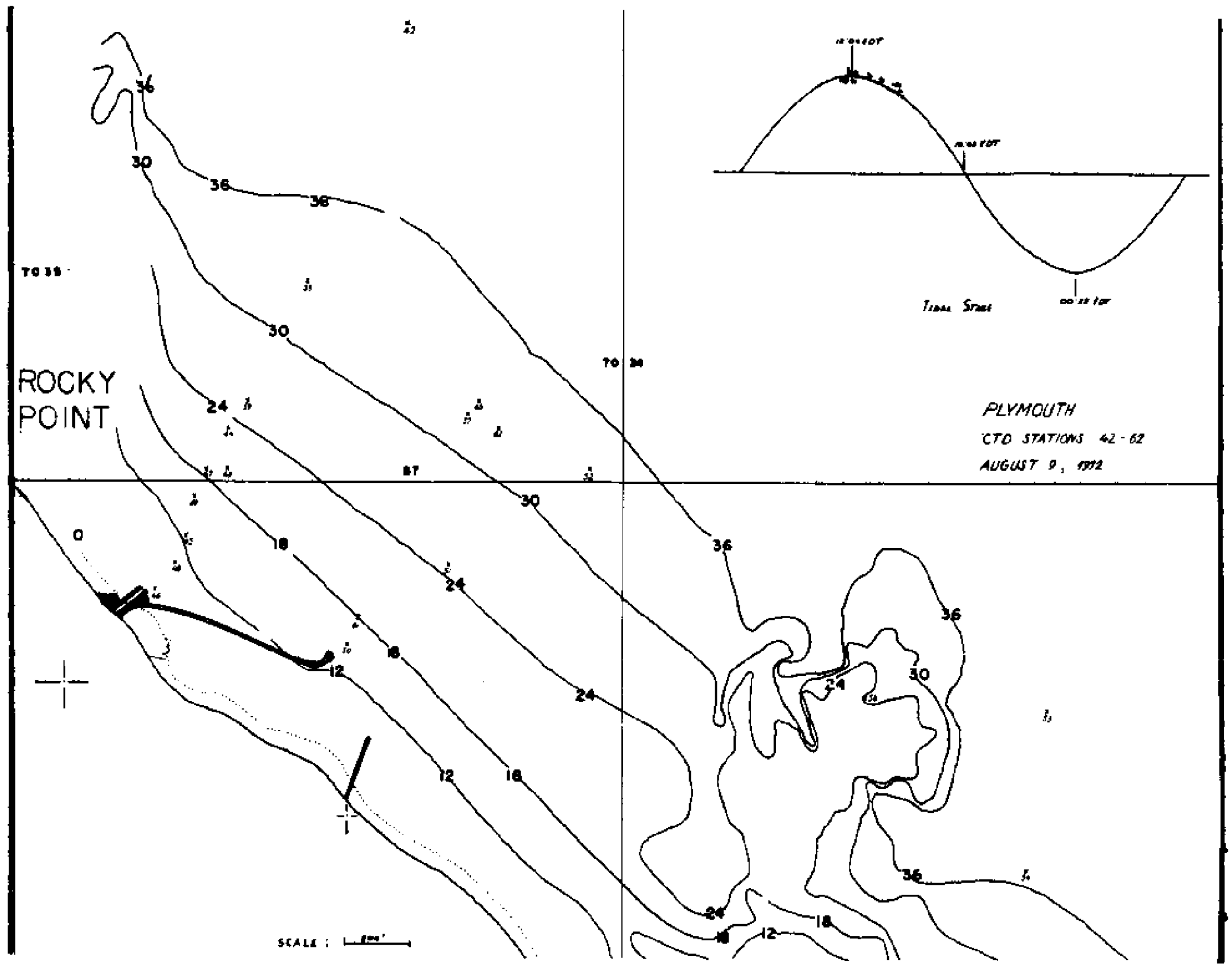

FIGURE 3.4 AUGUST 9 C.T.D. STATIONS

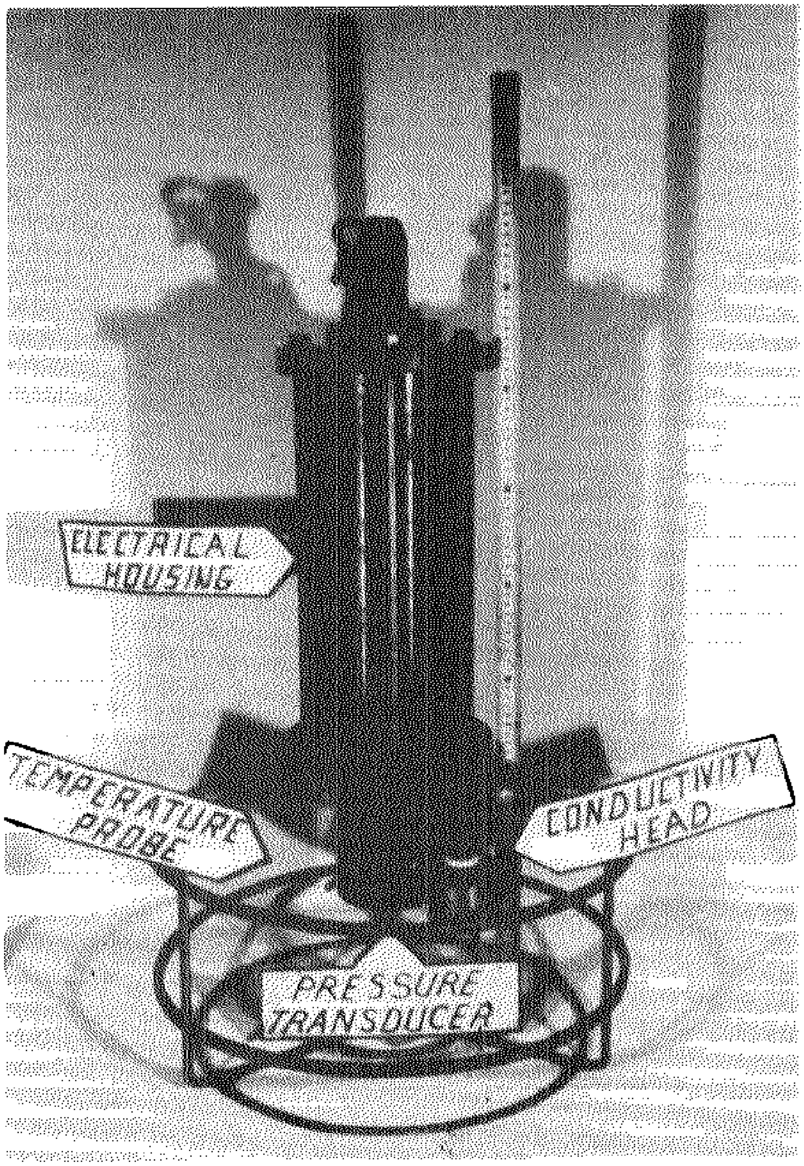

Figure 3.5 The Conductivity-Temperature-Depth Instrument

clock signal on a 8-track Precision Instrument tape recorder. This analog magnetic tape is then reduced to digital format which is converted to hard copy output on IBM 360/70. Graphic output is provided by a Houston Instrument x-y plotter. The accuracy of the sensors is 0.01°C for temperature, 0.5 feet for depth and 0.02 M Mho/cm for conductivity. The range of each sensor is 0 to 20°C for temperature, 0 to 370 feet of water for depth and 10 to 60 M Mho/cm for conductivity. The system is linear to 0.01 percent for all sensors and the temperature element has a time constant of 0.31 seconds. A listing of sample C.T.D. data is shown in Figure 3-6.

3.2.3 Current Drogues

The current drogues used during the survey were constructed of four x four foot 1/4" plywood sheets assembled in the form of a cross. The drogues were weighted to eliminate their buoyancy and suspended from 2' x 2' - 2" styrofoam surface floats. The depth of deployment varied as shown in Figures 3.7, 8 and 9.

Drogue studies were conducted during the June 13 and 14, 1972 survey and the August 8 and 9, 1972 survey period. Since power plant tests of the pumping system were conducted during the August 1972 survey period, current drogues were deployed in the mouth of the discharge channel to ascertain the effects of the non-heated discharge plume on the local current structure.

8/ 8/1972 CTD STATION NUMBER 1 DECIMATION = 1

DEPTH(METERS)	TEMPERATURE	SALINITY	SIGMA T	BRUNT VAISALA FREQ
0.256	11.746	32.911	25.036	-0.112E-01
0.389	11.743	32.908	25.034	-0.539E-01
0.365	11.738	32.916	25.042	-0.196E-01
0.546	11.738	32.907	25.034	-0.128E-01
0.600	11.742	32.906	25.034	-0.272E-01
0.824	11.745	32.885	25.016	-0.372E-01
0.950	11.749	32.862	24.998	0.559E-01
0.920	11.751	32.850	24.988	-0.394E-01
0.999	11.749	32.833	24.975	-0.540E-01
1.053	11.739	32.809	24.959	-0.393E-01
1.156	11.720	32.783	24.942	-0.158E-01
1.271	11.686	32.771	24.939	0.886E-02
1.428	11.645	32.763	24.941	-0.721E-02
1.561	11.605	32.753	24.940	-0.155E-01
1.725	11.564	32.738	24.936	0.124E-01
1.876	11.523	32.731	24.938	0.382E-01
1.991	11.480	32.744	24.956	0.210E-01
2.245	11.433	32.748	24.967	0.273E-01
2.378	11.392	32.752	24.978	0.482E-01
2.463	11.356	32.770	24.998	0.130E-01
2.566	11.325	32.765	25.000	0.881E-01
2.578	11.290	32.769	25.010	0.852E-02
2.657	11.255	32.762	25.010	0.310E-01
2.742	11.213	32.763	25.019	0.263E-01
2.863	11.166	32.764	25.028	-0.363E-01
2.754	11.120	32.772	25.043	-0.228E-01
2.893	11.064	32.750	25.035	-0.678E-01
2.863	10.994	32.753	25.050	-0.178E-01
2.997	10.918	32.730	25.045	-0.223E-01
3.124	10.819	32.699	25.039	0.402E-01
3.257	10.698	32.700	25.061	0.412E-01
3.403	10.572	32.706	25.087	0.315E-01
3.628	10.447	32.708	25.110	-0.163E+00
3.615	10.322	32.723	25.143	0.358E-01
3.749	10.200	32.719	25.161	0.312E-01
3.967	10.076	32.721	25.183	0.144E+00
3.986	9.961	32.747	25.223	0.720E-01
4.046	9.858	32.767	25.255	0.963E-01
4.095	9.763	32.807	25.302	0.853E-01
4.149	9.684	32.844	25.344	0.404E-01
4.247	9.626	32.853	25.366	0.623E-01
4.265	9.571	32.851	25.367	-0.486E-01
4.186	9.505	32.862	25.387	0.248E-01
4.307	9.428	32.856	25.395	-0.956E-01
4.277	9.340	32.875	25.424	0.793E-01
4.319	9.247	32.892	25.451	0.487E-01
4.398	9.150	32.897	25.471	0.394E-01
4.508	9.056	32.901	25.489	-0.879E-01
4.483	8.962	32.907	25.508	0.245E-01
4.666	8.874	32.904	25.520	-0.891E-01

FIGURE 3.6 SAMPLE C.T.D. DATA

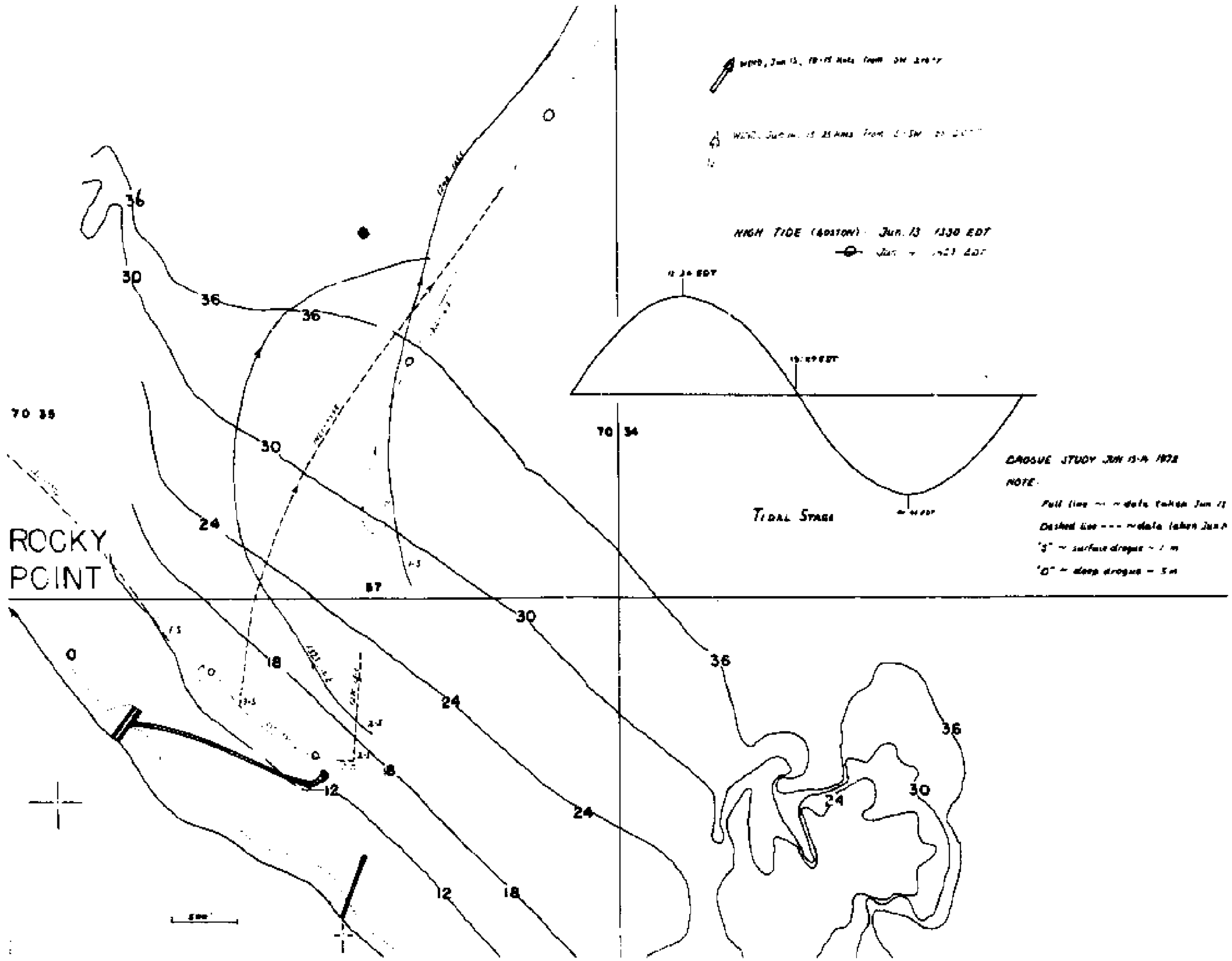

Figure 3.7 June Drogue Study

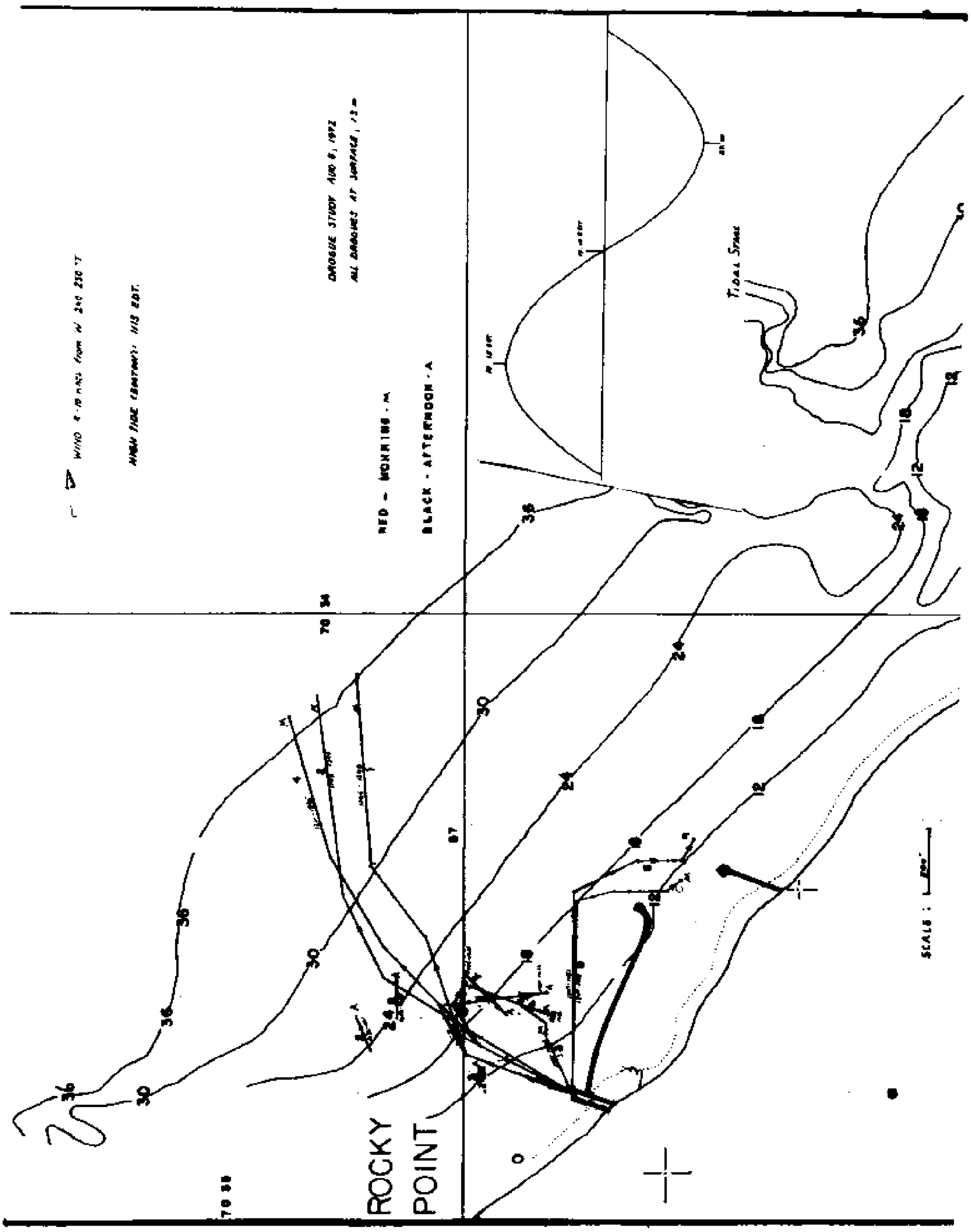

FIGURE 3.8 AUGUST 8 DROGUE STUDY

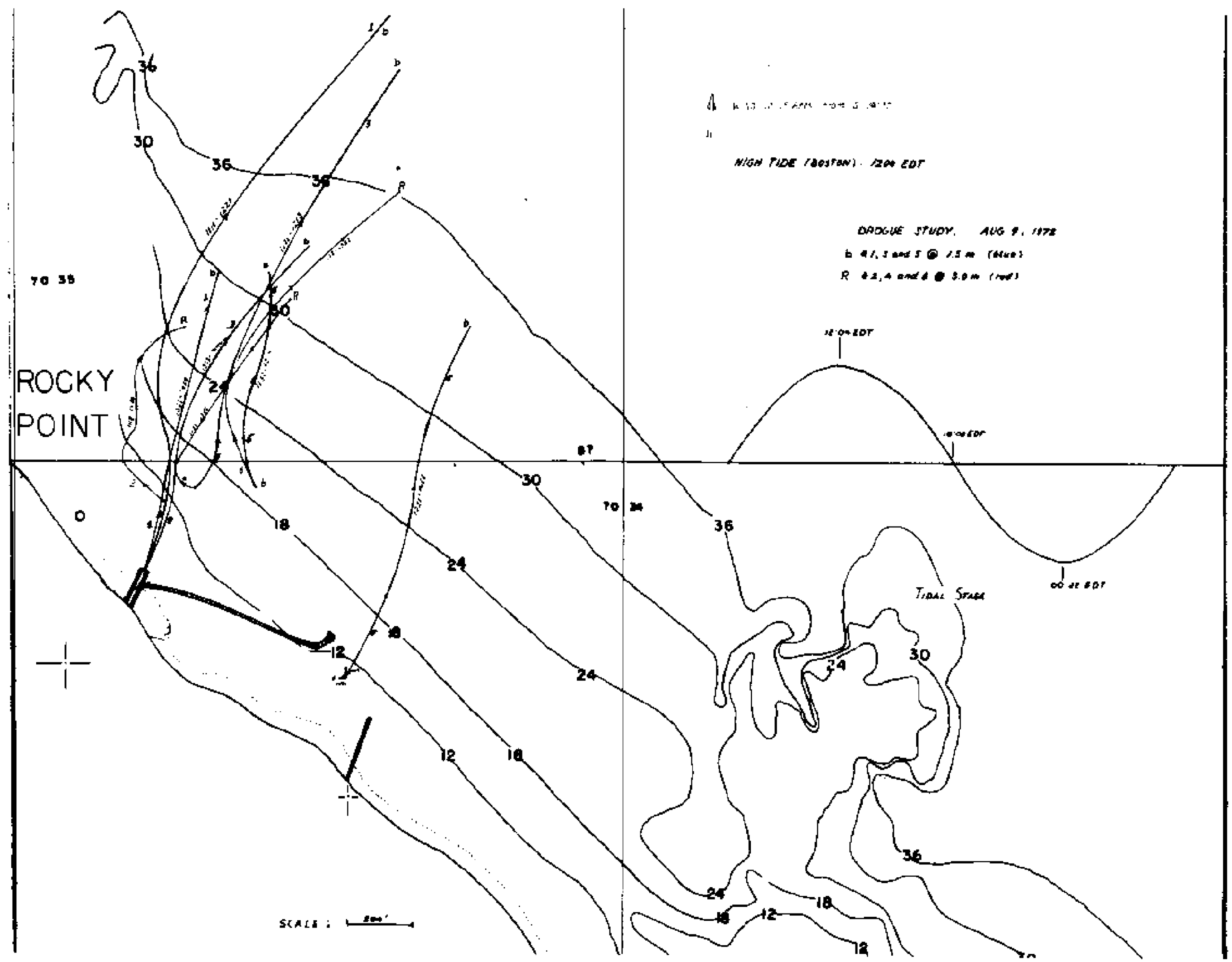

FIGURE 3.9 AUGUST 9 DROGUE STUDY

3.2.4 Positioning Controls and Station Location

Positioning control and location was provided by the use of a Mark IV Sextant. Control points were established from prominant features visible in the field and marked on the U.S.G.S. map of the Manomet Massachusetts Quadrangle. The location of two easily visible points were determined in this manner. A third point was established at the shore along the centerline of the south jetty shown in Figure 1-1. This third point was constructed of two 4 x 4 foot 3/8" plywood sections in the form of a cross. The M.I.T. marker signal, as this was called, was then painted flourescent orange. This marker stood 16 feet above the ground and approximately 40 feet above the water. These points are then used in a system of positioning known as "Three Point Fixes". Sextant sightings from both end points to the center point established the location of the desired station. The angles between each end point and the center were obtained and used to plot the location of the station. Reduction of the given position to latitude and longitude was accomplished by the use of a computer program written for this purpose. Use of position coordinates in latitude and longitude permitted the use of charts which did not contain the location of the original reference points.

3.3 Baseline Hydrographic Parameters

The hydrographic parameters can be summarized as follows: During the April 1972 survey, the water mass parameters were relatively constant. All stations sampled had a constant temperature profile of

$3.5^{\circ}C \pm 0.4^{\circ}C$. The salinity varied only slightly averaging 32.4 ppt. The plant log for these data shows that the condenser cooling water pumps were operating.

During the June 13 & 14, 1972 survey, the seasonal thermocline was at a depth of approximately 10 meters on June 13 and 7.5 meters on June 14. The thermocline exhibited a temperature difference of approximately $2^{\circ}C$ on both days. The salinity averaged 32.3 ppt showing a slight decrease since the April survey. The decrease in salinity is probably due to the longshore current carrying the less saline spring freshet waters from the numerous freshwater inflows north of the site. The average surface temperature was approximately $10.7^{\circ}C$ with a variation of $\pm 0.5^{\circ}C$. It was observed that the condenser cooling water pumps were operating on June 13. This pumping was found to have an effect in an area local to the discharge where the water mass appeared to be well mixed. The change in thermocline elevation seems to be related to tidal stage rather than wind conditions, since the wind directions and velocities were similar for both days. It appears that the thermocline rises on an ebbing tide. A three dimensional plot of temperature versus depth for selected stations is presented in Figures 3.10, 3.11 and 3.12.

During the August 1972 survey, most of the study was on the ebbing tide causing a condition of high salinity on the surface. The salinity averaged 33.5 ppt. The plant pumps were operating and the temperature of the discharged water was significantly lower than the surrounding ambient water temperature due to the pumping of cooler

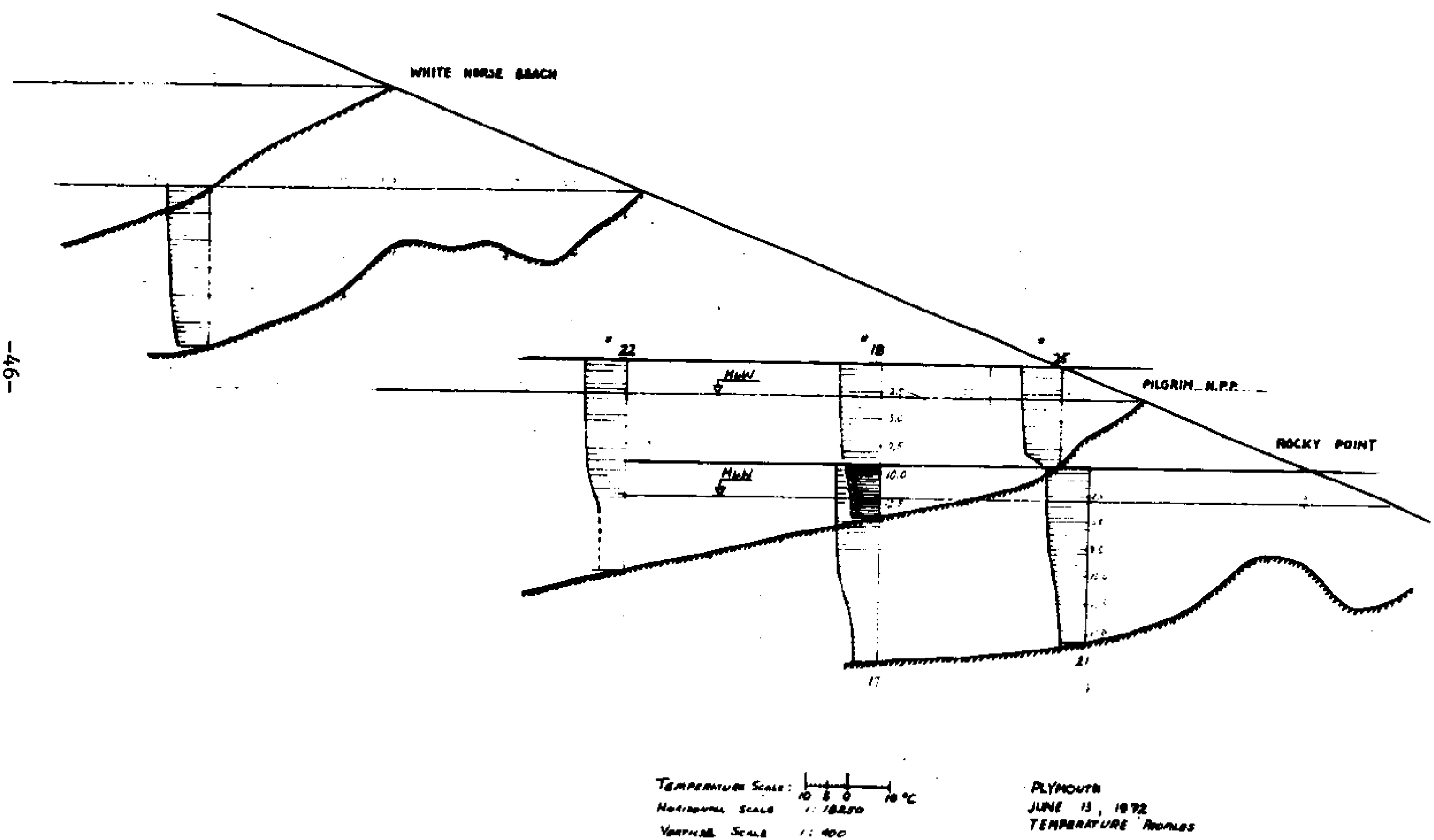

Figure 3.10 Selected 3-D Temperature Profiles, June 13

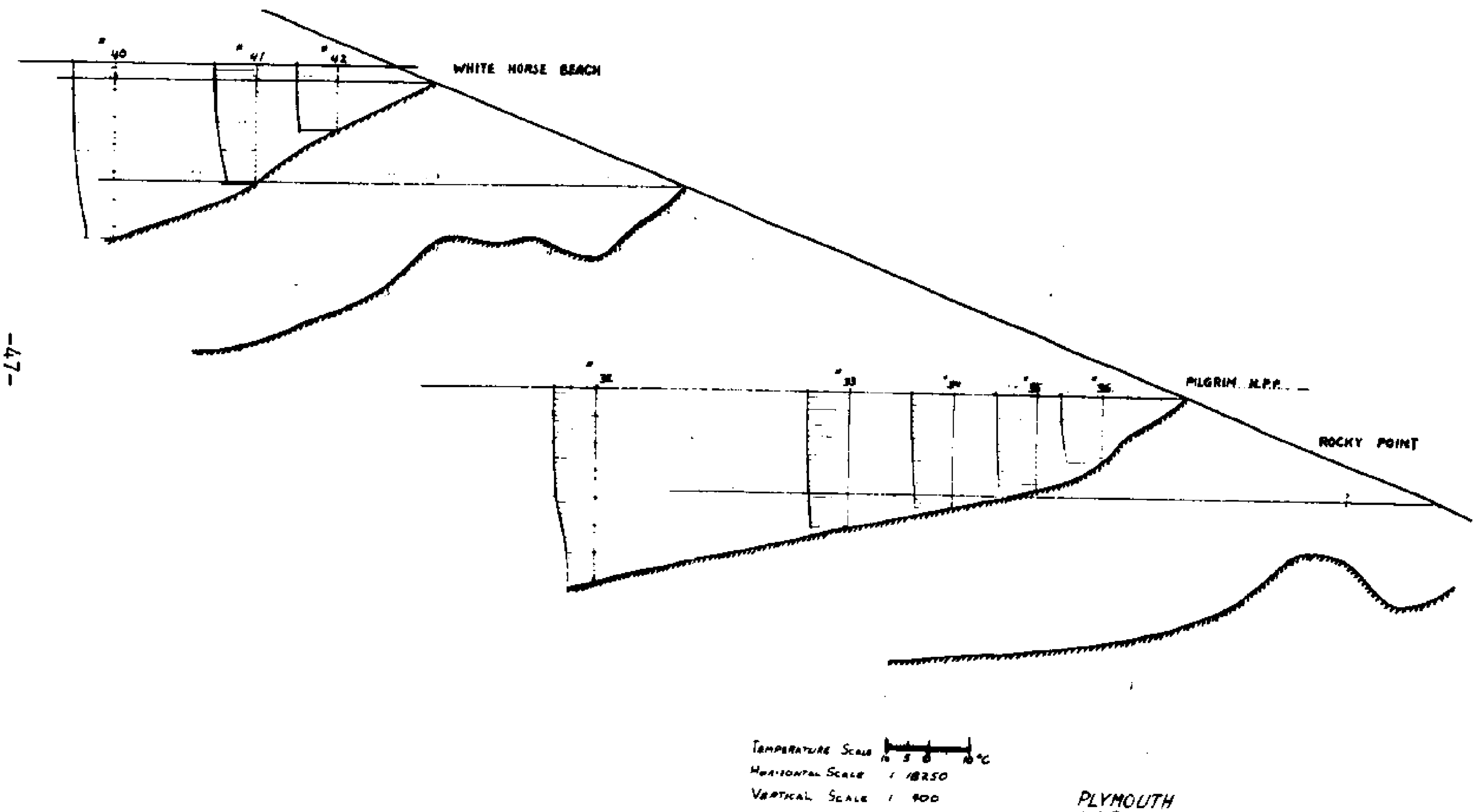

Figure 3.11 Selected 3-D Temperature Profiles, June 14

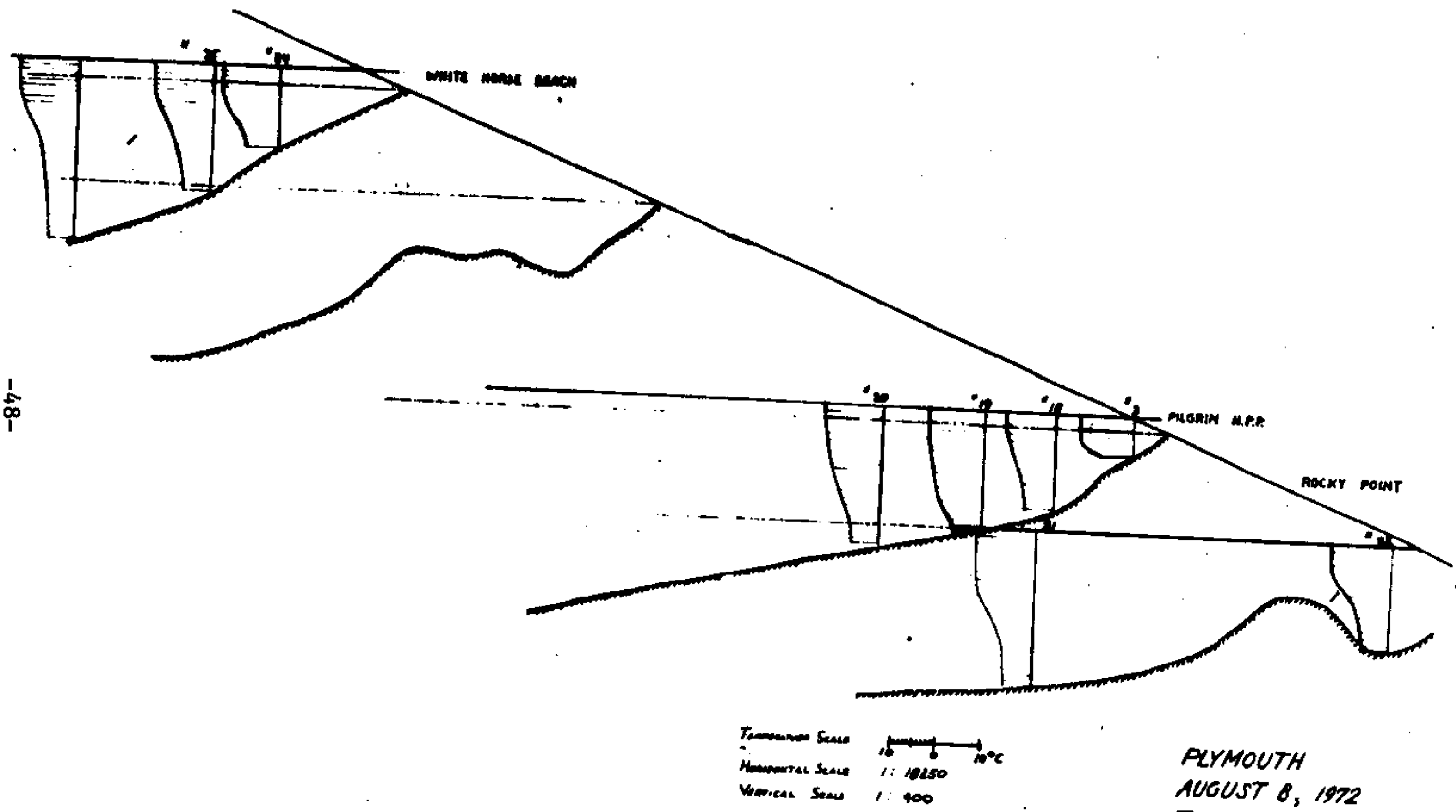

Figure 3.12 Selected 3-D Temperature Profiles, August 8

bottom water. The water temperature near the discharge plume was $10.1^{o}C$ at the surface and $6.7^{o}C$ on the bottom. The ambient surface water temperature was about $13.8^{o}C \pm 0.5^{o}C$. The temperature profiles taken at the intake showed the bottom two meters of depth in the intake channel carrying the cooler bottom water of $6.7^{o}C$. The thermocline was located at about 5 meters and the wind was from the west. Selected C.T.D. stations for August 8, 1972 are presented in Figure 3.12.

The surface salinity and temperature for the ambient water mass on August 9, 1972 was 32.6 ppt ± 0.3 ppt and $13.8 \pm 0.4^{o}C$, respectively. The bottom water temperature at the intake was about $11.5^{o}C$, and the temperature below the thermocline was $10^{o}C$; the depth of the thermocline was 5 meters. The wind, however, was from the south. The tidal stage during most of the survey on August 9, 1972 was on the ebbing tide.[5]

3.4 Baseline Data Summary

Three hydrographical surveys were conducted offshore of the Pilgrim Nuclear Power Station including two current field studies covering a period of eight months.

A definite 2-layer structure is found to develop in late spring with a thermocline depth varying between 5-10 m, apparently moving up and down with an ebbing and flooding tide, respectively. Little variation was found in hydrographic profiles (temperature and salinity versus depth) going along the coastline from north of

Rocky Point to White Horse Beach. The position of the thermocline did not change in the direction perpendicular to the coastline.

Surface currents were almost entirely governed by wind. The subsurface currents showed a significant dependence on tide, with a general tidal current direction going northwest on flooding tide and east to southeast on ebbing tide; however, some dependence on wind was evident as distance from the shore increased.

CHAPTER IV

PILGRIM NUCLEAR POWER STATION POST OPERATIONAL DATA STUDIES

4.1 Purpose of the On Line Data Study

The purpose of the on line data study is two-fold. The data collected since the power station has been in operation provide a basis by which the effectiveness of the discharge design can be compared with early thermal predictions made at the time of power plant licensing. The field data also provide a method by which the analytical model[2,3] can be tested against actual conditions. The use of published field data for the purpose of model correlation seldom includes enough information on ambient conditions.

The correlation of the analytical model with the field conditions existing as a result of the discharge design built at Plymouth for unit #1 should allow the prediction of the thermal effect of future additions.

4.2 On Line Procedures and Equipment

4.2.1 Measurement Procedures

The on-line area of study is smaller than that for the baseline phase of the thermal study. Reduction in the study area was necessary in order to allow repeatibility of the on-line transects in as limited a time as possible. The on-line data collection area is limited by the speed at which data can be collected. The design goal in establishing the on-line transects was to include the thermal plume within the study area regardless of the deflection of the plume. The horizonal profile data collected on this project necessitated the installation of fixed points in the field by which the operators of each of the two data collecting boats would be able to maintain the proper course at all times. The system used had to be simple to operate, reliable, easy to maintain and inexpensive to replace. The system employed was a simple set of lobster floats moored at the bottom with seventy-five pound mushroom anchors. Two buoy patterns were employed since the first pattern was destroyed in early March 1973 by an extremely violent "northeaster". Initially six transects and four auxiliary transects were designed. Each transect was marked by three buoys: a buoy at each end and a centerline buoy. The marker buoys were constructed such that variable water depth did not affect the position of each buoy. The transects chosen were laid out parallel to shore in the shape of a truncated "V" with the apex of the V towards the shore as shown in Figure 4.1. Selection of the transect widths was obtained from the Stolzenbach-Harleman analytical model.[2] Positioning of the marker buoys was obtained using sextants as described in Chapter 3. While this marker buoy pattern existed, C.T.D. temperature profile stations were taken at each buoy where the depth of water was not a factor for safe operation. The marker buoy pattern installed after the loss of the original "V" pattern system reduced the number of marker buoys. The replacement buoys described a zig-zag pattern as shown in Figure 4.2. Greater mobility and versatility was incorporated in the new pattern. The boat operator was able to follow a course in any direction without the confusion of buoys which were present in the

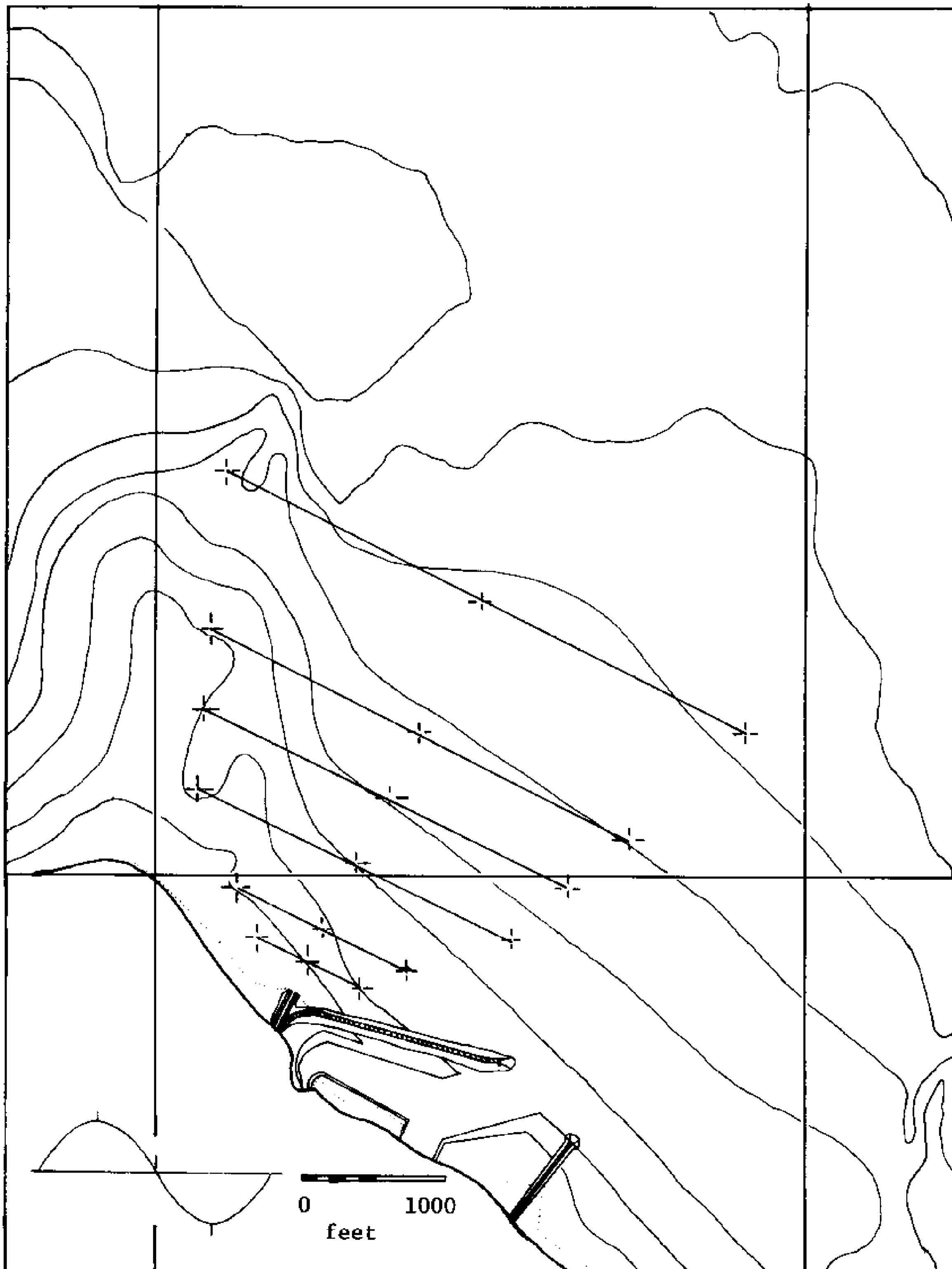

Figure 4.1 Initial Marker Buoy Pattern

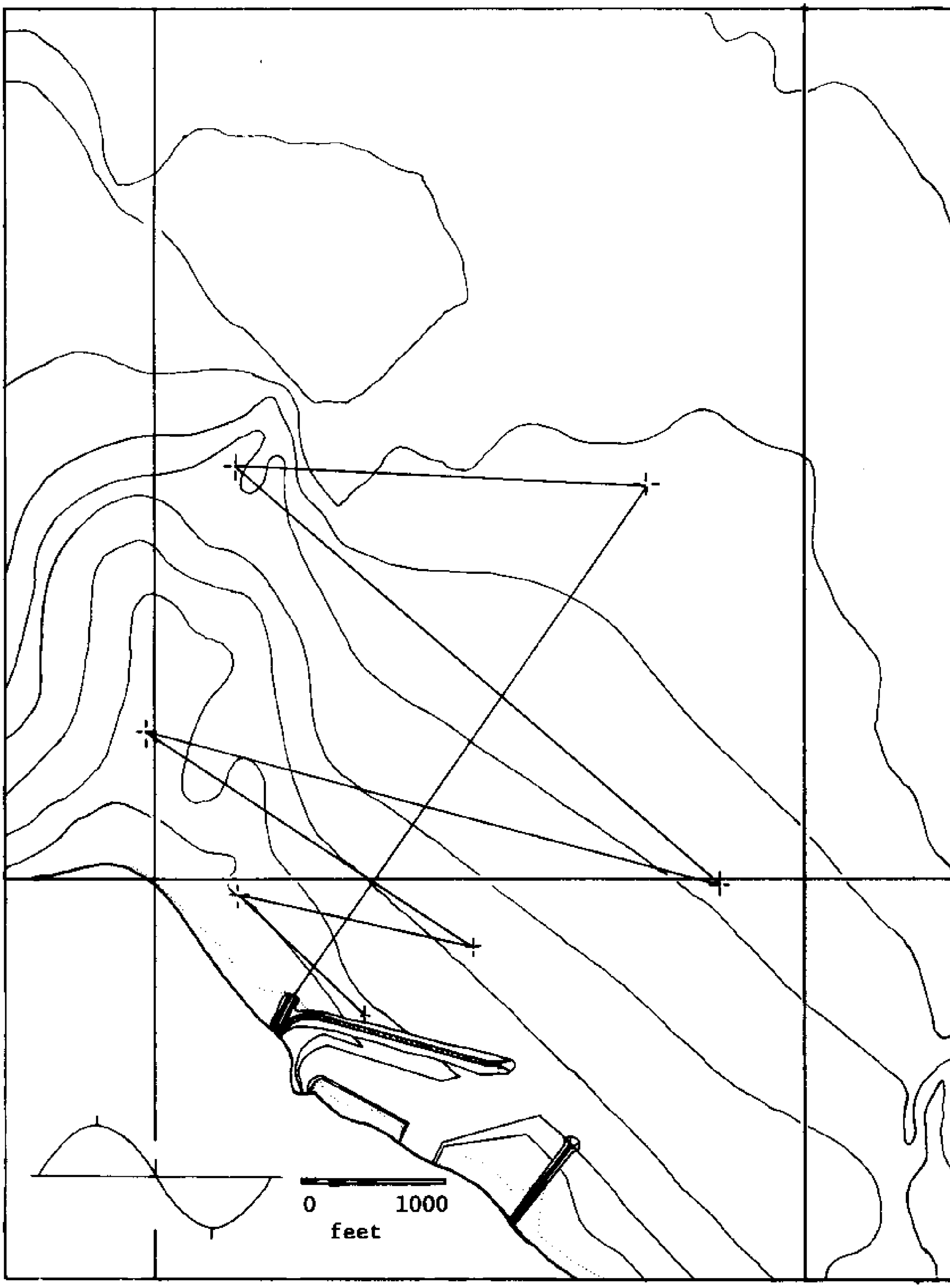

Figure 4.2 Replacement Marker Buoy Pattern

original system. Transect spacing in the original system also interfered with biological trawling studies conducted at the same time by the Massachusetts Division of Marine Fisheries at the power plant. Lobster "high flyers" were attached to each permanent position marker buoy in the new system during a field survey. Figure 4.3 shows the mooring system and the lobster "high flyer". The high flyer is constructed of a cylindrical surface float with a twenty-two foot vertical flagstaff. The addition of the "high flyer" at the position marker buoy was found to be advantageous since the buoys as originally deployed were visible for large distances only when the sun was behind the boat operator.

Horizontal profile data were collected from a sixteen foot Boston Whaler by towing two temperature thermistors at depths of 0.5 and 4.0 feet below the water surface along courses described by the marker buoy patterns. In the period between the loss of the original marker buoys and the replacement, horizontal transects were accomplished by taking the position of the beginning and end point of a transect. C.T.D. vertical temperature profiles were taken at each buoy of the original system as previously described above. After the establishment of the second marker system this could not be followed since centerline buoys no longer existed. Locations of C.T.D. stations were then determined by sextant.

The towed thermistor instrument is called the Small Boat Bathythermograph (S.B.B.T.) and is described below. Each thermistor was fabricated as a "fish" by adding tail fins. Both thermistors were

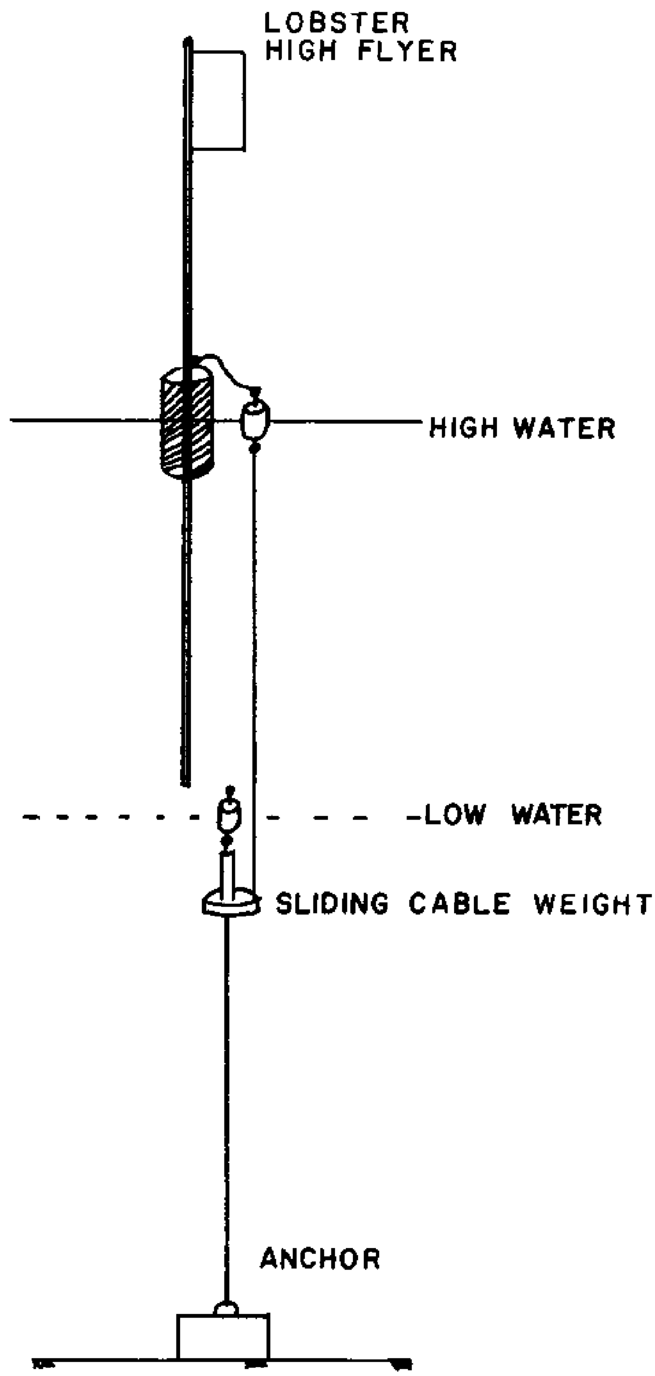

FIG. 4.3 MOORING SYSTEM & HIGH FLYER

suspended on a common carrier cable attached to a winch. The positioning of each thermistor was established in relation to the cable angle during towing operations. In operation the "fish" were extremely stable, tracking exactly parallel to the boat with no vertical or horizontal deviations. The actual water depths of the "fish" were 0.5 feet and 4 feet. During the initial survey period, equipment battery life was overestimated resulting in loss of data collected at the four foot level. At low tide of the April 1973 field trip the 4 foot level thermistor struck a rock which also resulted in loss of data.

Cross checks of the C.T.D. data and the Small Boat B.T. data were made periodically during each survey thus maintaining reliability of data from each source.

C.T.D. casts taken in the plume area proved to be of little value in determining the vertical temperature structure of the heated buoyant jet. Since the plume centerline position was not known until the surface isotherms were plotted, the C.T.D. stations taken in the field did not portray a representative position of the jet. Due to a sufficient water depth requirement for safe operation of the 63' foot survey boat used to take C.T.D. measurements, the most meaningful location for vertical profiles close to the discharge could not be surveyed. Since the C.T.D. must be lowered far enough into the water surface to keep the sensors below the water surface as the boat rolls, approximately three feet of surface water depth is not sampled during a cast. The surface three feet of water is the most significant range of water depth since an important percentage of the buoyant jet is located within this band in the far field. The C.T.D. has been used most productively in sampling the variation of ambient water conditions in the far field where the surface water layer is not important. Ambient water conditions for the three survey periods are presented in Figures 4.4, 4.5, and 4.6. For the March survey where slight ambient stratification exists and the April survey where more substantial stratification exists the depth averaged ambient water temperatures, $\overline{T}_{ambient}$, are used for determination of the model input parameters and data analysis. However, the isotherms are plotted using the ambient condition corresponding to the sampling depth of the plot.

4.2.2 Small Boat Bathythermograph

The small boat bathythermograph (S.B.B.T.) is an instrument developed at the Ralph M. Parsons Laboratory for near shore coastal research. The S.B.B.T. as originally developed gives a vertical profile of water temperature versus water depth. This equipment has the capability of computer compatibility. The temperature sensor is a Fenwal "15K" thermistor. The depth signal is generated by a potentiometer attached to the main cable pulley which is calibrated using the pulley rotation for S.B.B.T. depth. Both temperature and depth signals are fed to a water tight container housing three voltage controlled oscillators. Two oscillators are for temperature and depth; the third oscillator generates a clock frequency which is used as control in the data break out system. Each oscillator generates an FM signal which is

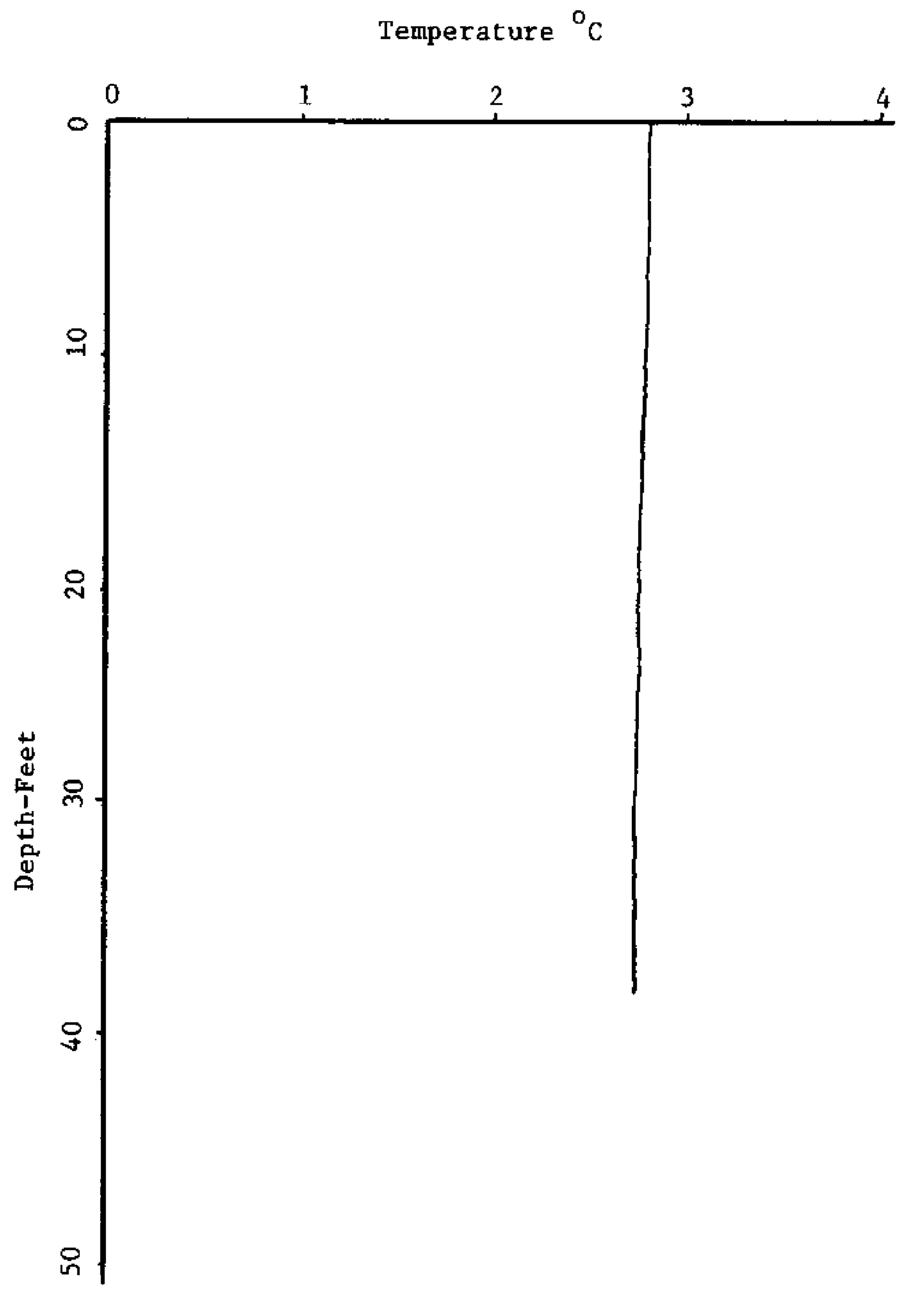

Location: Station A on Plate 4-1

Figure 4.4 1-26-73 Ambient Conditions

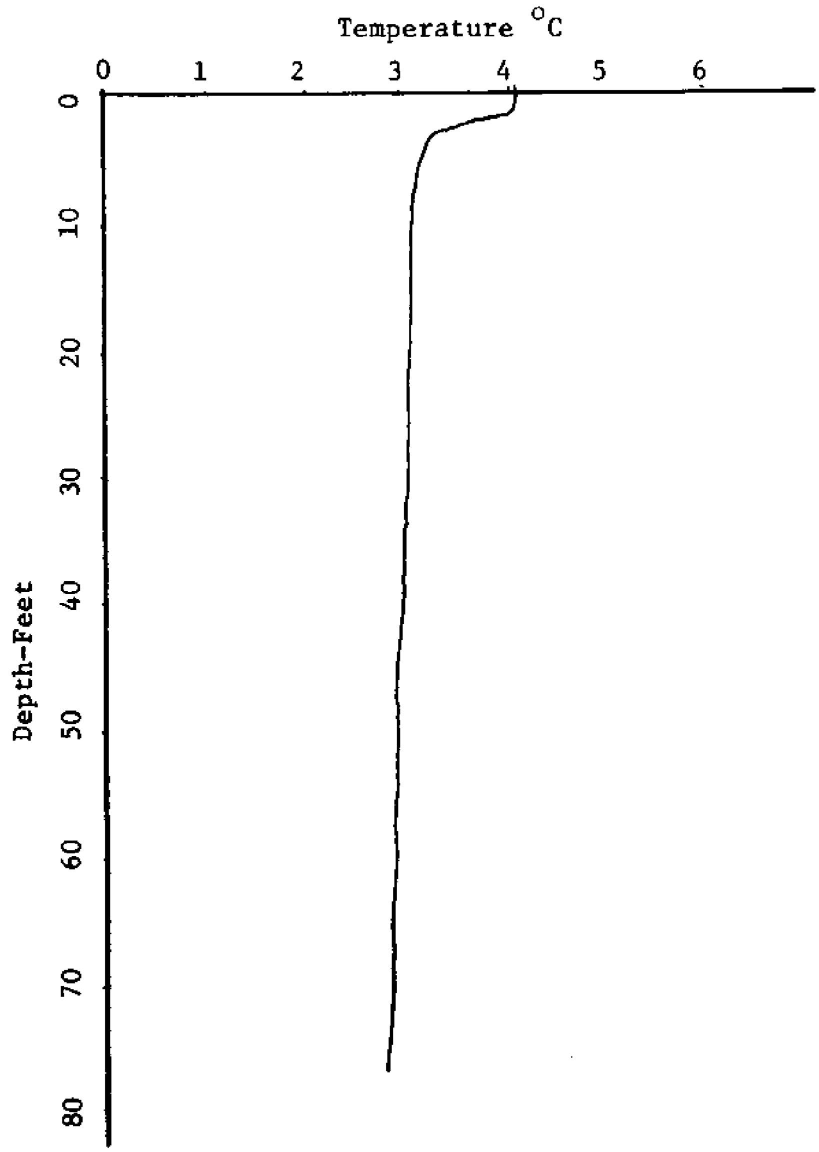

Location: Station B on Plate 4-8

Figure 4.5 3-25-73 Ambient Conditions

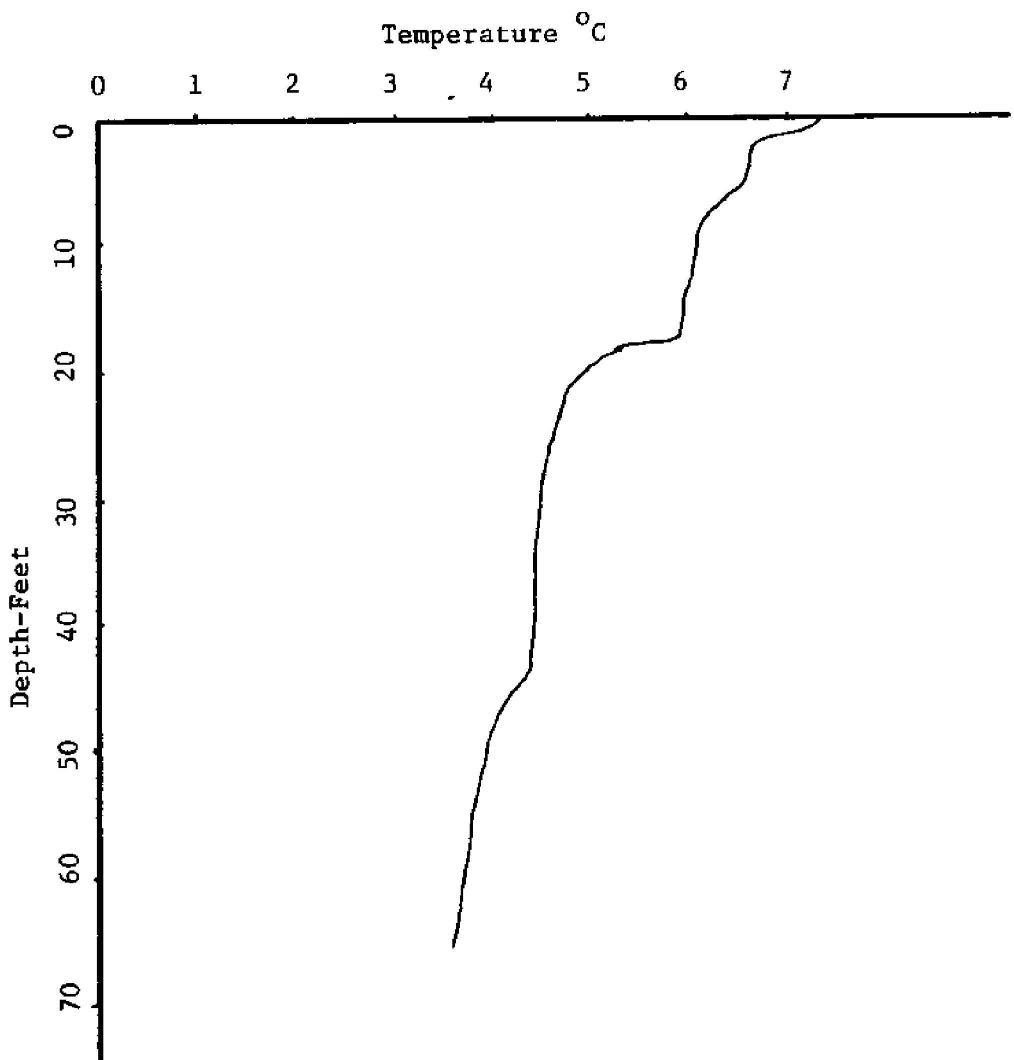

Location: Station B on Plate 4.16

Figure 4.6 4-19-73 Ambient Conditions

recorded on a portable cassette tape recorder contained in the water tight container. The FM signal is later demodulated, digitized, and recorded on IBM compatible magnetic tape. This system was modified for horizontal profiles by the addition of stabilizing fins to the thermistors and direct read out of temperature information on a dual channel Rustrak Strip Chart Recorder, Model #388. This direct read out recorder was added to give the operator in the field the ability to determine the edge of the thermal plume should the plume extend beyond the limits of the established transects. The cassette tape recording system was found to be limited in this long record type of employment due to the limitation of only fifteen minute recording time per side of cassette tape. Most records were longer than fifteen minutes using this horizontal profile technique. Accuracy using the tape cassette system was not sufficient for this work; therefore, direct read out of the strip chart recorder maintained the original design accuracy. The unmodified S.B.B.T. is shown in Figure 4.7.

The S.B.B.T. has a temperature range of 0 to 30°C, with an accuracy of 0.1°C. The response time (63% of reading) is 0.4 second, 0.2°C linearity, and a resolution of 0.05°C. The strip chart recorder has been modified to maintain an accuracy of 0.1°C. A variable range switch yielding ranges of 0 - 6, 6 - 12, 12 - 18, 18 - 24, 24 - 30, and 0 - 30°C was used to maintain the original design accuracy. Movements of the strip chart recorder are galvanometers equipped with center pivoted, balanced styli. This type of stylus eliminates boat movement contributions to the data. The equipment capabilities and accuracies

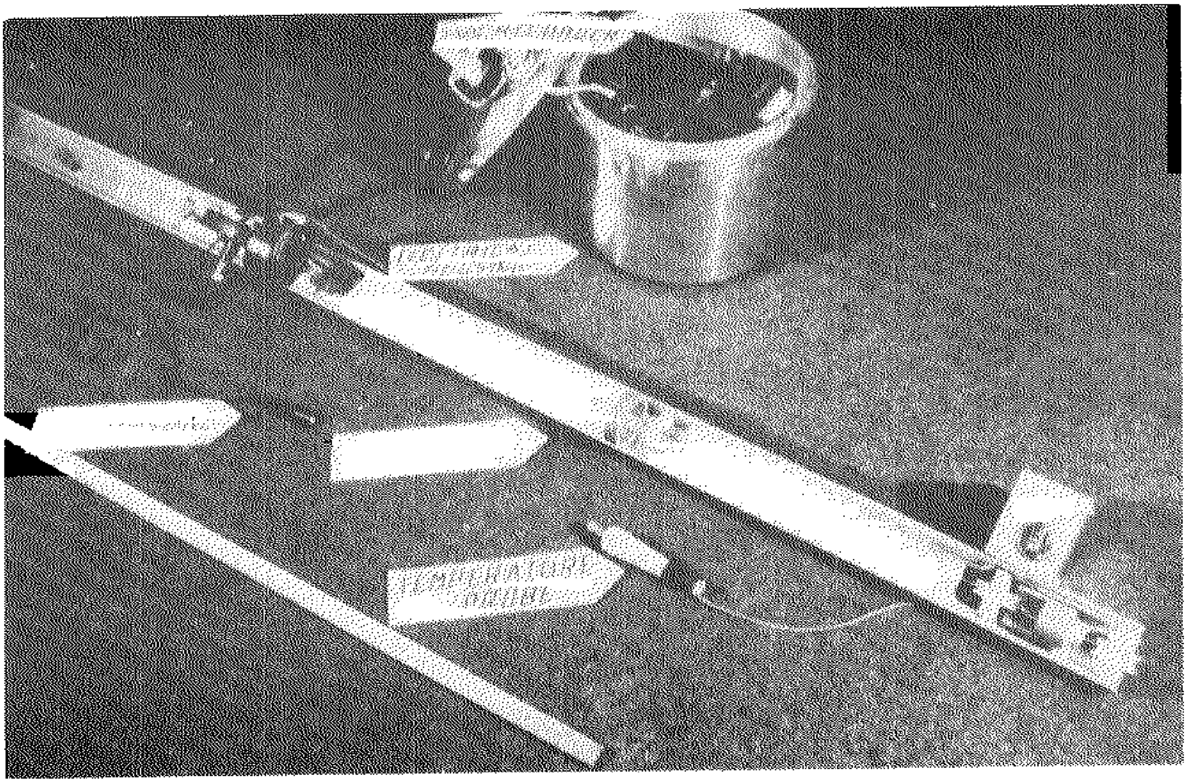

Figure 4.7 The Small Boat Bathy-Thermograph

used in this study compare very favorably with those used on a similar survey conducted by the Argonne National Laboratory for the Lake Michigan Studies.[6]

4.3 On-line Temperature Data

4.3.1 Data Reduction and Processing

Data reduction in any field project is a major concern. The reduction procedure was the major consideration in the development of the field equipment used on this project. However, since the Small Boat Bathythermograph was not capable of the extended records needed for the horizontal transects employed and the accuracy of the computer compatible system was not sufficient for the thermal studies contemplated, hand reduction from the strip chart records was necessary.

Horizontal boat speed and strip chart advance are assumed constant. The distance between fixed points established in the field is known and applied to the record length for a given transect. Thus each division on the strip chart represents a specified distance in the field. The absolute temperatures are plotted on a scale drawing of the offshore areas at Pilgrim Nuclear Power Station. Isotherms, in increments of $1^{o}C$ temperature rise above ambient, are interpolated. Ambient temperature is determined from vertical C.T.D. profiles taken at various places outside the thermal plume. The four foot isotherms plotted for the April 1973 field survey are referenced to the same surface ambient temperature value as the surface isotherms even though the ambient condition for this day was stratified. The thermocline was located at a depth of 7 feet exhibiting a $2^{o}C$ difference.

Vertical profiles generated by the C.T.D. are reduced to plots of surface temperature percentage versus depth. Vertical profiles taken at the "centerline" marker buoys (the 1st marker system) do not necessarily represent vertical profiles on the thermal plume center line since the thermal plume fluctuated in location with respect to an undeflected centerline. The areas of all the closed surface isotherms and those which can be extrapolated are computed by planimeter.

4.3.2 Summary of Horizontal Field Data

A summary of all the horizontal profile data collected follows: Data presented represents field studies conducted on January 26, 1973; March 25, 1973 and April 19, 1973.

Figure 4.8 is an illustration of the loci of the limit of distances reached by the $4^{o}C$ isotherm as determined from the three study periods. During the study period the $4^{o}C$ isotherm did not exceed this limit.

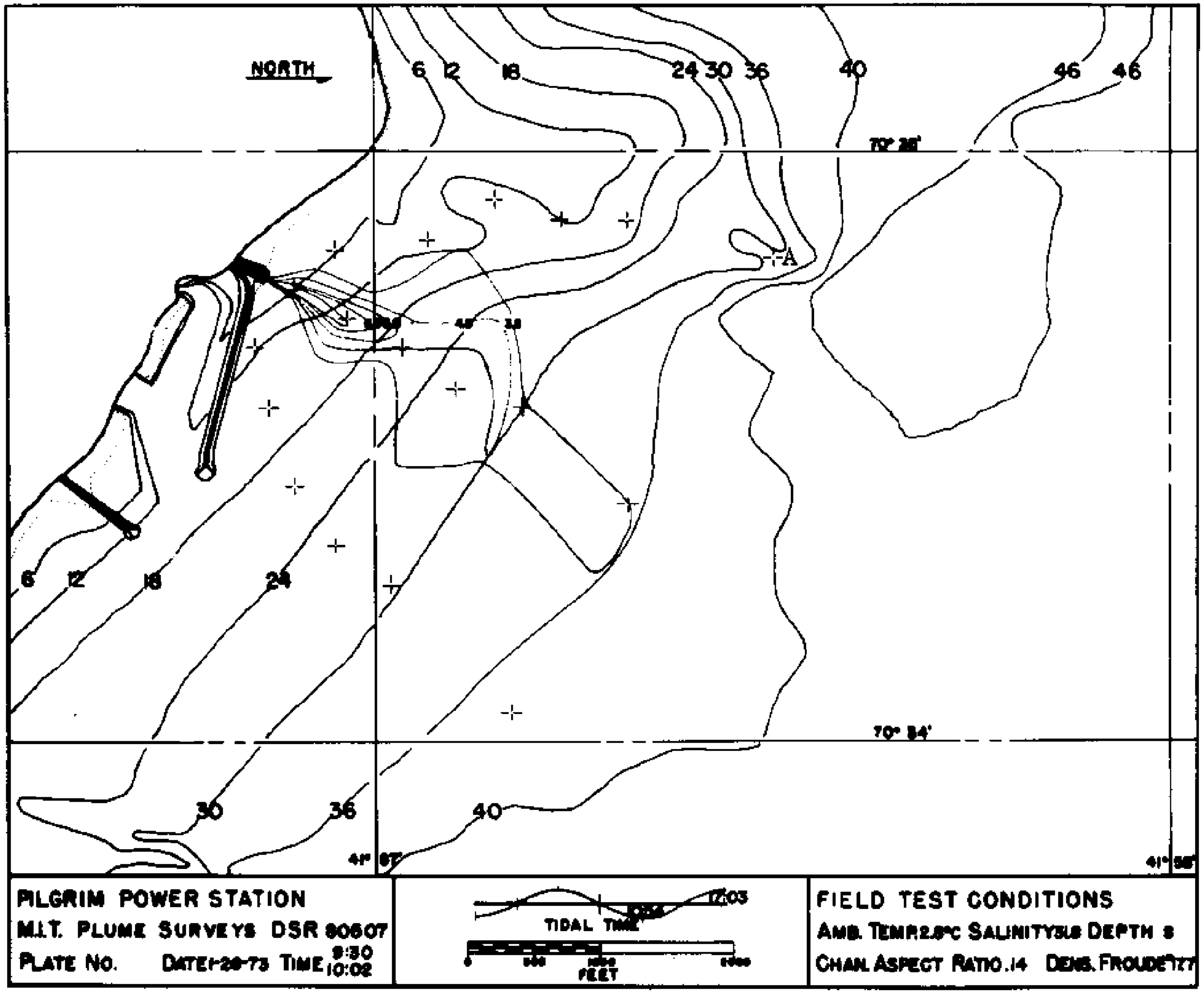

Plate 4.1 January Isotherms, $\mathbb{F}_o$ = 17.7, Surface

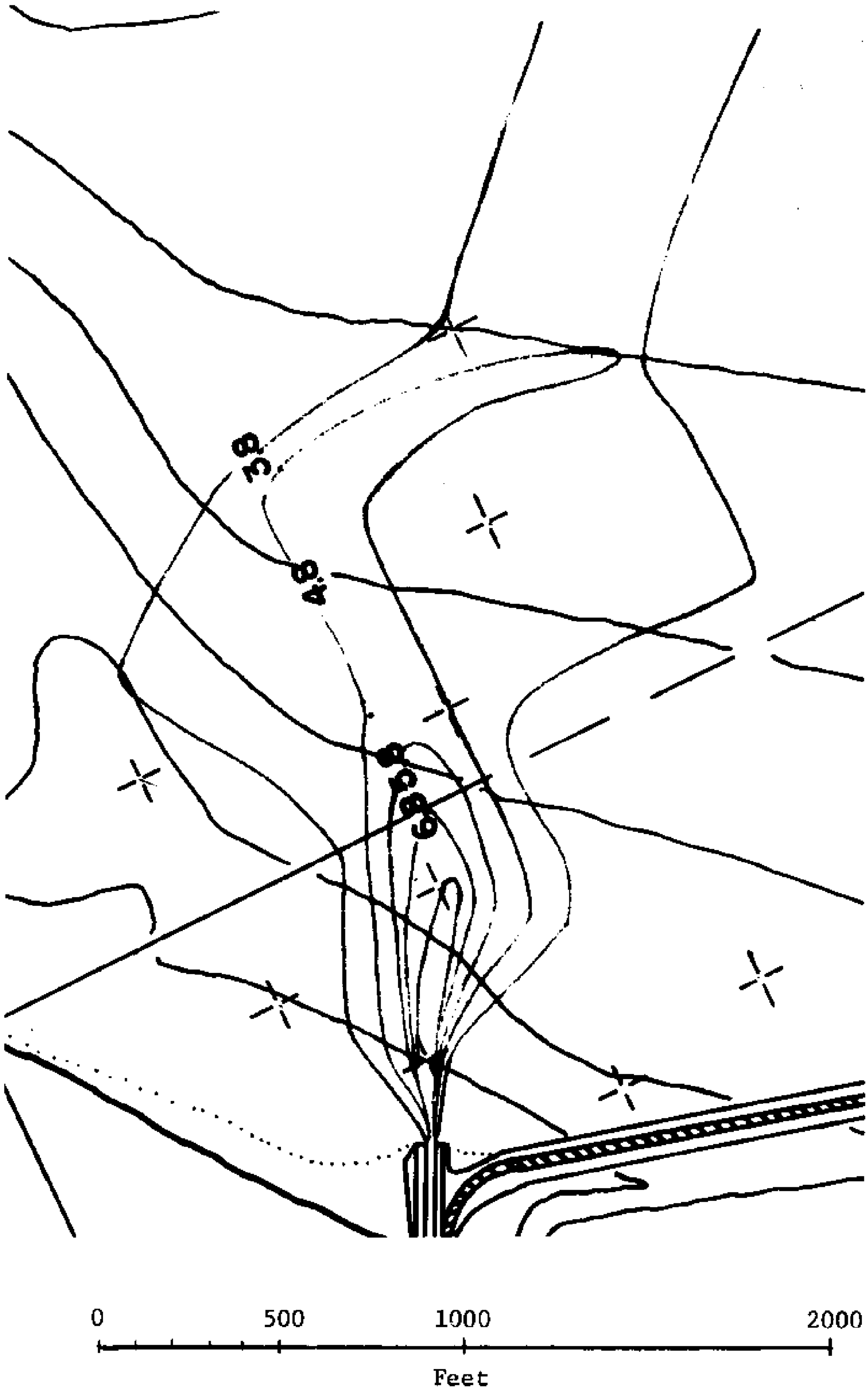

Plate 4.2 January Isotherms, $IF_o = 17.7$

Local to Discharge, Surface

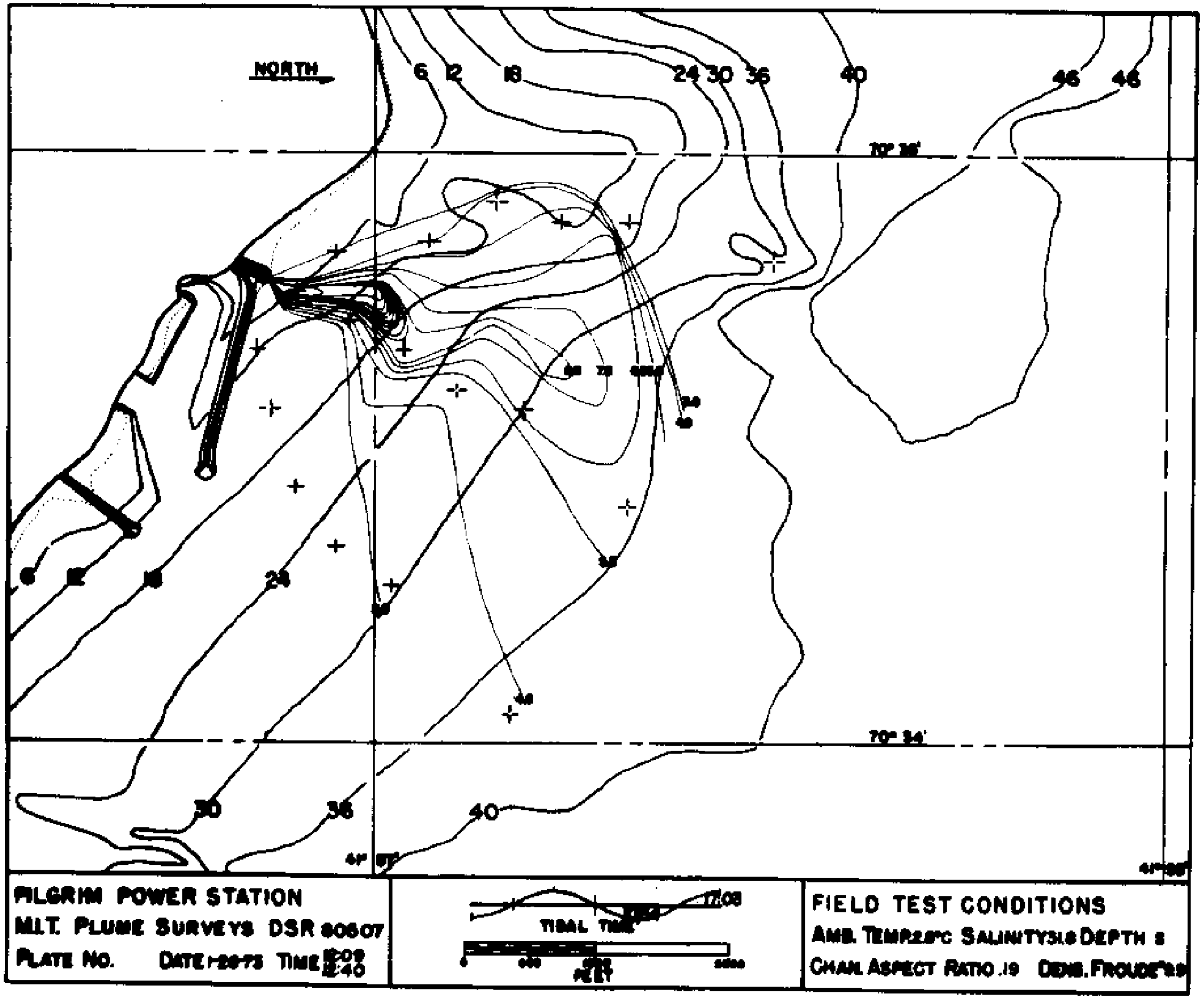

Plate 4.3 January Isotherms, $IF_o = 9.9$, Surface

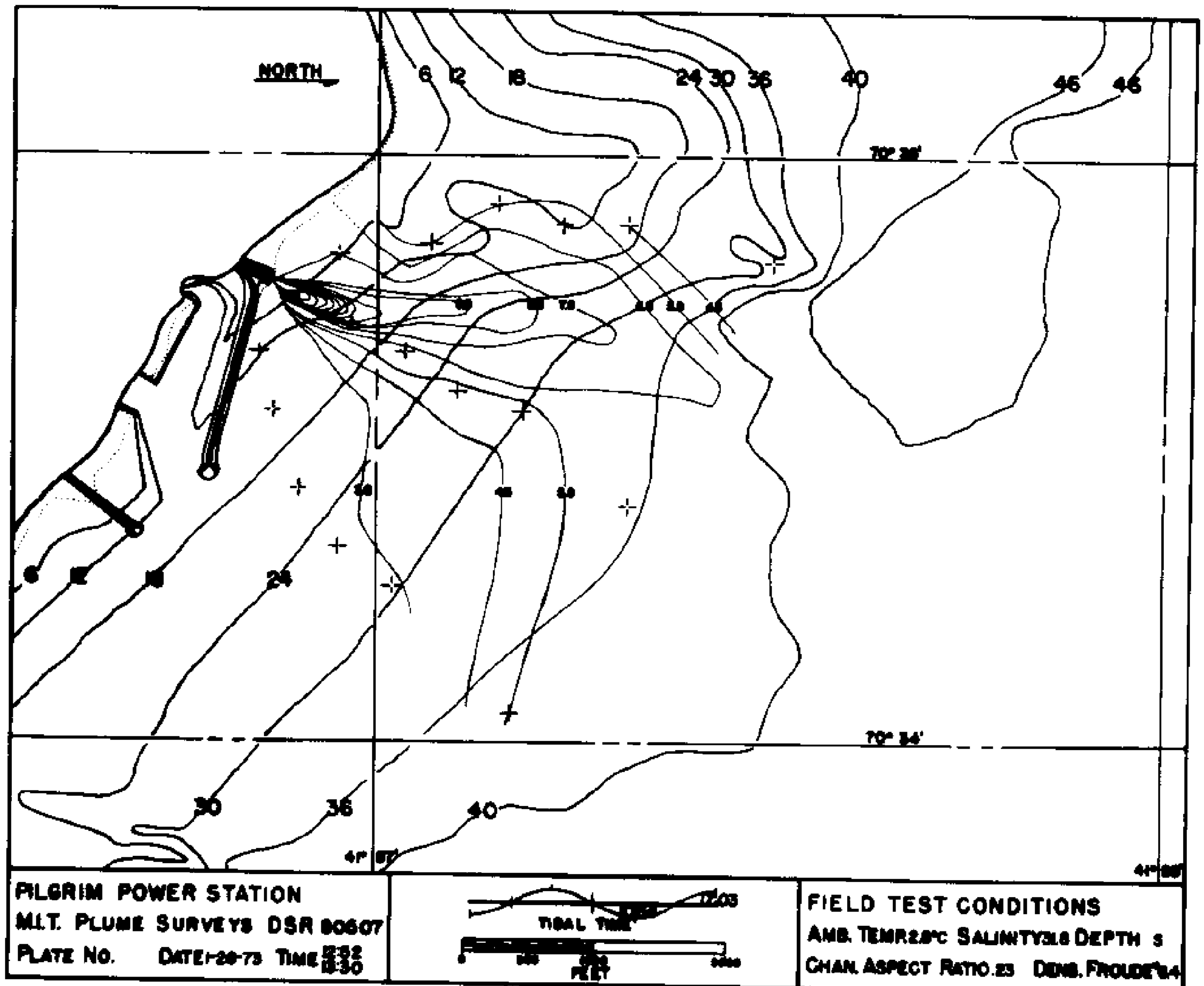

Plate 4.4 January Isotherms, $\mathbf{F}_o = 6.4$, Surface

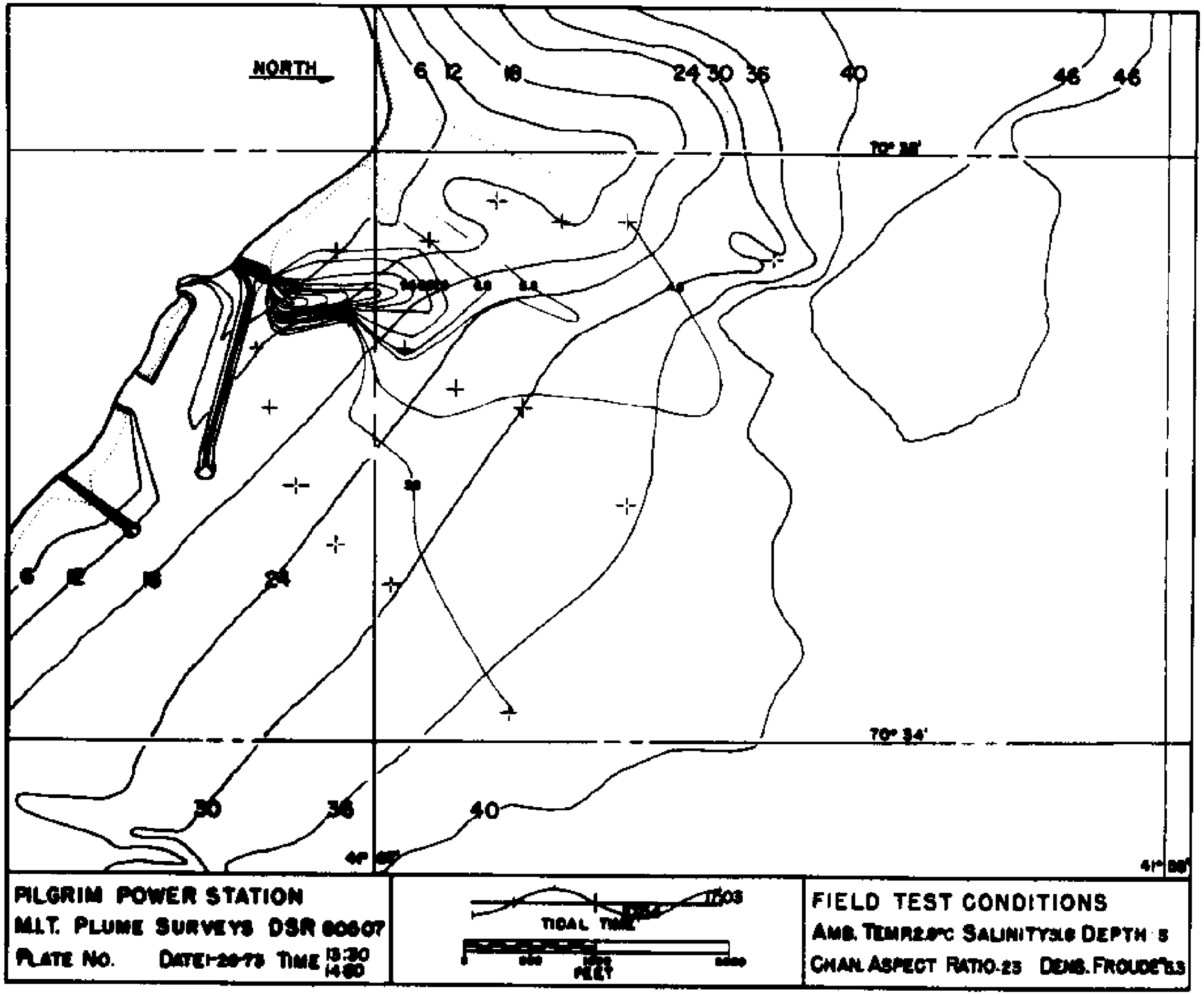

Plate 4.5 January Isotherms, $\mathbb{F}_o = 5.3$, Surface

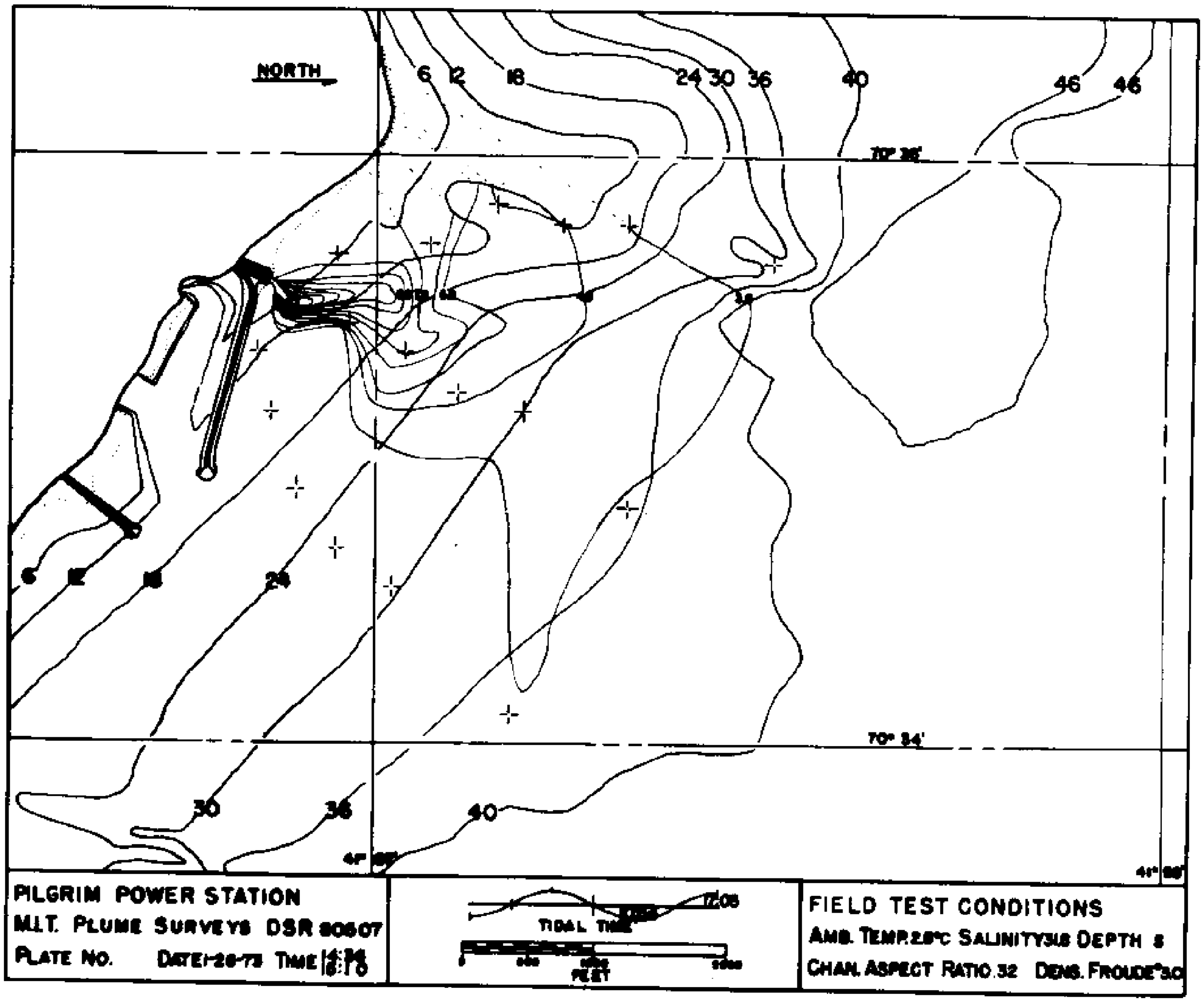

Plate 4.6 January Isotherms, $\mathbb{F}_o$ = 3.0, Surface

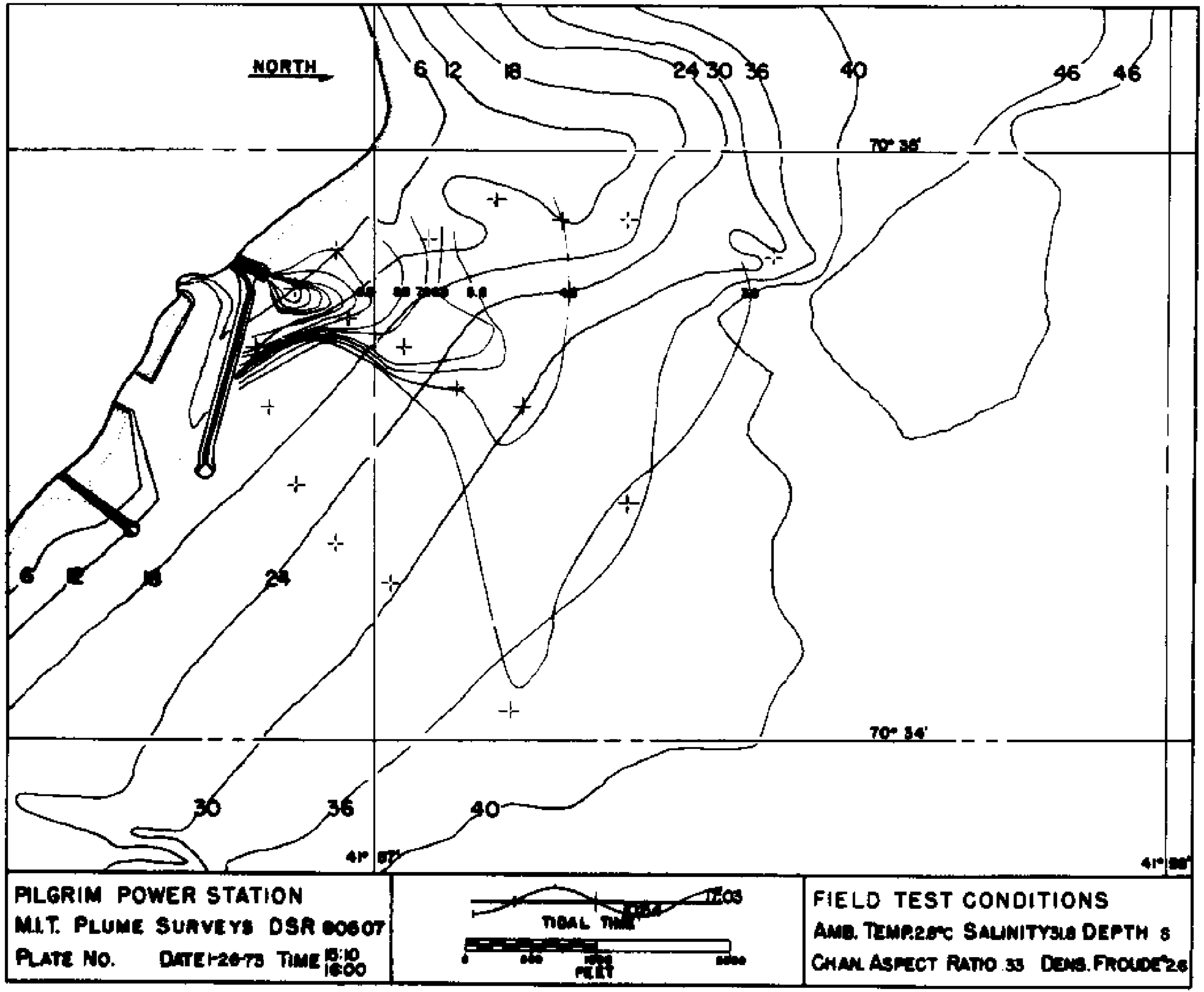

Plate 4.7 January Isotherms, $IF_o = 2.6$, Surface

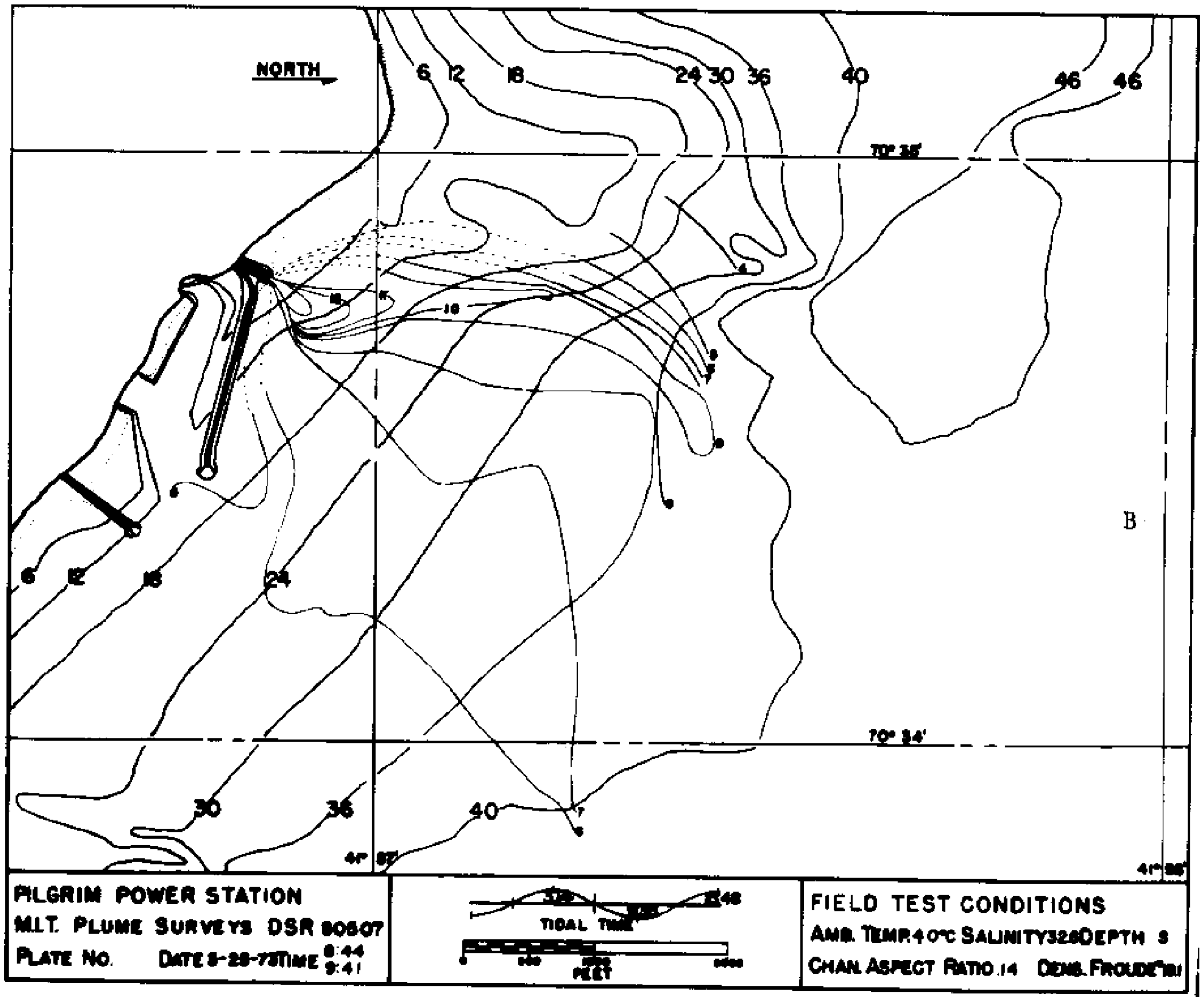

Plate 4.8 March Isotherms, $\mathrm{IF}_o = 18.1$, Surface

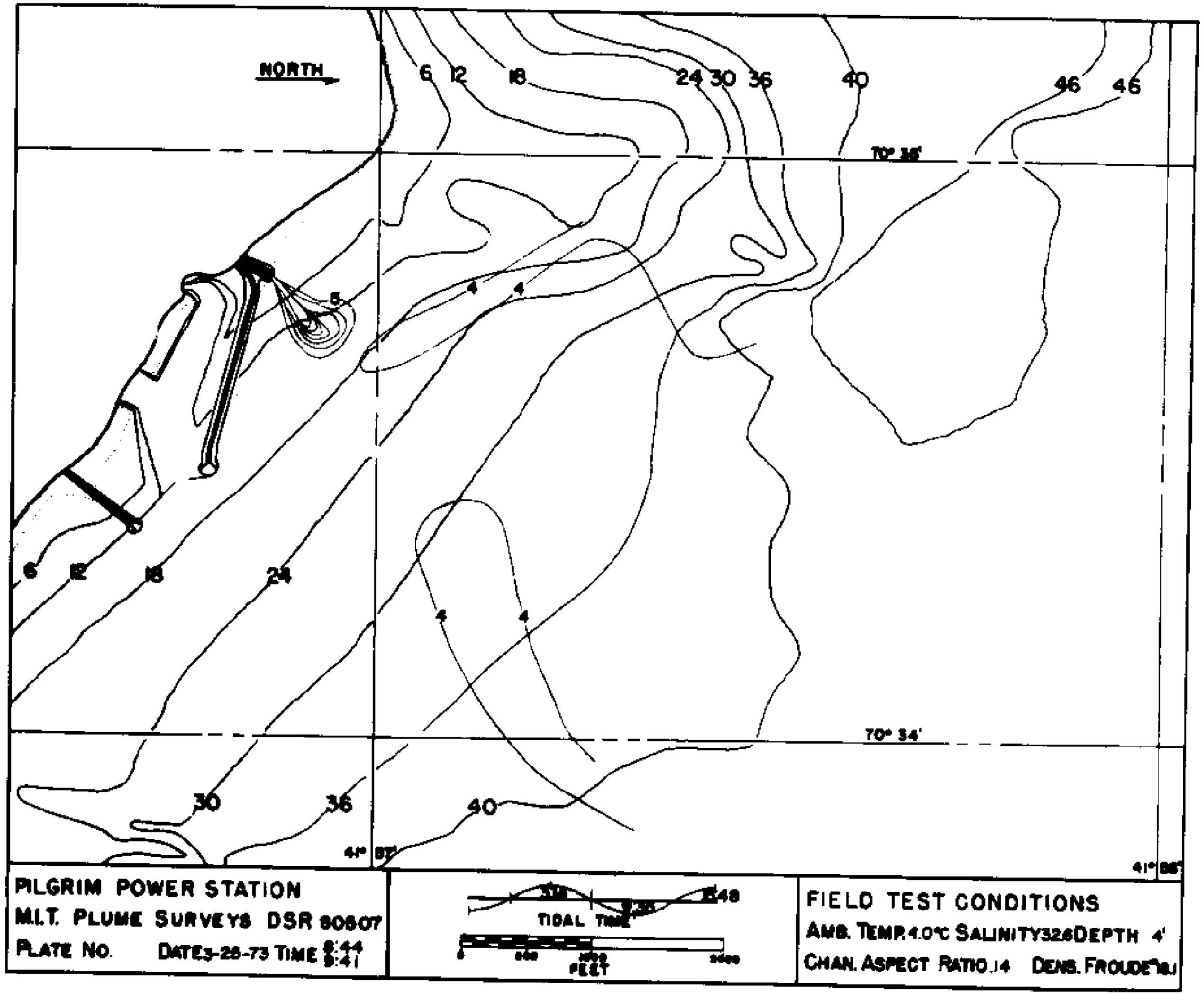

Plate 4.9 March Isotherms, IF_o = 18.1, 4 Feet

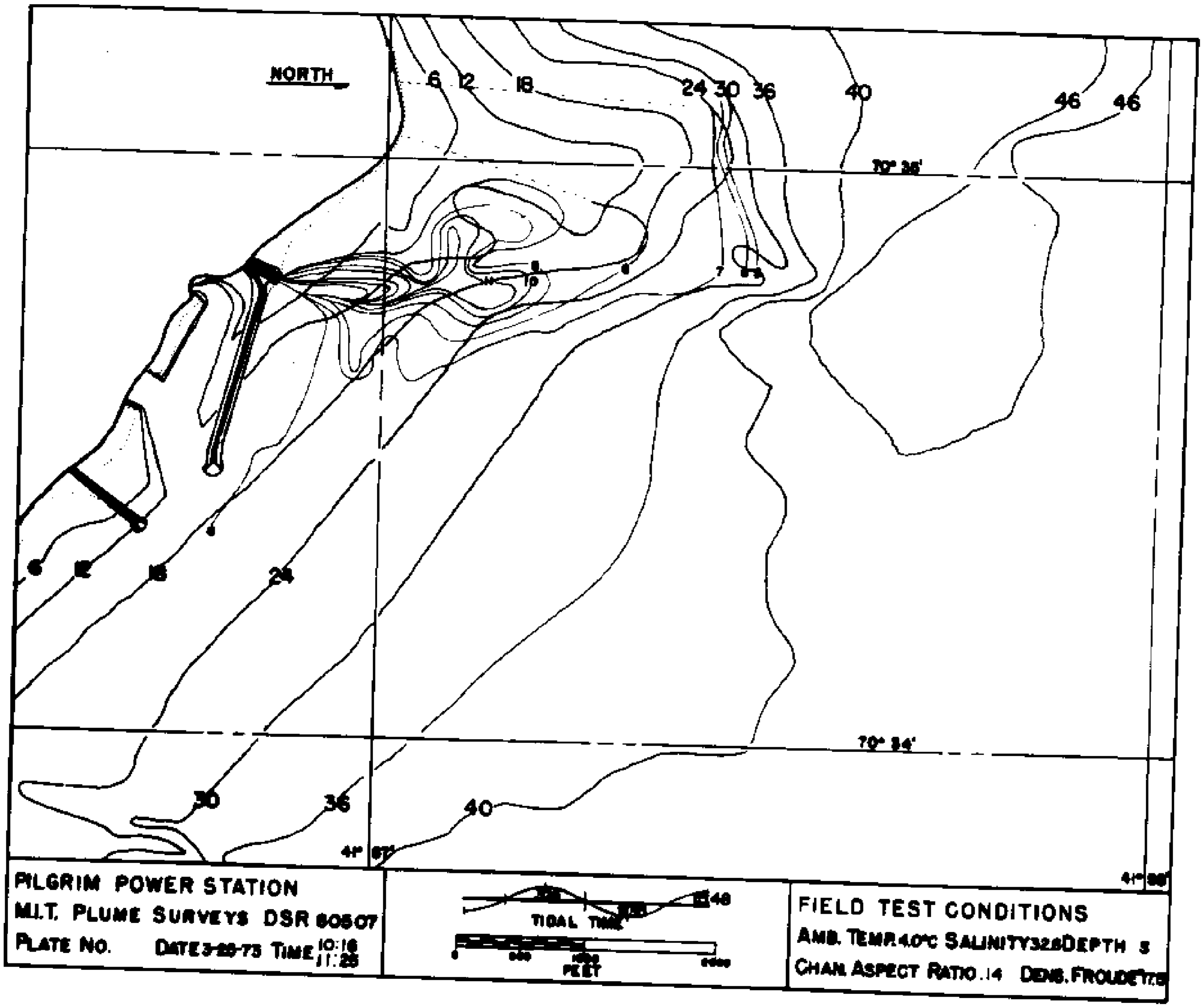

Plate 4.10 March Isotherms, IF_o = 17.5, Surface

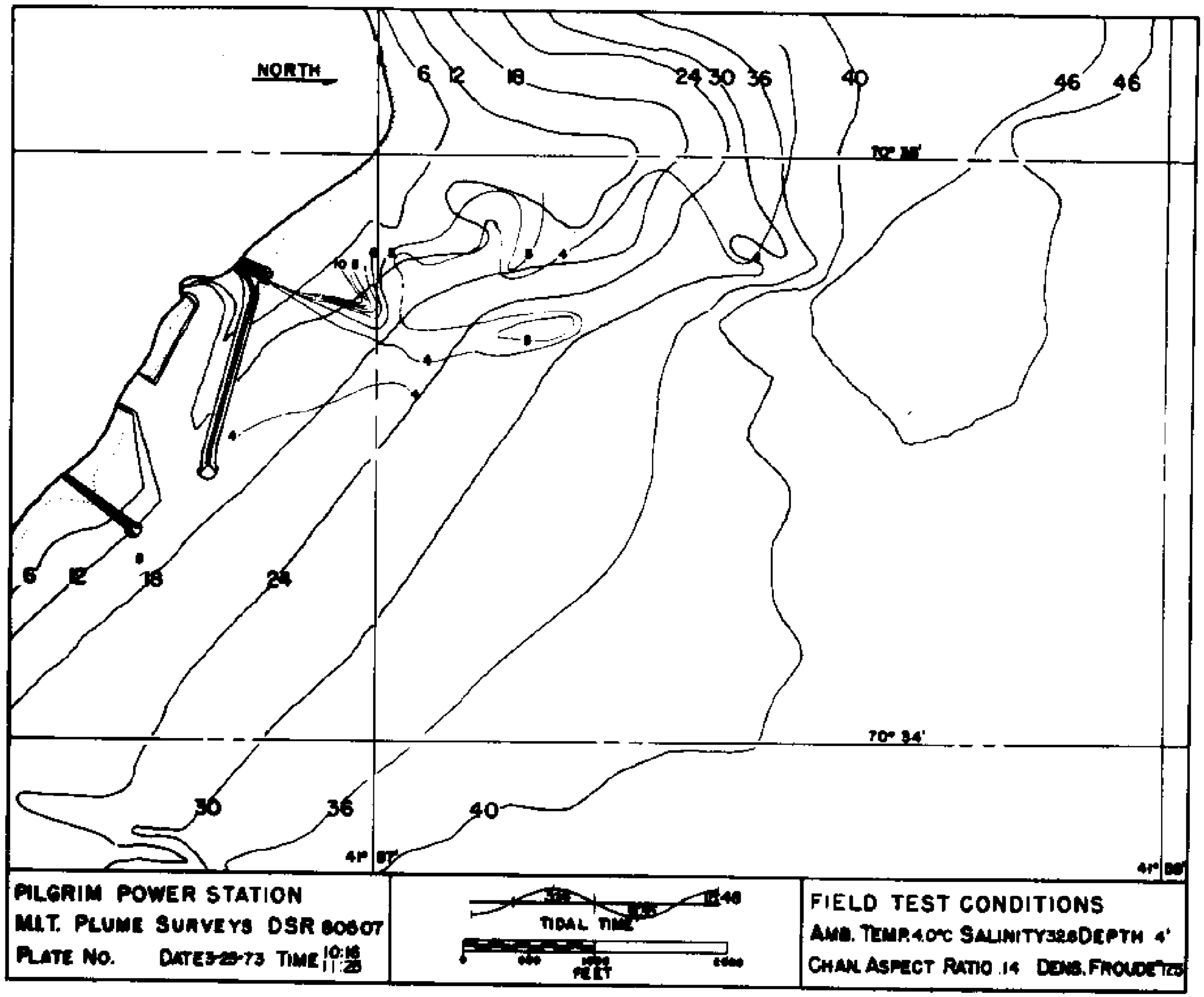

Plate 4.11 March Isotherms, IF_o = 17.5, 4 Feet

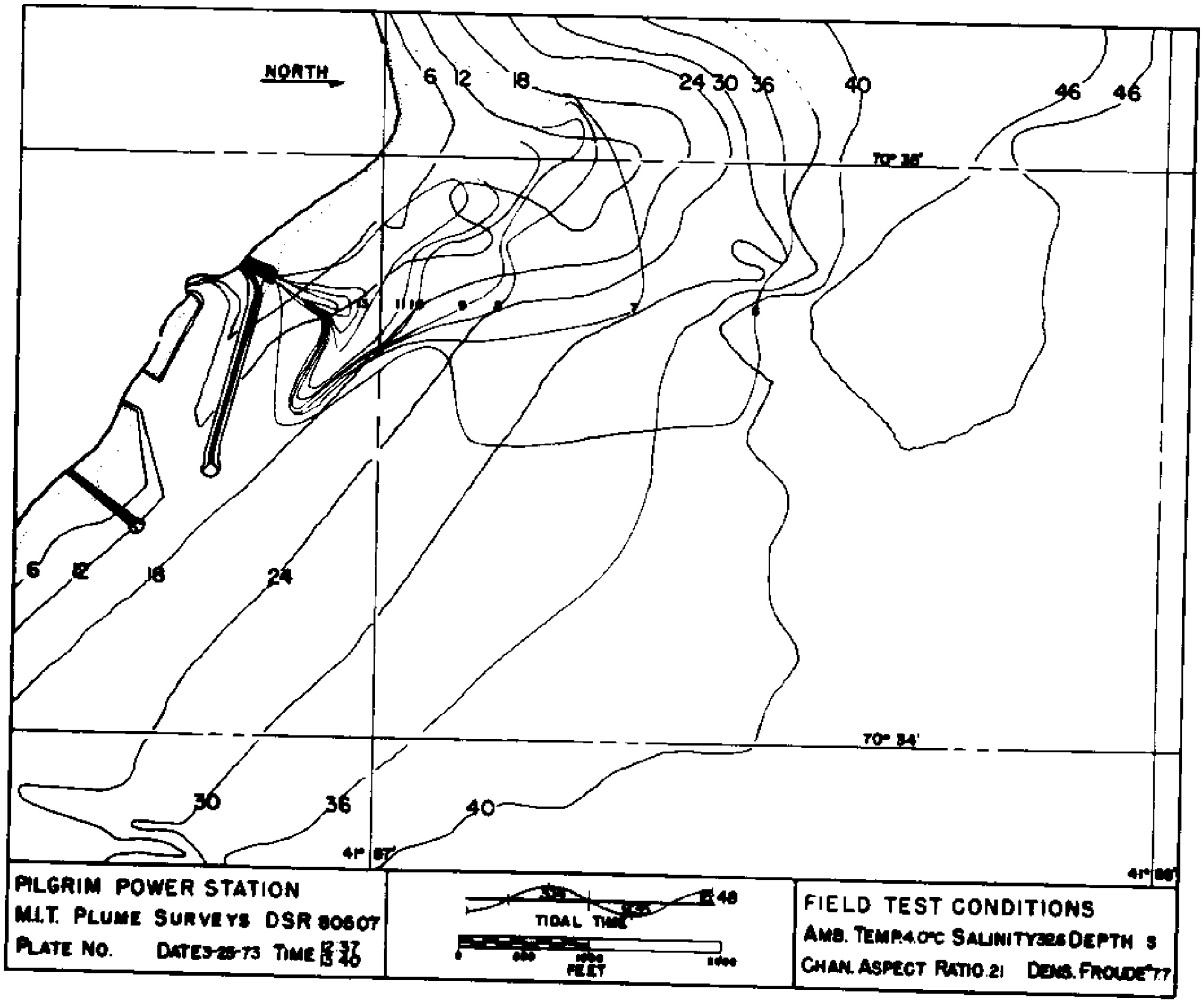

Plate 4.12 March Isotherms, $IF_o = 7.7$, Surface

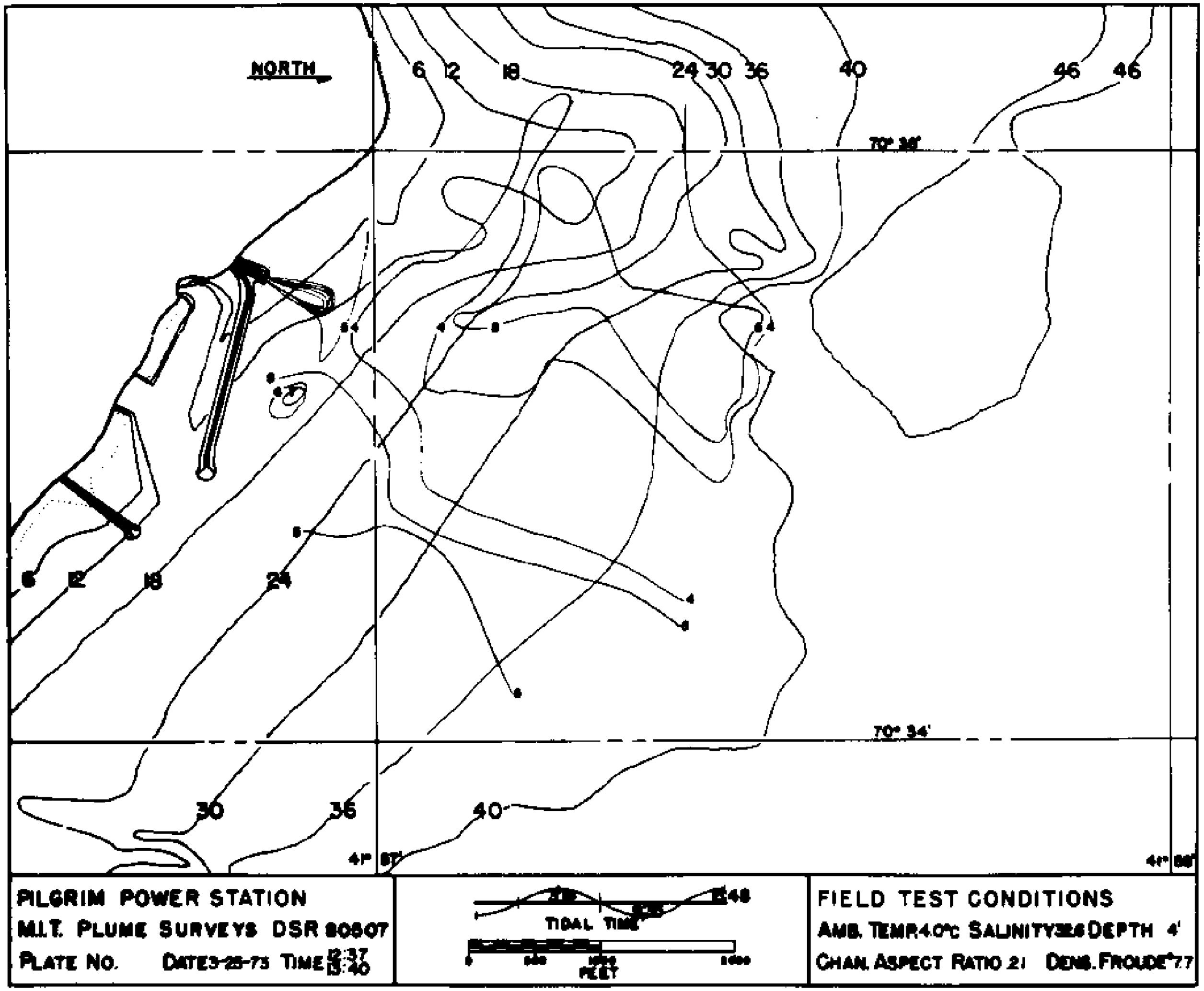

Plate 4.13 March Isotherms, IF_o = 7.7, 4 Feet

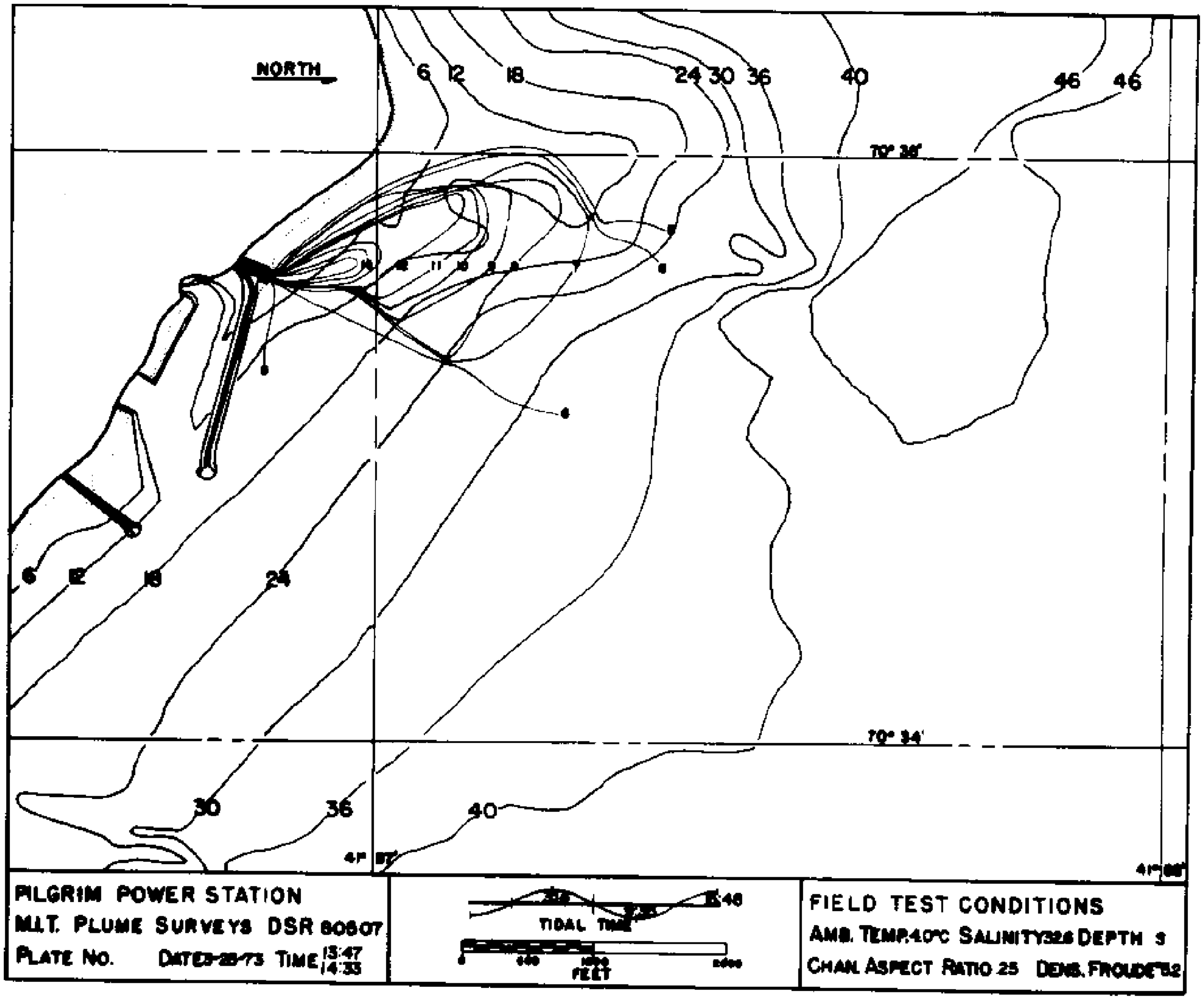

Plate 4.14 March Isotherms, $IF_o = 5.2$, Surface

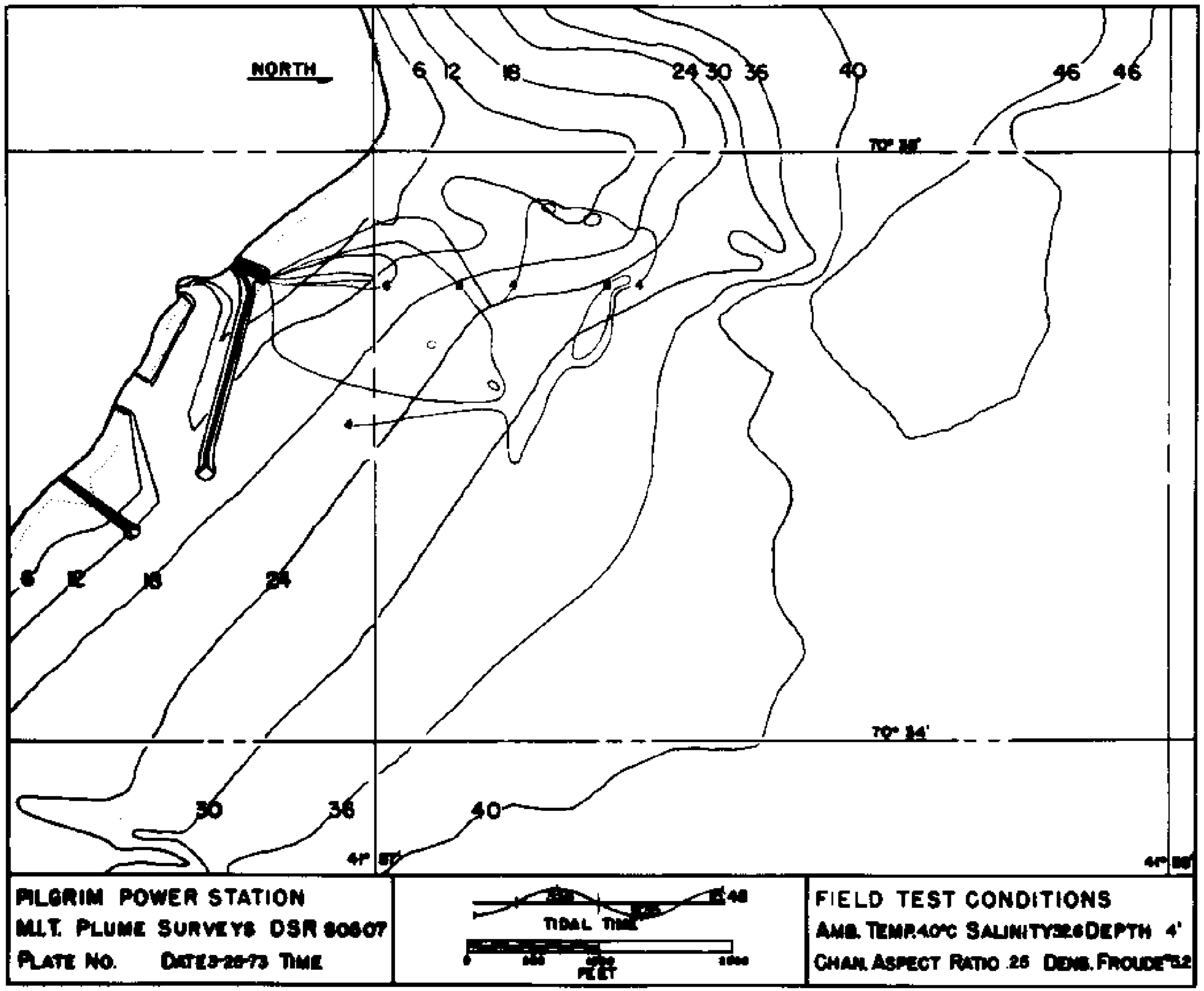

Plate 4.15 March Isotherms, $\mathbb{F}_o = 5.2$, 4 Feet

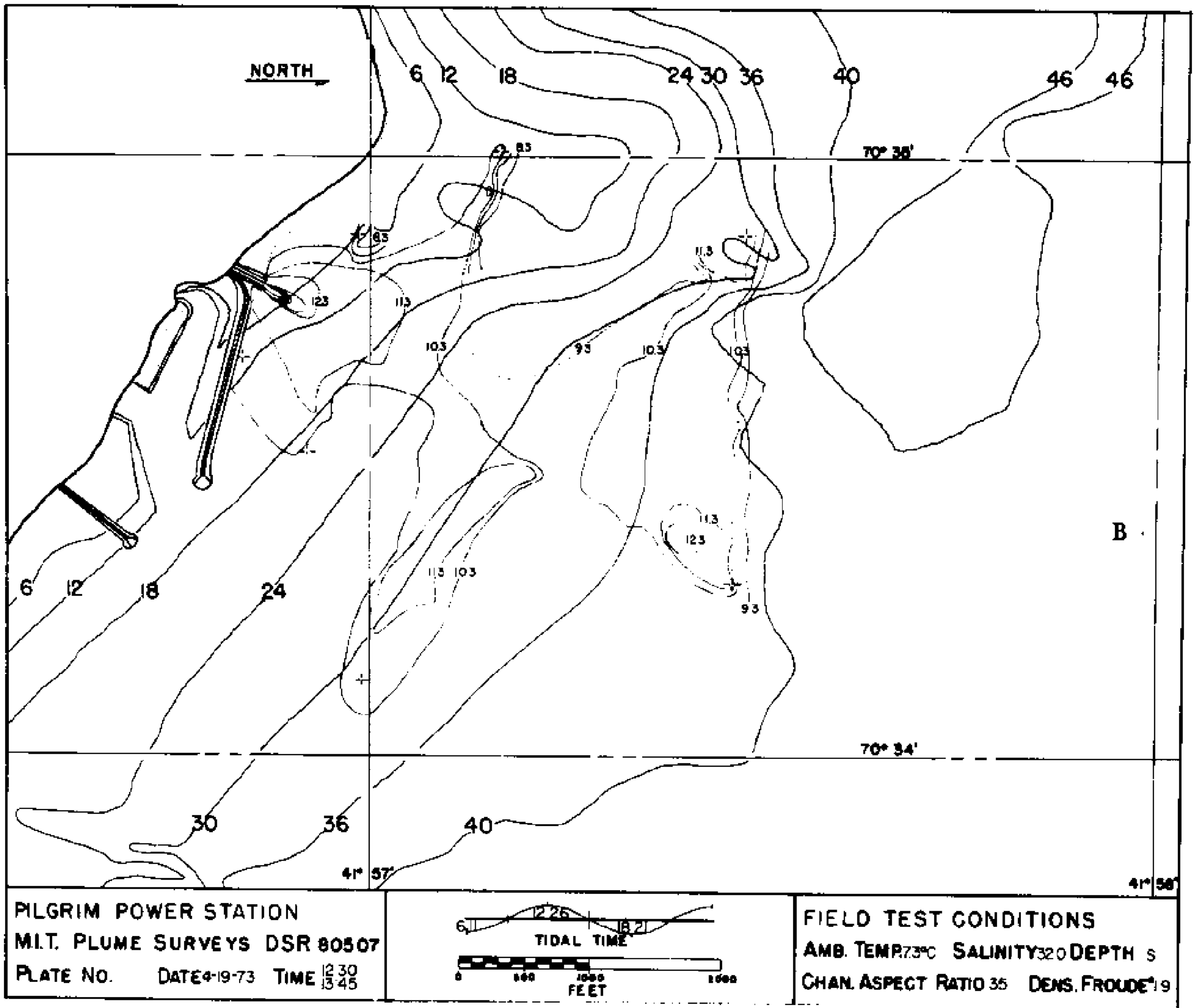

Plate 4.16 April Isotherms, $IF_o = 1.9$, Surface

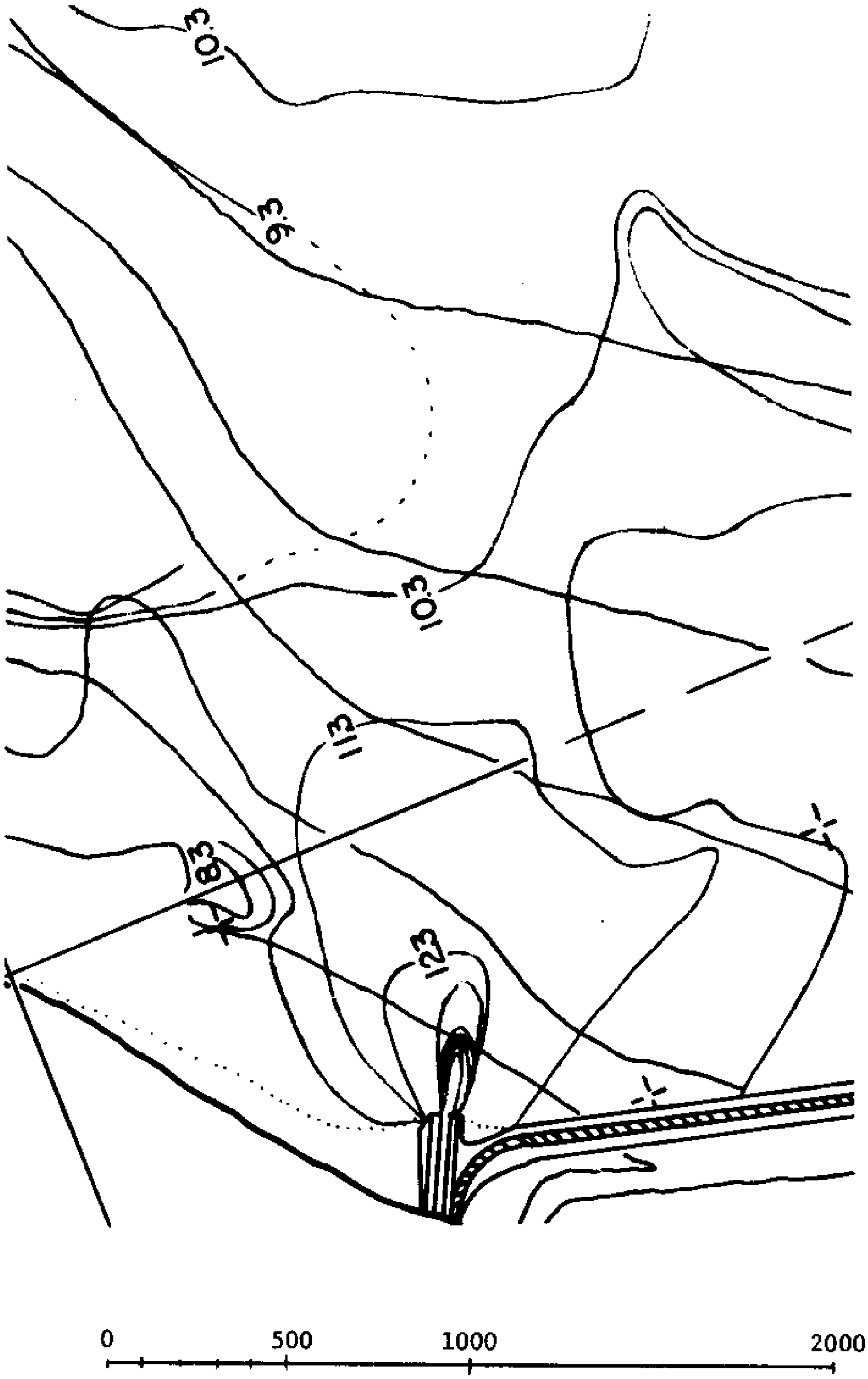

Plate 4.17 April Isotherms, $\mathbb{F}_o = 1.9$

Local to Discharge, Surface

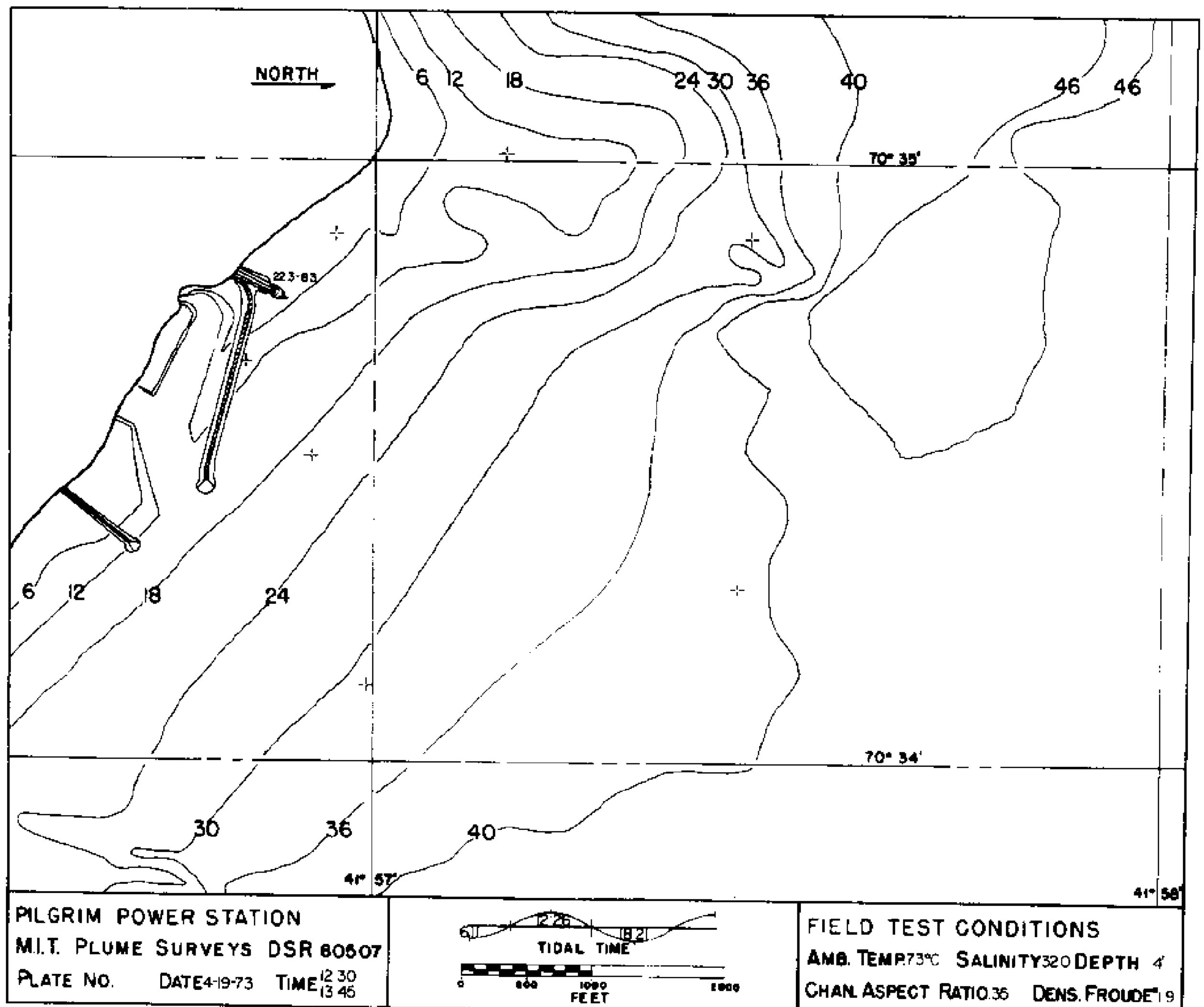

Plate 4.18 April Isotherms, IF_o = 1.9, 4 Feet

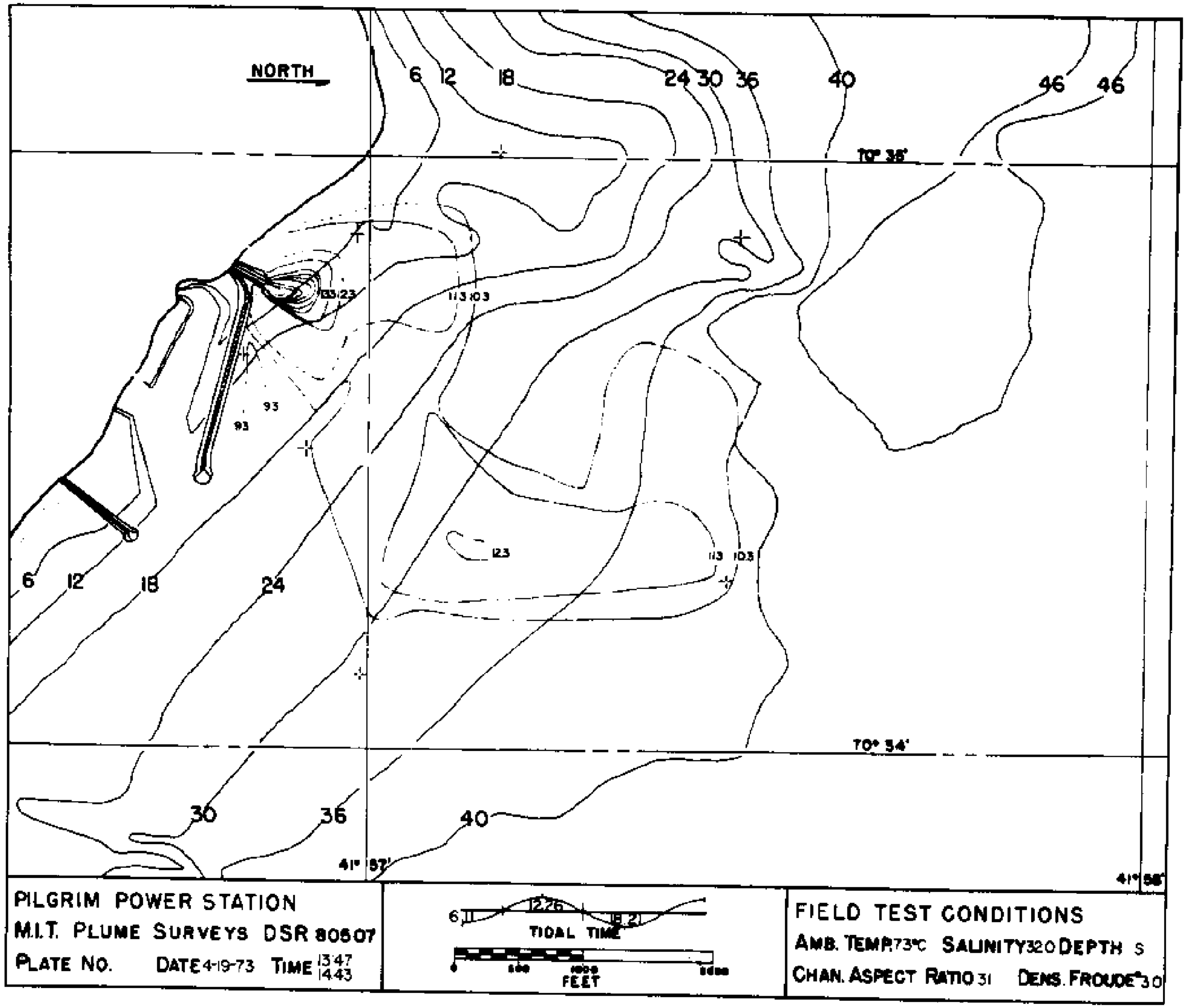

Plate 4.19 April Isotherms, IF_o = 3.0, Surface

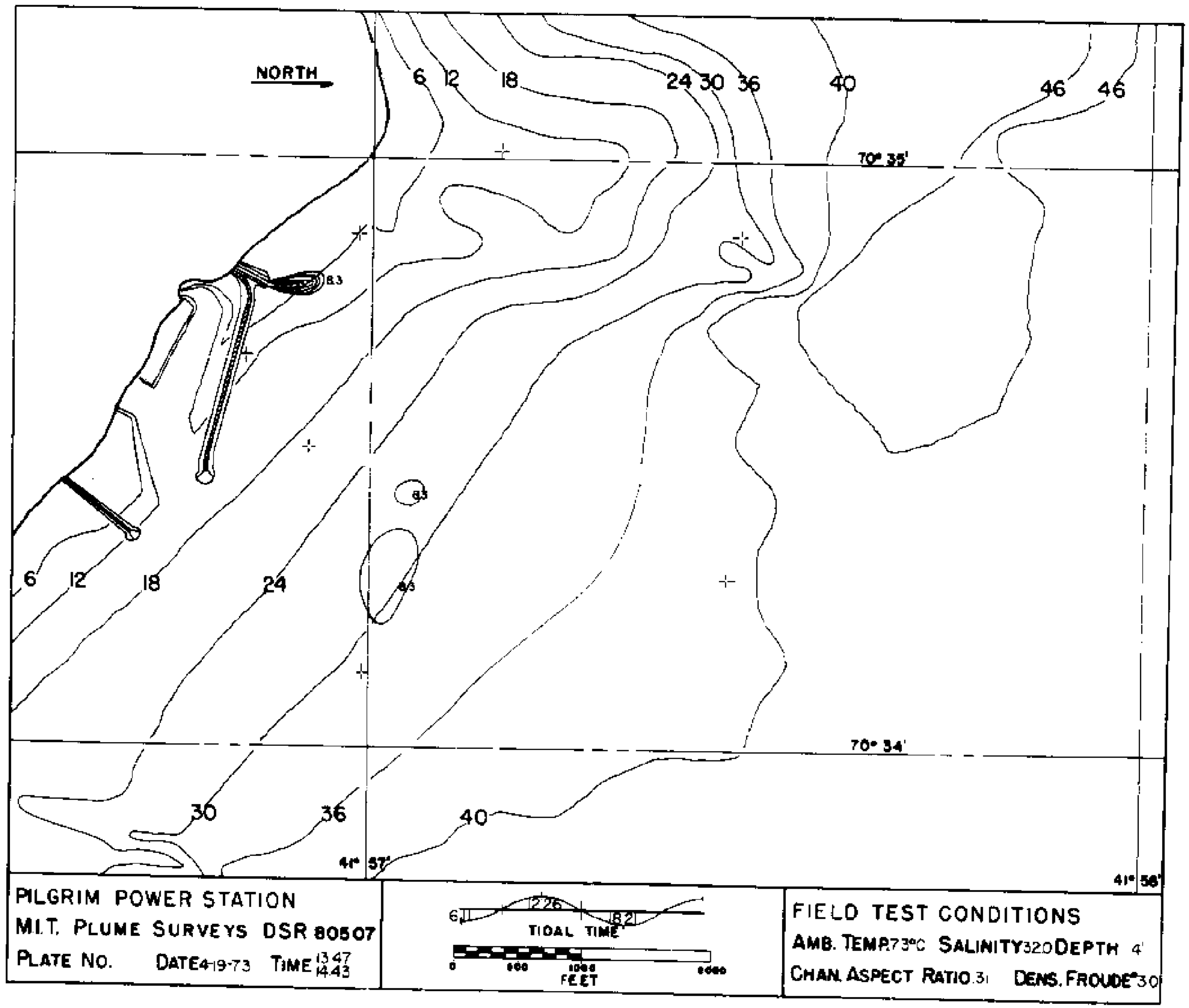

Plate 4.20 April Isotherms, $IF_o = 3.0$, 4 Feet

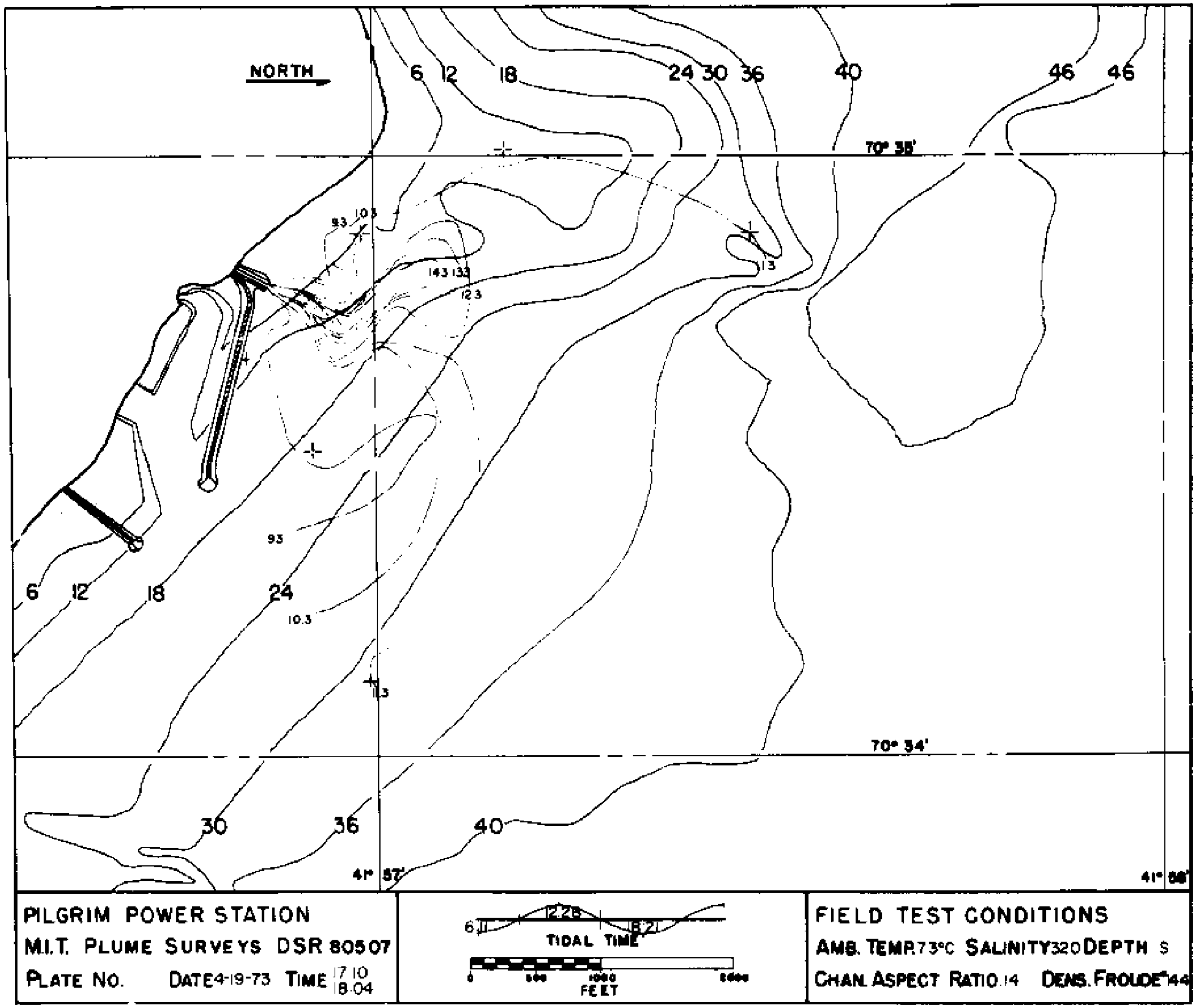

Plate 4.21 April Isotherms, IF_o = 14.4, Surface

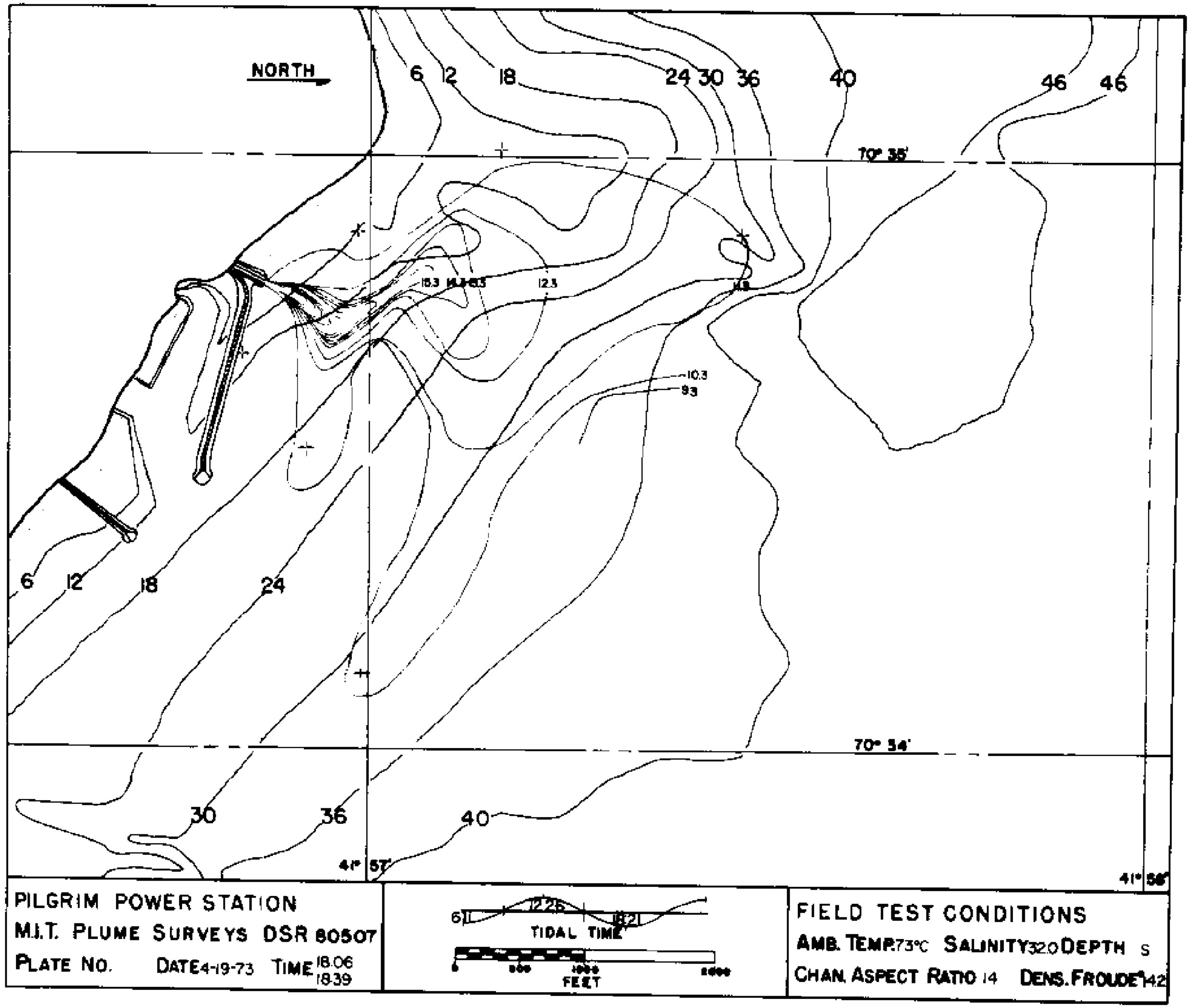

Plate 4.22 April Isotherms, IF_o = 14.2, Surface

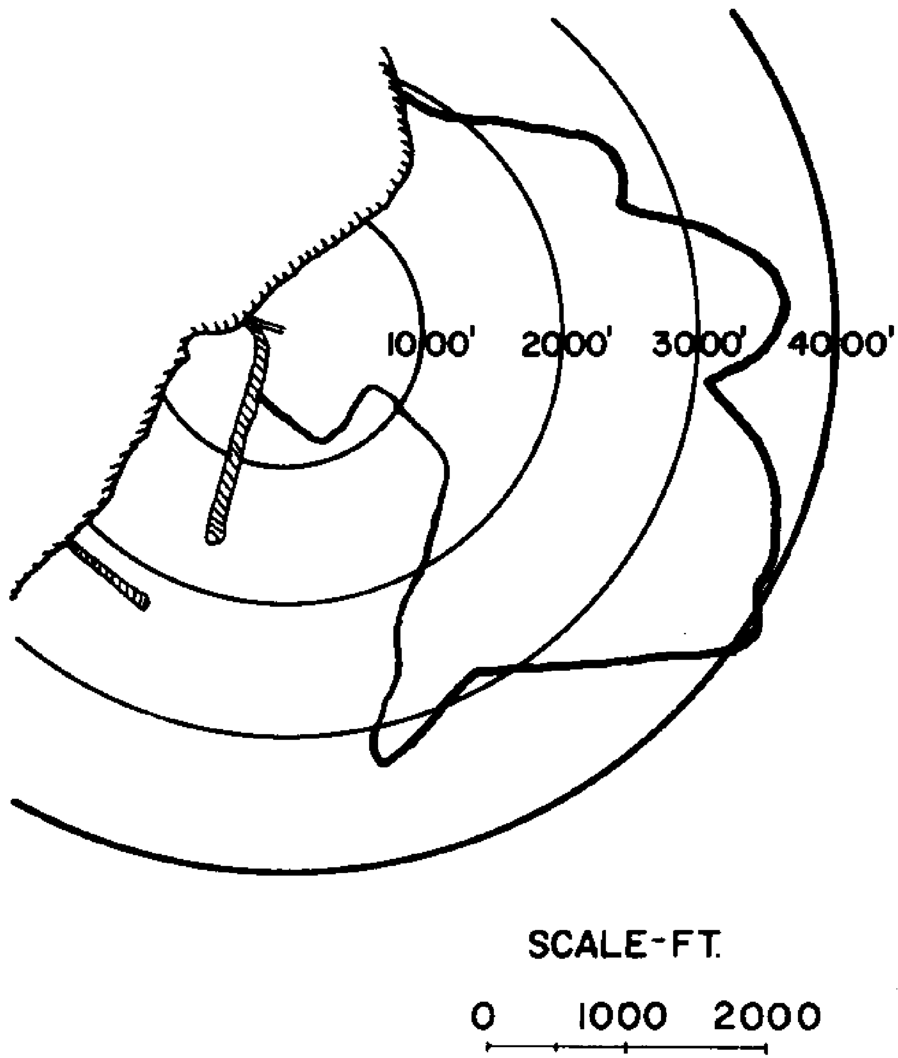

FIG. 4.8 THREE SURVEY 4°C ISOTHERM LIMIT

CHAPTER 5

COMPARISON OF FIELD DATA WITH THEORY

5.1 Analysis of Field Data

Areas of surface isotherms were determined for each surface plot by planimeter. A summary of this data is shown in Table 5.1. Plume centerline distances to a given surface isotherm were determined. Plots of nondimensional $\Delta T_c/\Delta T_o$, where ΔT_o is the rise in temperature across the condenser and ΔT_c is temperature observed less the ambient temperature, versus the centerline distance to the ΔT_c isotherm of interest are shown in Figures 5.4 through 5.8. Ambient temperatures are determined from the vertical temperature profiles shown in Figures 4.5, 4.6, and 4.7 for each of the three survey days. The ambient temperature values used for each survey are listed in Table 5.1. ΔT_o, the rise across the cooling water condensers, is not a constant due to small changes in plant operation. Calculation of the temperature rise across the condenser is an average of the hourly temperature rise across the condenser from data provided by the power plant. The average ΔT_o represents the ΔT_o of the power plant during the period that each complete run of the field transects was made. A listing of the ΔT_o used for each survey is included in Table 5.1. The discharge configurations were determined from the time of survey in relation to high and low tide as given in Tide Tables published by the U.S. Department of Commerce for 1973.[7] Water density at the ambient temperature was determined from the water conductivity and temperature

TABLE 5.1

FIELD SURFACE ISOTHERM - AREA TABLES

IF_o = 1.9 A = .35 Date: 4-19-73 Ambient Temp. = 7.3°C ΔT_o = 15.0 °C

T_c	$\Delta T_c = T_c - T_a$	Area Enclosed Acres
13.3	6	1.0
12.3	5	3.4
11.3	4	28
10.3	3	76

IF_o = 3.0 A = .31 Date: 4-19-73 Ambient Temp. = 7.3°C ΔT_o = 15.1°C

T_c	$\Delta T_c = T_c - T_a$	Area Enclosed Acres
17.3	10	0.9
16.3	9	1.3
15.3	8	2.0
14.3	7	2.5
13.3	6	4.0
12.3	5	7.0
11.3	4	75
10.3	3	156

IF_o = 14.4 A = .14 Date: 4-19-73 Ambient Temp. = 7.3°C ΔT_o = 16.4°C

T_c	$\Delta T_c = T_c - T_a$	Area Enclosed Acres
18.3	11	1.0
17.3	10	1.1
16.3	9	1.5
15.3	8	2.8
14.3	7	4.3
13.3	6	7.7
12.3	5	14

TABLE 5.1 (Continued)

$\mathbb{F}_o$ = 14.2 A = .14 Date: 4-19-73 Ambient Temp = 7.3°C ΔT_o = 17.0°C

T_c	$\Delta T_c = T_c - T_a$	Area Enclosed Acres
19.3	12	0.8
18.3	11	1.1
17.3	10	1.8
16.3	9	2.8
15.3	8	4.0
14.3	7	7.5
13.3	6	14
12.3	5	31
11.3	4	42

$\mathbb{F}_o$ = 18.1 A = .14 Date: 3-25-73 Ambient Temp = 4.0°C ΔT_o = 15.0°C

T_c	$\Delta T_c = T_c - T_a$	Area Enclosed Acres
13.0	9	1.2
12.0	8	2.7
11.0	7	5.2
10.0	6	14
9.0	5	29

TABLE 5.1 (Continued)

$F_o = 17.5$ $A = .14$ Date: 3-25-73 Ambient Temp $4.0^{o}C$ $\Delta T_o = 15.5^{o}C$

T_c	$\Delta T_c = T_c - T_a$	Area Enclosed Acres
16.0	12	0.6
15.0	11	2.1
14.0	10	2.9
13.0	9	4.1
12.0	8	5.9
11.0	7	12
10.0	6	19
9.0	5	30
8.0	4	66
7.0	3	125

$F_o = 7.7$ $A = .21$ Date: 3-25-73 Ambient Temp = $4.0^{o}C$ $\Delta T_o = 15.9^{o}C$

T_c	$\Delta T_c = T_c - T_a$	Area Enclosed Acres
15.0=	11	.4
14.0	10	1.1
13.0	9	1.9
12.0	8	13
11.0	7	34 (est.)
10.0	6	48 (est.)
9.0	5	62 (est.)
8.0	4	77 (est.)
7.0	3	108 (est.)

TABLE 5.1 (Continued)

$\mathrm{IF}_o = 5.2$ $A_s = .25$ Date: 3-25-73 Ambient Temp = $4.0^\circ C$ $\Delta T_o = 16.0^\circ C$

T_c	$\Delta T_c = T_c - T_a$	Area Enclosed Acres
15.0	11	1.8
14.0	10	3.8
13.0	9	4.1
12.0	8	10
11.0	7	15
10.0	6	19
9.0	5	24
8.0	4	34
7.0	3	49

$\mathrm{IF}_o = 17.7$ $A_s = .14$ Date: 1-26-73 Ambient Temp = $2.8^\circ C$ $\Delta T_o = 16.2^\circ C$

T_c	$\Delta T_c = T_c - T_a$	Area Enclosed Acres
7.8	5	0.8
6.8	4	1.9
5.8	3	3.7
4.8	2	13
3.8	1	49

TABLE 5.1 (Continued)

IF_o = 9.9 A_s = .19 Date: 1-26-73 Ambient Temp = 2.8°C ΔT_o = 16.4°C

T_c	$\Delta T_c = T_c - T_a$	Area Enclosed Acres
18.8	16	0.6
17.8	15	1.3
16.8	14	2.2
15.8	13	2.5
14.8	12	2.8
13.8	11	2.9
12.8	10	3.0
11.8	9	3.1
10.8	8	3.6
9.8	7	4.0
8.8	6	9.5
7.8	5	21
6.8	4	50

IF_o = 6.4 A = .23 Date: 1-26-73 Ambient Temp = 2.8°C ΔT_o = 17.0°C

T_c	$\Delta T_c = T_c - T_a$	Area Enclosed Acres
17.8	15	0.30
16.8	14	0.61
15.8	13	0.84
14.8	12	0.95
13.8	11	1.1
12.8	10	1.2
11.8	9	1.6
10.8	8	2.8
9.8	7	6.1
8.8	6	11
7.8	5	25
6.8	4	61

TABLE 5.1 (Continued)

$\mathbb{F}_o = 5.3$ $A = .25$ Date: 1-26-73 Ambient Temp = 2.8^oC $\Delta T_o = 16.9^oC$

T_c	$\Delta T_c = T_c - T_a$	Area Enclosed Acres
15.8	13	.3
14.8	12	.6
13.8	11	1.0
12.8	10	1.3
11.8	9	3.0
10.8	8	3.9
9.8	7	5.9
8.8	6	9.6
7.8	5	15
6.8	4	28
5.8	3	37
4.8	2	144

$\mathbb{F}_o = 2.6$ $A = .33$ Date: 1-26-73 Ambient Temp = 2.8^oC $\Delta T_o = 16.9^oC$

T_c	$\Delta T_c = T_c - T_a$	Area Enclosed Acres
15.8	13	.5
14.8	12	1.0
13.8	11	1.8
12.8	10	2.4
11.8	9	4.5
10.8	8	8.3
9.8	7	10
8.8	6	21
7.8	5	32

generated by the C.T.D. The water temperature and conductivity were reduced to density values by use of sea water density tables as published by USC and GS.[8]

Densimetric Froude numbers and aspect ratios given in Table 5.2 were determined as follows: the depth, h_o, at the exit of the discharge channel was assumed to follow the daily tide predictions for Boston using a sinusoidal interpolation between high and low water values. The schematic discharge channel (see Table 5.2) is assumed to have the same instantaneous cross sectional area as the "as built" section. Therefore, the half width $b_o = 15 + h_o$(ft.) and the aspect ratio $A = h_o/b_o$. The instantaneous cross sectional area is $30h_o + 2h_o^2$(ft.^{2}) and the exit velocity for the discharge channel is obtained by dividing the nominal condenser water pumping rate of 720 cfs by the instantaneous area. All variables needed for the densimetric Froude number determination are known except the value of $\Delta\rho_o/\rho_a$. The temperature of the discharged water is assumed to be given by summation of ΔT_o and the ambient water temperature. The ambient salinity is used for the determination of the outlet water density from the sea water density tables. Ambient water density is determined from the ambient salinity and temperature noted in Figures 4.5, 4.6, and 4.7; ambient salinity is noted in the information block of each surface isotherm plate. In cases of significant ambient stratification a depth averaged temperature is used to determine the temperature to be used for determination of ρ_a. The densimetric Froude number as defined in Chapter 1 is calculated for the time period corresponding to each temperature survey

TABLE 5.2 SUMMARY OF FIELD SCHEMATIZATIONS

Date	$A = \frac{h_o}{b_o}$	$\mathbb{F}_o = \frac{U_o}{\sqrt{g \frac{\Delta\rho_o}{\rho_a} h_o}}$	U_o ft/sec	h_o - ft.	h_{max} - ft.
4-19-73	.35	1.9	1.9	8.2	9.0
1-26-73	.33	2.6	2.1	7.5	9.5
4-19-73	.31	3.0	2.5	6.8	9.5
3-25-73	.25	5.2	3.6	5.0	15
1-26-73	.25	5.3	3.6	5.0	16
1-26-73	.23	6.4	4.1	4.5	17
3-25-73	.21	7.7	4.7	4.0	19
1-26-73	.19	9.9	5.6	3.5	22
4-19-73	.14	14.2	8.3	2.5	24
4-19-73	.14	14.4	8.3	2.5	24
3-25-73	.14	17.5	8.3	2.5	30
1-26-73	.14	17.7	8.3	2.5	30
3-25-73	.14	18.1	8.3	2.5	30

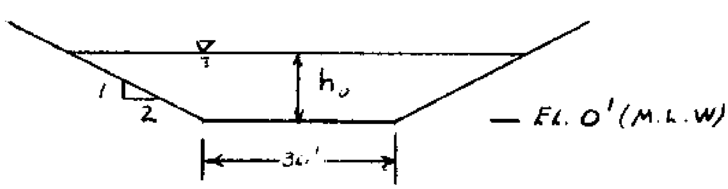

Discharge Channel (as built)

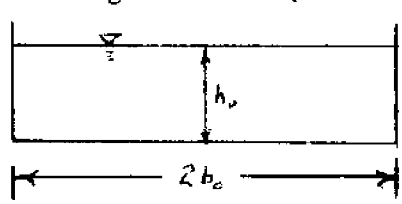

Schematic Discharge Channel

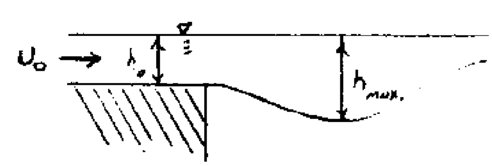

Schematic of h_{max}

using the tabulated value of U_o, h_o and $\Delta\rho_o/\rho_a$. Current measurements in the receiving water were not available for any of these surveys due to the heavy frequency of winter storms which caused the loss of current meters and inability to service the remaining current meters maintained by the Boston Edison Company at the site. Wind data from the Boston Edison meterorological tower was available for the January survey period only. On other dates an average wind velocity was estimated. Values to be determined for the analytical model calculation, with or without the effect of bottom slope, for each model run are: densimetric Froude number, aspect ratio, and the surface heat loss coefficient. Heat loss coefficients were determined from equations and graphs given by Ryan and Harleman.[9] Heat loss coefficients used as model input are in the dimensionless form k/u_o. k is determined from the relationship, $k = K/\rho c$, where K is the heat loss coefficient in btu/ft^2-day-^{o}F, ρ is the water density and c is the volume specific heat of water. k has dimensions of ft/sec. K is a function of the humidity, temperature difference between water surface and air, and wind velocity. The wind velocity was estimated to be 10 mph and 8 mph for the March and April surveys respectively. The other variables were either provided by the power plant or recorded from a local weather station.

Model sensitivity to the heat loss coefficient and to cross currents in the receiving water was tested for densimetric Froude numbers and aspect ratios ranging over the entire tidal range. Three values of the heat loss coefficient were used in the analytical model (no bottom slope). The model showed little sensitivity in $\Delta T_c/\Delta T_o$ versus distance to variations in distances of 1500 feet or less from the discharge as shown in Figure 5.1. This finding is consistent with that found by Stolzenbach and Harleman.[2] In order to insure the proper analytical model centerline temperature reduction at distances greater than 1500 feet, the correct heat loss coefficient for each field survey was determined as mentioned above for the field conditions existing at the time of each survey.

Cross current sensitivity in the results of $\Delta T_c/\Delta T_o$ versus distance of the analytical model was determined by input of three values of cross current to the model. The results of the analysis are shown in Figure 5.2. The analytical model is not sensitive to cross current. The results from each run of the analytical model were compared to the corresponding field data.

Two versions of the analytical model were used for comparison: the Stolzenbach-Harleman model[2] and the Harleman, Stolzenbach, Adams model.[3] The major difference between these models is that the former includes the effect of bottom slope and the latter does not.

5.2 Comparison of Field Results with the Analytical Model

Table 5.2 shows a summary of the field parameters including the quantity h_{max}, the maximum penetration of the discharge jet below the water surface in receiving waters of infinite depth. A sketch of h_{max} is shown in Table 5.2. h_{max} is determined by Stolzenbach, Harleman and Adams:[3]

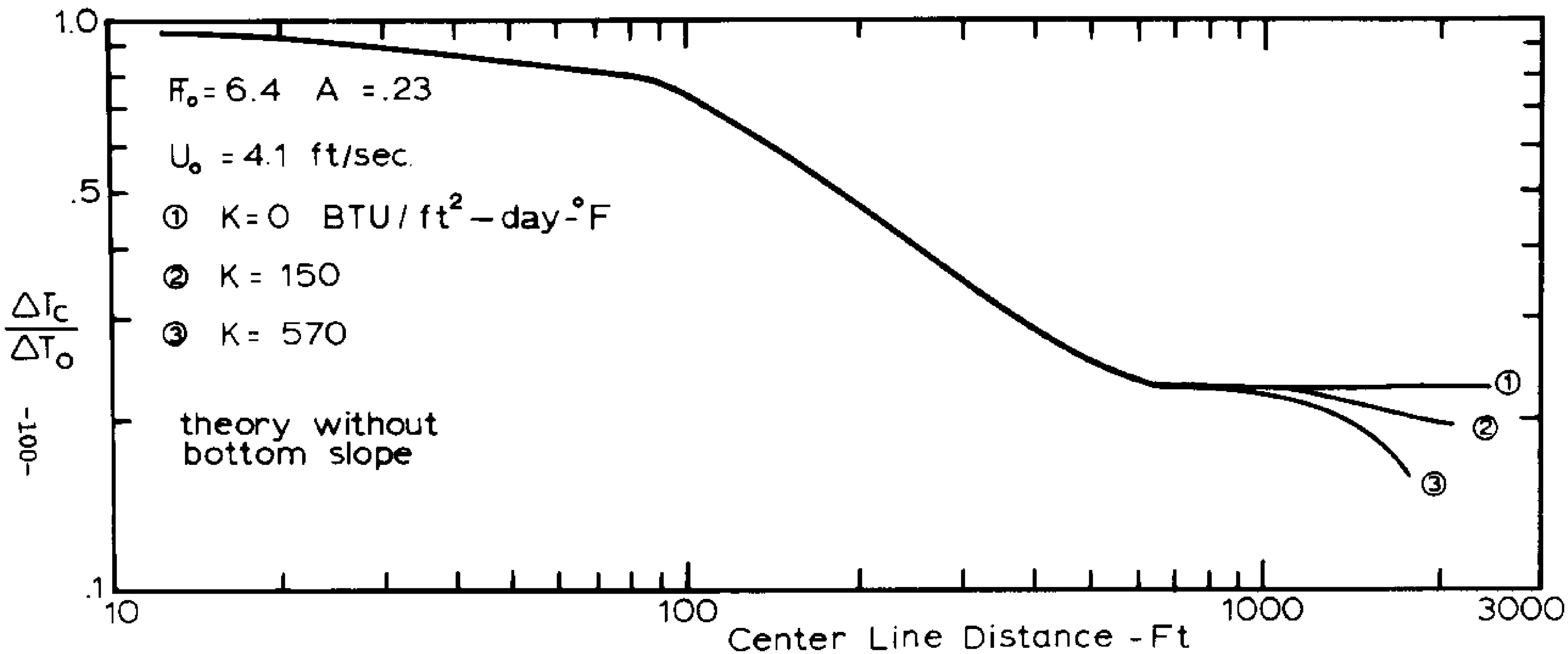

Fig. 5.1 : Heat Loss Coefficient Sensitivity

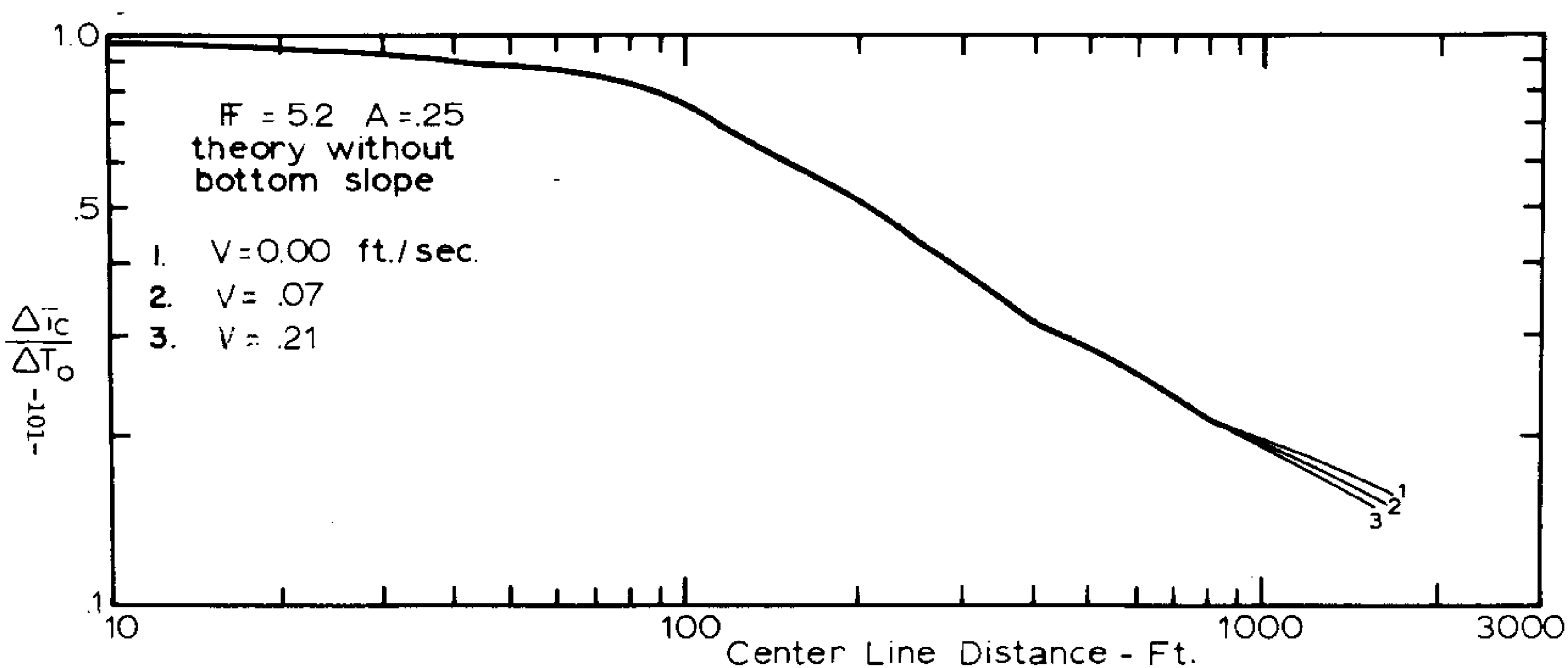

Fig. 5.2 Cross Flow Sensitivity

$$h_{max} = .42\sqrt{h_o b_o}\sqrt{IF' + 1} \quad \text{for} \quad IF' \leq 3.0$$

where

$$IF' = IF_o A^{1/4} \quad \text{and} \quad A = \frac{h_o}{b_o}$$

or

$$h_{max} = .42\sqrt{h_o b_o}\ IF' \quad \text{for} \quad IF' > 3.0$$

This parameter is important in this study because it determines the degree of interaction between the discharge jet and the sloping bottom at the site. When the discharge channel depth h_o, is less than the maximum jet penetration (h_{max}) the bottom can be expected to interfere with jet spreading and reduce the entrainment of the receiving water into the jet. Further discussion of h_{max} is given below.

The field data is characterized in three phases based on the variation of the densimetric Froude number and aspect ratio due to the changing tidal elevations at the exit of the discharge channel. The phases are high tide, mid tide and low tide. The densimetric Froude number and aspect ratio of the heated discharge is relatively constant for a period of an hour or more during both the high and low tide phases. Thus conditions in the field, at high and low tide are more consistent with the steady state assumption used in the analytical model. The mid tide phase of the tidal elevation curve is a phase in which the densimetric Froude number and aspect ratio are changing rapidly. Thus field data obtained during this phase are not consistent with the steady state assumption made for model useage. Since both versions of the analytical model (with and without bottom slope) are based on the steady state assumption, the time of travel in the discharge jet was analyzed to determine the length of time required to reach the end of the near field mixing region several thousand feet offshore. If the water discharged had a travel time of major significance in traversing to the limit of the survey area (such that the schematization of the discharge cross section was affected by a corresponding tidal change in depth), then a new schematization would be necessary to fit the data. The study showed a travel time less then two hours to the most distant transect at high tide. All other tidal stages had smaller times of travel.

The tidal phases discussed earlier are characterized in Figure 5.3. The high tide phase had Froude numbers ranging from 1.9 to 3.0 and an aspect ratio from .35 to .31, mid tide values of Froude numbers ranged from 5.2 to 9.9 and aspect ratio from .25 to .19. The low tide Froude numbers ranged from 14.2 to 18.1 while the aspect ratio was constant at 0.14. The constant aspect ratio at low tide is caused by the free overfall at the end of the discharge channel as discussed in Chapter 2.

The field data during these tidal phases (Figure 5.3) are reasonably well grouped considering that ΔT_o (the condenser temperature rise) is not a constant, surface winds are variable in magnitude and direction, and recirculation occurs at certain times. The grouping of

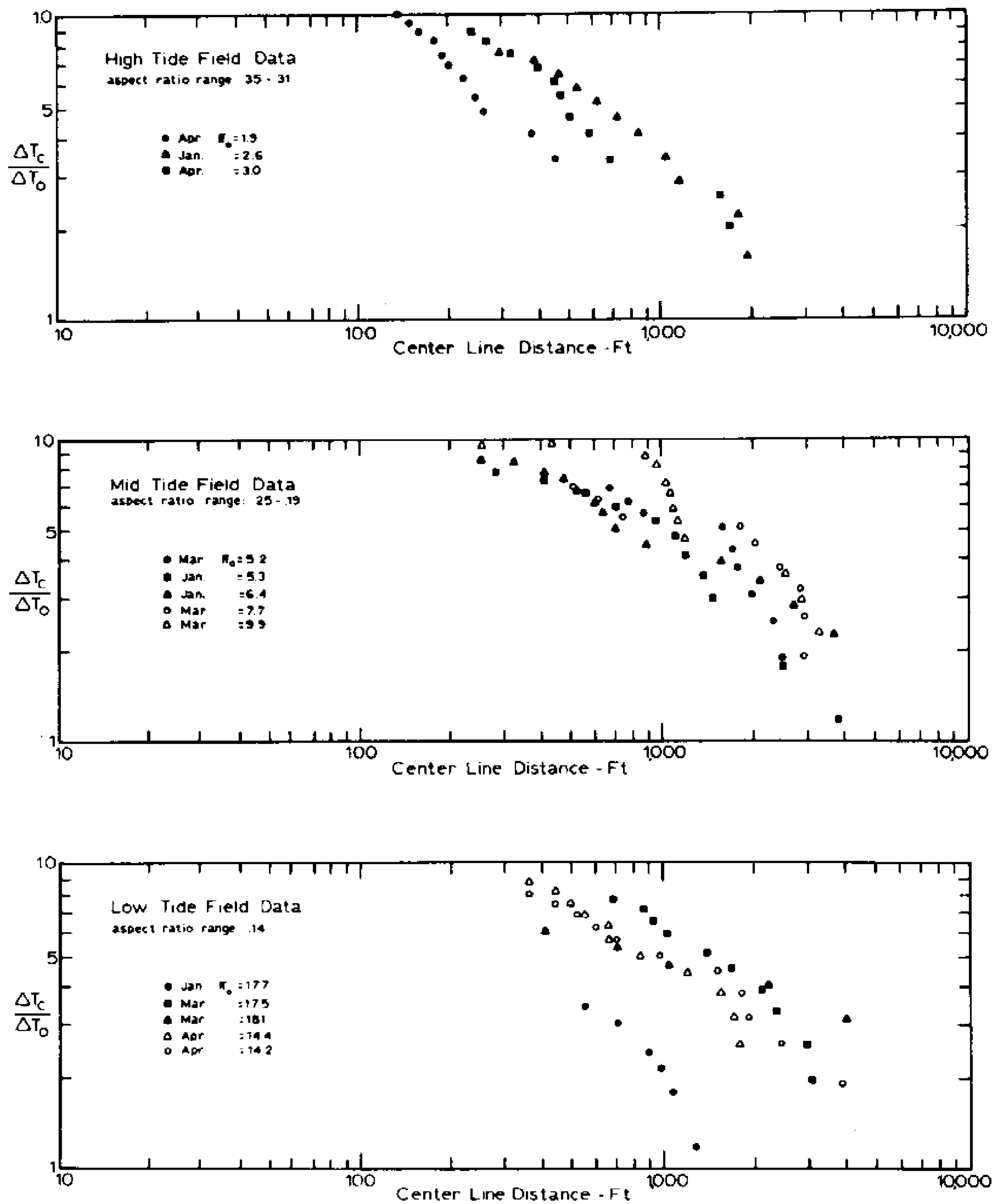

Fig. 5.3 Field Data Grouped by Tidal Range Aspect Ratio

the data suggests that the relative insensitivity of centerline temperature reduction to cross currents (see Figure 5.2) is reasonable.

There are two major exceptions to this relatively tight grouping. One is the low tide data for 1-26-73 with $\mathbb{F}_o$ = 17.7 and A = .14. The other exception is the high tide data collected on 4-19-73 with $\mathbb{F}_o$ = 1.9 and A = .35. Each exception will be discussed below in the comparison of theory by tidal phase.

5.2.1 High Tide Phase

Figure 5.4, 5.5, and 5.6 are comparisons of the theoretical surface centerline temperatures with the field data collected during the high tide phase.

Figure 5.4 compares theory with field data collected during the high tide phase on 4-19-73. Both theories with and without bottom slope, predict the centerline temperature reduction conservatively. The curve drawn from the theory without bottom slope best exhibits the characteristics of the field data and agrees reasonably well in the range of greatest dilution which is near the discharge. The theoretical value of the maximum jet penetration, h_{max}, for these data, as shown in Table 5.2 shows that the maximum jet penetration is 9 feet, which corresponds to h_o. The four foot isotherms for these data show a limited zone close to the discharge affected by the jet. Thus the jet should exhibit good dilution since the bottom does not affect entrainment and the theory without bottom slope should agree.

Two additional field data comparisons of centerline temperatures during the high tide phase are shown in Figures 5.5 and 5.6.

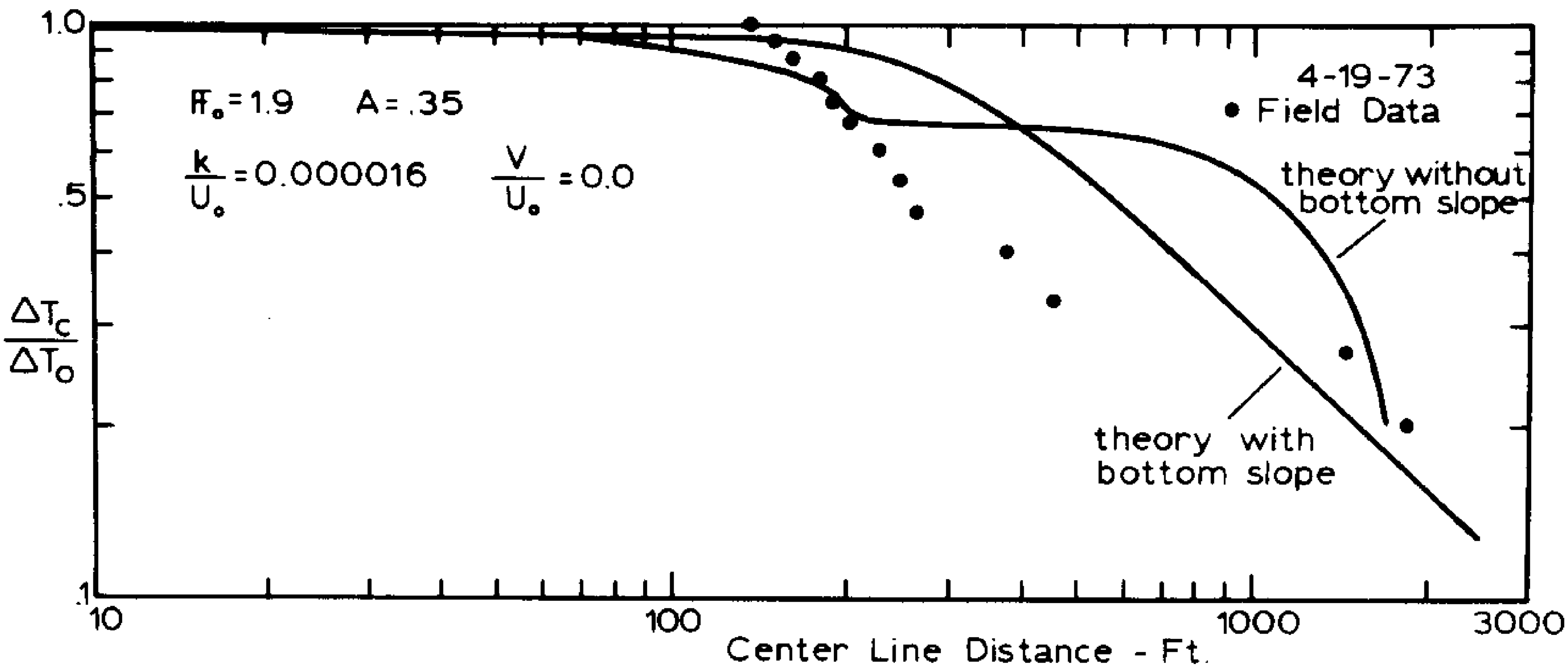

Fig. 5.4: Comparison of Data with Theory

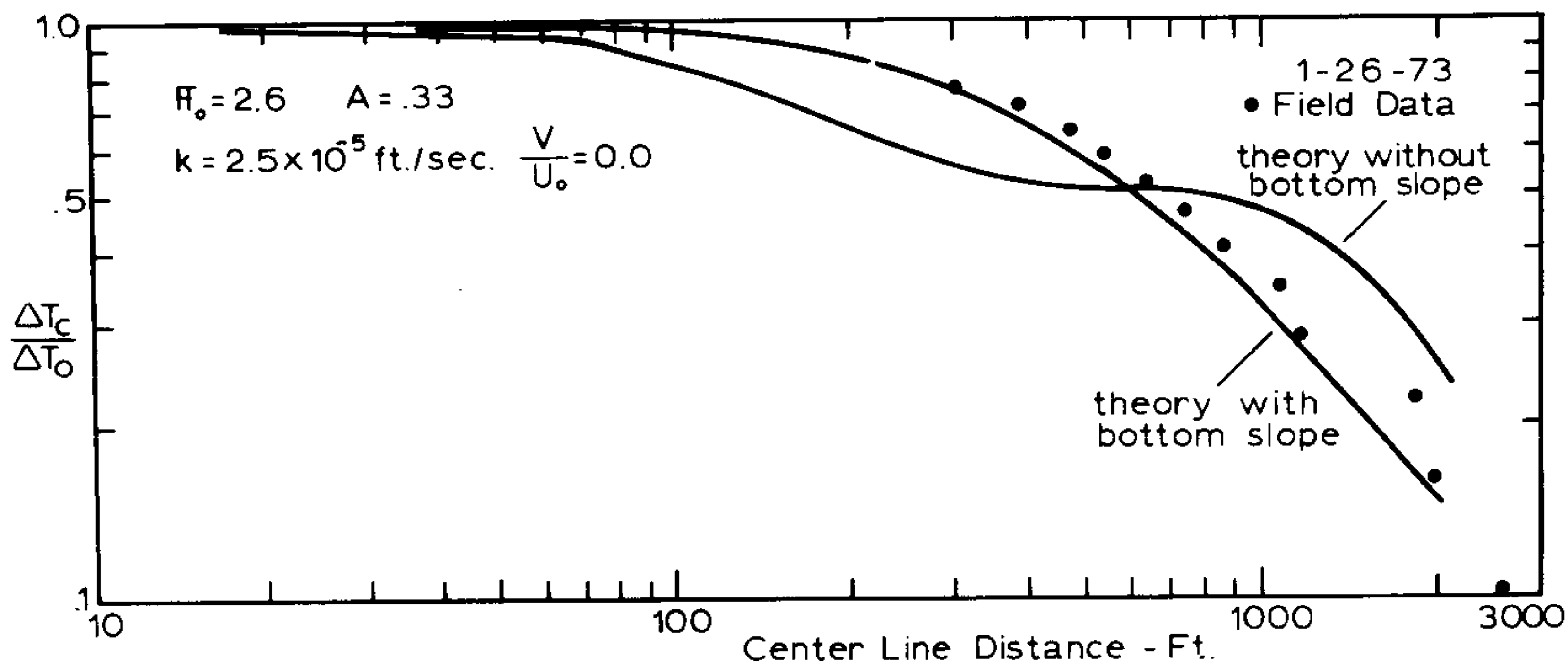

Fig. 5.5: Comparison of Data with Theory

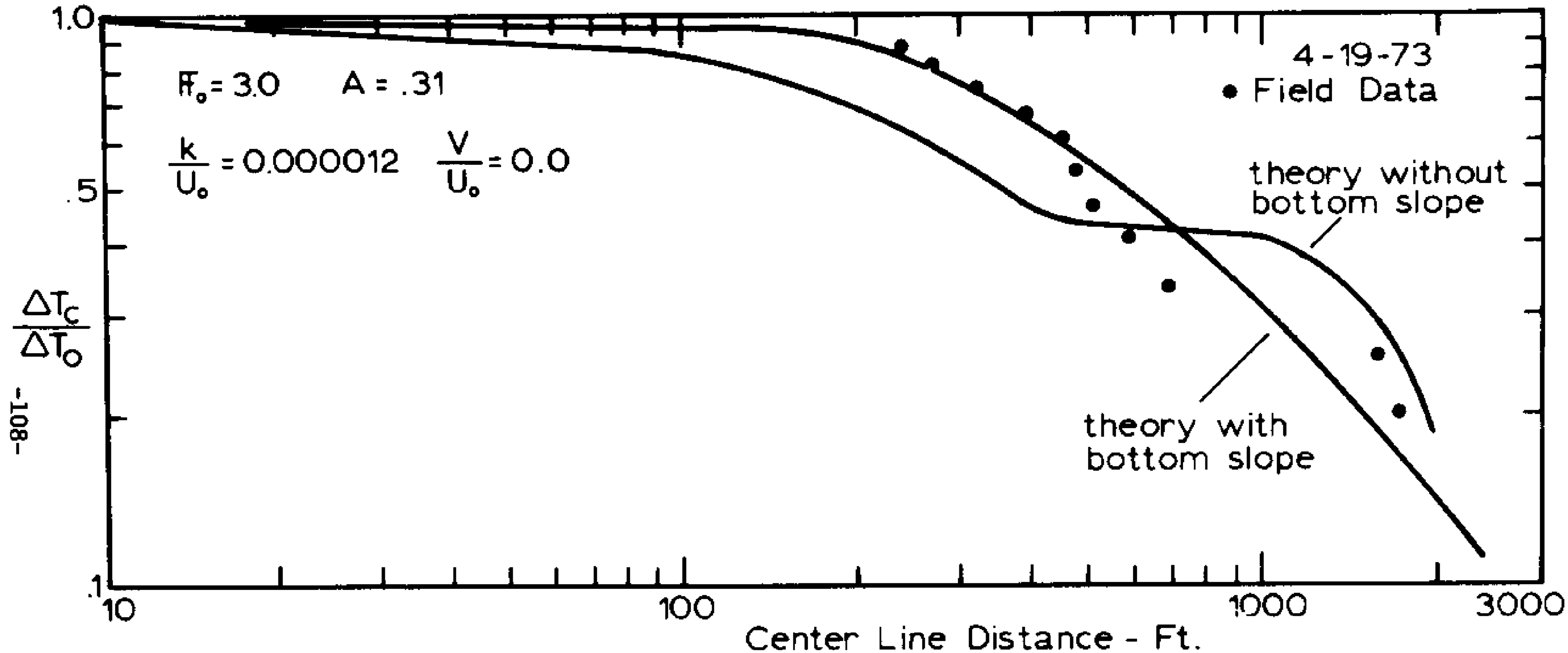

Fig. 5.6: Comparison of Data with Theory

Again an analysis is made of the theoretical maximum jet penetration, h_{max} for this data as shown in Table 5.2. The maximum theoretical jet penetration predicted for both groups shown in Figures 5.5 and 5.6 is 9.5 ft and the depth of water at the exit of the discharge channel is 7.5 ft and 6.8 ft, respectively. The isotherms at a depth of 4 ft show that there is relatively little interaction between the jet and the bottom. Therefore the treatment of point of separation of the jet from the bottom as described in Chapter 2 by the theory with bottom slope is valid and the agreement between field data and theory is good.

Area comparisons between theory and field measurements are shown in Table 5.3. Predicted surface isotherm areas are determined from the analytical model output as shown in Reference 3.

The theory output gives the values of $\overline{\Delta T}$, $\bar{s}$ and $\bar{b}$ as a function of $\bar{x}$. All values are non-dimensional as shown in Figure 2.4:

$$\bar{s} = s/\sqrt{h_o b_o}$$

$$\bar{b} = b/\sqrt{h_o b_o}$$

$$\overline{\Delta T} = \Delta T_c/\Delta T_o$$

The surface isotherm area (A_*) for a given temperature rise of interest (ΔT_*) is determined by:

$$A_* = 2h_o b_o \int_0^{\bar{x}_*} [\bar{s}+\bar{b}(1-\Delta\bar{T}_*/\Delta\bar{T})^{2/3}]d\bar{x}$$

TABLE 5.3

COMPARISON OF ANALYTICAL MODEL DATA TO CORRESPONDING FIELD DATA

High Tide Phase

Field Data Isotherm Value - ^{o}C	Field Data Area Acres	Theory Area Acres
$\mathbb{F}_o$ = 1.9 A = .35		
6	1.0	18
5	3.4	37
4	28	59
3	76	89
$\mathbb{F}_o$ = 3.0 A = 3.1		
10	0.9	0.9
9	1.3	1.3
8	2.0	1.8
7	2.5	2.4
6	4.0	3.1
5	7.0	3.8
4	75	13
3	156	34
$\mathbb{F}_o$ = 2.6 A = .33		
13	.5	0.4
12	1.0	0.5
11	1.8	0.8
10	2.4	1.0
9	4.5	1.8
8	8.3	3.7
7	10	6.4
6	21	9.0
5	32	14

TABLE 5.3 (Continued)

Low Tide Phase

IF_o = 17.7 Isotherm - °C	January Low Tide Field Data Area Acres	Combined Theories Area Acres
5	0.8	2.6
4	1.9	5.1
3	3.7	14
2	13	41
1	49	

where

$$\overline{\Delta T}_* = \Delta T_*/\Delta T_o$$

$$\bar{x}_* = \text{the value of } x/\sqrt{h_o b_o} \text{ where } \overline{\Delta T} = \overline{\Delta T}_*$$

Area computations using $\bar{s}$ and $\bar{b}$ calculated from the bottom slope theory were found to be in error by comparison with laboratory experiments conducted for the User Manual.[3] Due to this fact, a combined theory of area computation was used to predict theoretical surface isotherm areas. The combined theory uses the same equations as above but the output from both the bottom affected and nonbottom affected model is necessary. The $\overline{\Delta T}$ as a function of $\bar{x}$ is used from the bottom affected analytical model output and the $\bar{s}$ and $\bar{b}$ as a function of $\bar{x}$ is used from the nonbottom slope analytical model results. Therefore to determine the surface area (A_*) for a particular temperature rise of interest (ΔT_*) in a bottom affected jet, all values mentioned above are obtained from the specified analytical model run (bottom and nonbottom affected) and substituted into the equation for A_*. Although this is a highly empirical procedure, area agreements between theory and field for bottom affected jets are good when the agreement between field and theory centerline reduction curves are good. This method of surface isotherm area computation for bottom affected jets is referred to as the "combined theory" in Table 5.3.

5.2.2 The Mid Tide Phase

The mid tide phase is a phase in which the steady state assumption used in the analytical model is violated. Because of the rapidly changing Froude number and aspect ratio, agreement between the analytical model and field data should not be expected. The tight grouping of the field data in this phase as shown in Figure 5.3 seems to suggest that the combination of changing Froude number and aspect ratio as well as the effect of jet bottom contact is the controlling mechanism, since the wind and wave conditions were variable on the different survey dates. An example of theory in comparison with mid tide field data is shown in Figure 5.7. The poor agreement as expected between the theory with or without bottom slope and the field data is a result of the violation of the steady state assumption used in the analytical model. As seen in Table 5.1 the greatest isotherm surface areas occur during this tidal phase due to the residual effects from the preceding high tide (low Froude number) portion of the tidal cycle. During this period the temperature of the water being entrained in the buoyant jet is greater than the ambient temperature. This results in higher surface temperatures at a given distance and larger surface areas contained within a given isotherm.

5.2.3. The Low Tide Phase

The low tide phase, as characterized by the free overall condition at the discharge channel exit, is a phase in which the Froude number and aspect ratio are constant over a period of an hour or more for each survey date. A comparison between the field data and theory

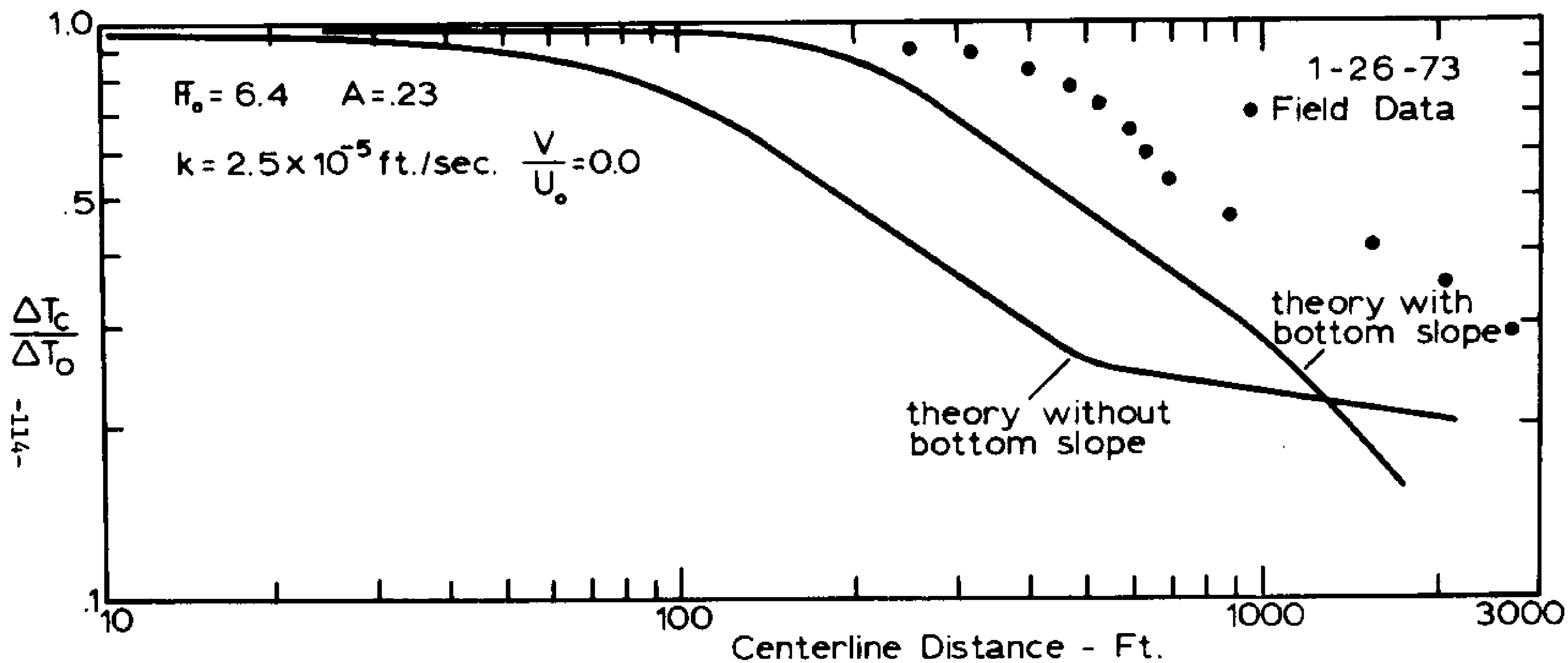

Fig. 5.7 : Comparison of Data with Theory

with bottom slope is in reasonable agreement as shown in Figure 5.8. An analysis of the maximum jet penetration indicates that $h_{max} = 30$ ft. Since the 30 foot depth contour is not reached until a distance of approximately 3000 feet from the discharge exit, the theory predicts that the jet will remain in contact with the shore bottom for the entire near field region. Thus the treatment of the point of jet separation in the model with bottom slope is justified. As expected, the theory without bottom slope indicates centerline temperatures which are too low.

Isotherm surface area comparisons between the combined theory and the January low tide field data are shown in Table 5.3. The agreement is good, the combined theory predicts the surface isotherm areas conservatively. A conservative surface area prediction is expected since the bottom slope analytical model treatment of the point of jet separation remains valid.

Changes in the discharge channel geometry occurred between the January and March survey period due to the winter storms mentioned earlier. Several cap stones of the discharge structure fell into the mouth of the discharge channel. The presence of these obstructions although not changing the water depth in the discharge channel at low tide has changed the velocity field of the jet at the discharge channel exit. Since the new geometry is not known, it is difficult to determine the correct input parameters for the analytical model. Therefore the field results at low tide for field data collected after the changes in the discharge channel are not predicted by the theory (with or without bottom slope).

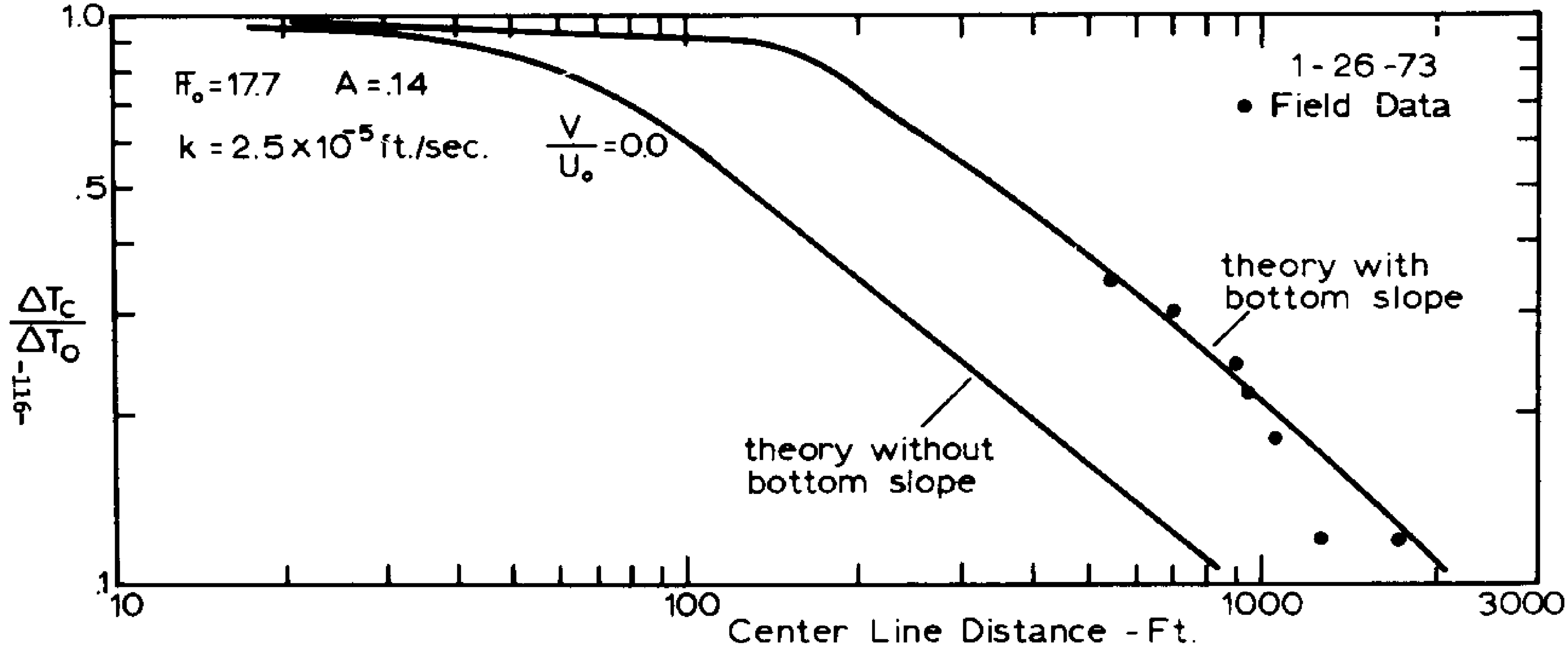

Fig. 5.8 : Comparison of Data with Theory

5.3 Time Weighted Average of Field Data

Due to the variation of Froude number and aspect ratio with time at the site, a method of comparison between theory and field data for the three phases was sought which reduces the unsteady effects of tidal elevation variation. A time weighted average of the field data was employed since the existance of a given field condition is variable, being a function of the sinusoidal tidal elevation versus time curve.

A time weighted average of the January field data was used since the January data is the most continuous record of field results through a half tidal cycle. Time weighting factors were determined using the time of existance of a given field condition in relation to the total time under consideration, which is half a tidal cycle.

The time weighting factor was applied to field and analytical model results for the centerline temperature reduction versus distance. The analytical model output was obtained by two methods. One method was to time weight the output of each model run and sum the results for each distance. The other method was to time weight the input to the analytical model for each field condition and run the sum in the analytical model with the time weighted averaged input. The analytical model with bottom slope was used for the averaging since the buoyant jet is affected by the shore bottom through most of the tidal cycle. The results of the time weighted average are shown in Figure 5.9.

The weighted average of the individual outputs from the model and the weighted average of all the inputs to the model almost coincide which is expected. The time weighted average of the field data is in

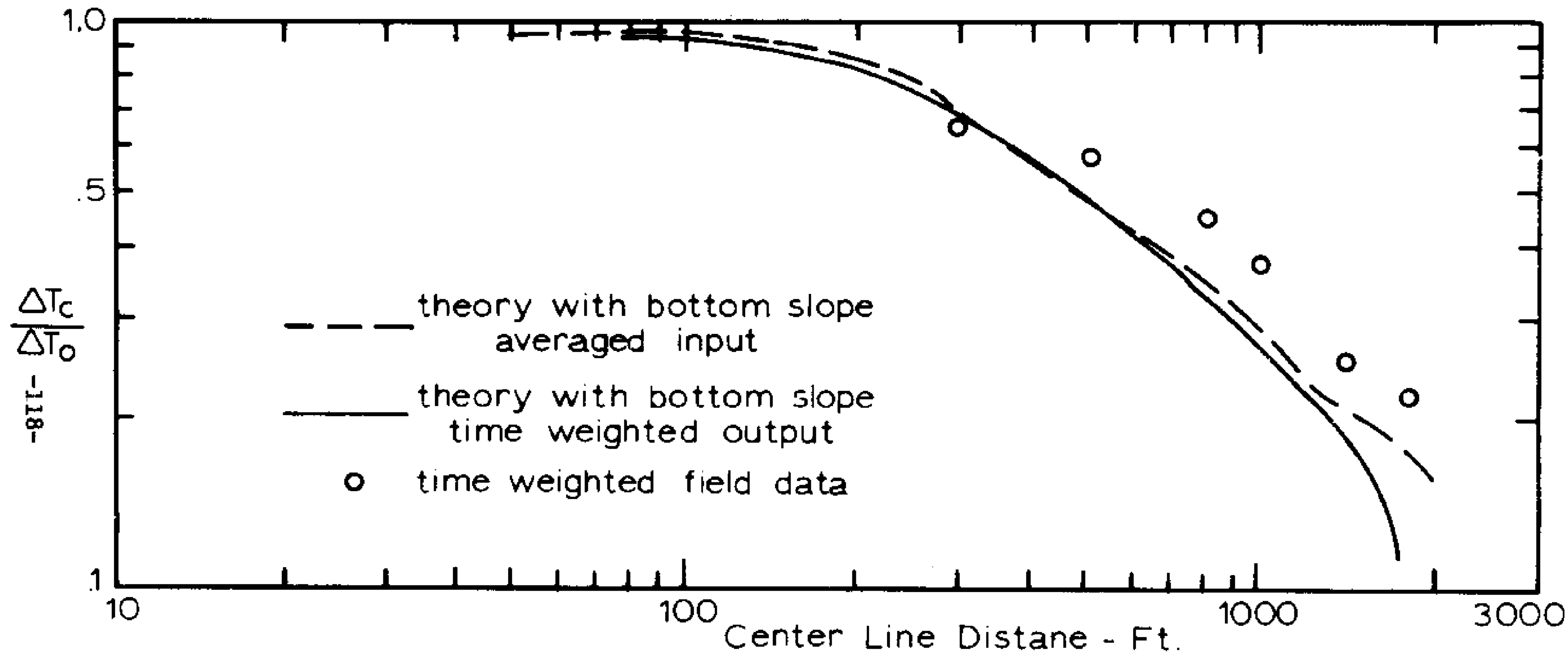

Fig. 5.9 Time Weighted Average Comparison

reasonable agreement with the theory. These results suggest that the violation of the steady state assumption for the analytical model in the mid tide phase is a major contributing factor to unsatisfactory agreement between theory and field for the mid tide phase.

CHAPTER 6

SUMMARY AND CONCLUSIONS

6.1 Objectives

The increased need for electric power in the United States has resulted in the need for new power generating facilities. Power generating facilities discharge waste heat to the environment. Public and governmental awareness of potential thermal pollution has resulted in the need to predict the thermal affects of contemplated power plant construction on the environment.

The characteristics of electric power plant waste heat discharged to the ocean by a once through cooling water system was studied. The study consisted of field measurements of the heated surface buoyant jet of the Pilgrim Nuclear Power Station located at Plymouth, Massachusetts. Field Measurements were conducted to define the thermal plume characteristics of the Pilgrim Nuclear Power Station heated discharge as affected by tidal stage and variability of the ambient water conditions. The variability of the ambient water conduction is a function of wind velocity, coastal current, and the ambient water temperature stratification.

Correlation was sought between the field data collected and a steady state analytical model for heated surface buoyant discharges for the prediction of the heat affected zone. Two versions of the analytical model were used for prediction of the heat affected zone in the receiving water body, one considers the effects of the shore body, the other does not.

6.2 Comparison of Theory with Field Data

Comparisons were made between the analytical model and field data on the basis of observed and predicted plume centerline temperature reduction versus distance as well as observed and predicted surface isotherm areas. The sensitivity of both versions of the analytical model to the heat loss coefficient and to cross currents was determined. An evaluation of the usefulness of the steady state analytical model in conditions of rapidly varying jet characteristics due to tide level changes was made. The ability of the bottom slope version of the analytical model to predict the affects of shore bottom interaction are determined in relation to the tidal elevation variation at the site.

6.3 Results

The field results were grouped into three characteristic periods of time within a tidal cycle based on the jet Froude number and aspect ratio of the discharge which is a direct function of the tidal elevation. The phases are characterized by the high, mid and low tide phase. Analytical predictions for field results of both centerline temperature reduction versus distance and surface isotherm areas show good agreement when discharge conditions are relatively constant for a period of an hour or more. Theoretical predictions of centerline temperature reduction versus distance and surface isotherm areas for the mid tide phase when the jet characteristics are changing most rapidly do not agree with the field results. An attempt to reduce the unsteadiness of the field conditions by time weighted average (1/2 tidal cycle) and comparison to the time weighted average of the theory was made for the centerline temperature reduction versus distance field results. The results were reasonably successful but the unsteady influence of the mid tide phase could not be completely eliminated by this method. Sensitivity of the analytical model to cross currents and heat loss coefficient were determined to be minimal.

Changes in channel geometry at the mouth of the discharge channel occurred due to winter storms. Since the discharge channel geometry is not known exactly, a precise comparison with the analytical model is difficult particularly at low tide when the effects of changes in the exit section are most important.

Winter weather conditions at the site prohibited continuous ambient current measurement by the power company. Ambient current measurements were not made for the survey periods due to loss of current meters and inability to service the remaining meters at the proper intervals.

6.4 Future Work

The bottom slope version of the analytical model requires more work in order to provide the proper surface spreading equations in a unified model. The effect of shore bottom interference for cases where the buoyant jet maintains significant bottom contact before the jet separates from the bottom should be analyzed.

The points of jet separation from the shore bottom as formulated in the analytical model with bottom slope[2] is not adequately predicted. The inclusion of the proper point of jet separation and surface spreading should allow conservative predictions of plume centerline temperature reduction and surface isotherm areas for heated surface buoyant jets affected by bottom slope for steady state conditions.

Development of a transient theory for heated surface buoyant jets in tidal regions should be pursued.

Conservative predictions for power plant discharges throughout the tidal range are necessary for confidence in predictions of the heat affected zone as required by the Atomic Energy Commission for future plants located on oceans or bays.

Measurements should be made to determine the actual discharge channel configuration. Temperature measurements at the intake and in the discharge channel for inplant data correlation should be made during field survey periods. The concept of automatic data reduction should be pursued further but an understanding of the field space requirements versus the size and weight of the necessary equipment is mandatory. Due to the shallow near shore areas involved in this type of survey, a small boat is necessary. If the equipment necessary for automated data reduction is large and requires substantial electrical power then a small survey craft may not suffice. Horizontal temperature profiles at the surface and at the four foot depths were generally sufficient to define the thermal plume. Measurements at greater depths are difficult due to bottom obstructions.

Vertical temperature profiles at various points in the plume would be most useful. The small boat bathythermograph as originally conceived is the proper instrument for the existing field conditions. The automatic data reduction system used in the small boat bathythermograph should be improved. Implementation of an automatic navigation system would speed data collection. Again the automatic navigation system used must be small enough to fit in a small boat. Cost justification for all these additional improvements can be based on the increase of data collected and reduced for each hour spent in the field. Weather delays increase overhead of any operation, so if more data can be taken in a similar time period, the necessity of frequent consecutive surveys may be reduced.

REFERENCES

1. Harleman, D.R.F. and Stolzenbach, K.D., "A Model Study of Proposed Condenser Water Discharge Configurations for the Pilgrim Nuclear Power Station at Plymouth, Massachusetts", Technical Report No. 113, Ralph M. Parsons Laboratory for Water Resources and Hydrodynamics, Department of Civil Engineering, M.I.T., May 1969

2. Stolzenbach, K.D. and Harleman, D.R.F., "An Analytical and Experimental Investigation of Surface Discharges of Heated Water", Technical Report No. 135, Ralph M. Parsons Laboratory for Water Resources and Hydrodynamics, Department of Civil Engineering, M.I.T., February 1971

3. Stolzenbach, K.D., Adams, E.E. and Harleman, D.R.F., "A Users Manual for Three Dimensional Heated Surface Discharge Computations", Technical Report No. 156, Ralph M. Parsons Laboratory for Water Resources and Hydrodynamics, Department of Civil Engineering, M.I.T., September 1972

4. Boston Edison Company Report. "Pilgrim Nuclear Power Station Environmental Report Supplement, Operating License Stage", Report to A.E.C. by Boston Edison Company, November 1971

5. Progress Report to Boston Edison Company. "December 31, 1972 Progress Report for Oceanographic Studies at Pilgrim Nuclear Power Plant", M.I.T., 1973

6. Frigo, P.D. and Frye, D.E., "Physical Measurements of Thermal Discharges into Lake Michigan: 1971", Special Report No. ANL/ES-16, Argonne National Laboratory, October 1972

7. Tide Tables, East Coast of North and South America 1973, U.S. Department of Commerce Publication, National Ocean Survey, Rockville, Maryland, 1973

8. U.S. Coast and Geodetic Survey Publication, "Density of Sea Water at Tide Stations on the Atlantic Coast, North and South America, USCGS Publication 31-2, U.S. Government Printing Office, 1955

9. Ryan, P.J. and Harleman, D.R.F., "An Analytical and Experimental Study of Transient Cooling Pond Behavior", Technical Report No. 161, Ralph M. Parsons Laboratory for Water Resources and Hydrodynamics, Department of Civil Engineering, M.I.T., January 1973